

**UCSF**

**UC San Francisco Electronic Theses and Dissertations**

**Title**

The Role of Ectodermally Derived Epithelium in the Development, Maintenance, and Pathogenesis of Tissues and Structures in the Craniofacial Complex

**Permalink**

<https://escholarship.org/uc/item/875453sd>

**Author**

Jones, Kyle Burke

**Publication Date**

2017

**Supplemental Material**

<https://escholarship.org/uc/item/875453sd#supplemental>

Peer reviewed|Thesis/dissertation

The Role of Ectodermally Derived Epithelium in the Development,  
Maintenance, and Pathogenesis of Tissues and Structures in the  
Craniofacial Complex

by

Kyle Burke Jones

DISSERTATION

Submitted in partial satisfaction of the requirements for the degree of

DOCTOR OF PHILOSOPHY

in

Oral and Craniofacial Sciences

in the

GRADUATE DIVISION

of the

UNIVERSITY OF CALIFORNIA, SAN FRANCISCO

**Copyright 2017**

**by**

**Kyle Burke Jones**

## DEDICATION AND ACKNOWLEDGEMENTS

I would like to dedicate this work to my beautiful and incredibly supportive wife, Kristin, along with my wonderful daughter, Anna. Kristin, you have sacrificed so much for me to complete this program and chase after my impossible dreams. None of this would have been possible without your love, advice, and support, particularly when times were difficult. I am forever grateful and in your debt. Thank you from the bottom of my heart for everything you have done for me and continue to do for me on a daily basis. I love you and look forward to the many amazing adventures that await our family in the future.

Next, I would like to thank my PhD mentor, Dr. Ophir Klein. Ophir, thank you for your mentorship and guidance in both my scientific endeavors and career. My project would certainly not be what it is today without your help and insight. Also, thank you for always pushing me to be the best scientist that you knew I could become. Most of all, thank you for your patience! This entire journey took a bit longer than I think either of us anticipated. Thank you for sticking with me and believing in my project. I will always have fond memories of my time in the lab and the many lessons I learned there. I look forward to your continuing friendship, mentorship, and successful collaborations in the future!

To my parents, Burke and Paula, thank you for your unwavering support. You have always seen the best in me and supported me in all of my endeavors as a young adult and now as an adult. I love you both and am so happy to be able to share this experience and moment with you.

Thank you, Roger Mraz, for being an incredibly helpful guide throughout this entire DDS/PhD process, as well as for being a genuine, selfless, and fierce friend. Thank you for always making the time to talk with me when I needed help as well as for lending an ear when I just needed someone to listen. Kristin and I look forward to our continued friendship in the future.

I particularly want to thank my residency director and mentor, Dr. Richard Jordan, for your infinitely valuable career guidance and support towards completion of my PhD and career in academia. Without your flexibility and help, I would not have been able to finish the PhD program nor be on my current career path. I look forward to working with you in the future as both a colleague and friend. I would also like to thank Dr. John Greenspan for your support and mentorship over these many years. Your guidance early on in my DDS/PhD career helped solidify my love for science and academia. Thank you for always finding time to speak with me despite your incredibly busy schedule. Also, thank you to Dr. Caroline Shiboski. You have been an ardent supporter throughout this experience, especially during my residency training. Thank you for your continued support.

Thank you to the Klein Lab members that I have had the pleasure of working with over the years, especially Adriane Joo, Saunders Ching, Kerstin Seidel, Alice Goodwin, Andrew Jheon, Vagan Tapaltsyan, Asoka Rathnayake, Brian Biehs, Jimmy Hu, Pauline Marangoni, Ysbrand Nusse, Hongfang Ma, Sachiko Furukawa, and Hua Tian. Thank you for all of the technical expertise and fruitful conversations we have had related to my project. Also, thank you to Henry Pinkard and Kaitlin Corbin for all of your amazing help and expertise with confocal imaging for my project. Lastly, thank you to Sarah

Knox and Jeff Bush for your support and helpful comments related to my project and career.

Finally, thank you to my collaborator, Dr. Allon Klein, for all of your time, knowledge, and energies devoted to this project. There is no way I could have done this without your insight and guidance. Also, thank you to my dissertation committee members, Dr. Allan Balmain, Dr. Todd Nystul, and Dr. Jason Rock. Your feedback and encouragement allowed me to reach higher with my project and explore new directions, which significantly improved the quality of my project. Thank you.

There are so many others that I would like to thank but just do not have the space necessary to do so. From clinical instructors to administrative staff, I have had the immense pleasure and honor of working with so many talented and genuinely good people here at UCSF. Of all the lessons I have learned from you during my PhD training, the most important has been the realization that science is a team sport. For projects to be successful, it requires the efforts of so many people. Thank you to all of those who have helped me throughout my training and that will continue to help me as I move forward in my career.

# **The Role of Ectodermally Derived Epithelium in the Development, Maintenance, and Pathogenesis of Tissues and Structures in the Craniofacial Complex**

by

Kyle Burke Jones

## **ABSTRACT**

The craniofacial complex comprises myriad cells types, tissues, and anatomic structures, all of which are vital for proper function. Two of these tissues, the ectodermally derived epidermis and oral epithelium, play integral roles in the embryonic development of several important craniofacial structures, such as hair follicles, sweat glands, and minor salivary glands. They are also important for maintaining epidermal and oral mucosal barrier integrity. Dysfunction in the development and/or integrity of these tissues can lead to serious clinical sequelae. One of the key cell types within the epidermis and oral mucosa that is crucial to maintaining homeostasis is the epithelial stem cell. While much work has been done in the epidermis to identify and characterize these cells, there is still relatively little known about stem cells within the oral epithelium. For example, where in the oral epithelium are these cells located? How can they be identified? Are they rare or numerous? What role do these cells play in oral disease? Identifying and characterizing epithelial stem cells will be crucial to understanding how they maintain tissue homeostasis as well as the role they may play in the development of various diseases in the craniofacial complex. Furthermore, an increased understanding of their organization and biology could lead to new treatment strategies.

This dissertation is organized into two main sections. The first section (Chapter 2) focuses on the identification of oral epithelial stem cells and their organization within the adult mouse using basic science approaches and techniques. The second section (Chapters 3 and 4) centers on the clinical sequelae that result from presumed defects in epithelial stem cell function, specifically in the context of X-linked hypohidrotic ectodermal dysplasia and various intraoral white lesions. These basic science and clinical research studies together highlight the importance of epithelial stem cell biology in the development and maintenance of epithelial tissues within the craniofacial complex.



## **TABLE OF CONTENTS**

|  |           |
|--|-----------|
| <b>CHAPTER 1: Introduction to Oral Epithelial and Epidermal Stem Cells in Tissue Maintenance and Disease .....</b> | <b>1</b>  |
| <b><u>1.1 Abstract</u> .....</b>   | <b>3</b>  |
| <b><u>1.2 Introduction</u> .....</b>   | <b>4</b>  |
| <b><u>1.3 Oral Mucosal and Epidermal Development and Histology</u>....</b>   | <b>4</b>  |
| <b><u>1.4 Methods Used to Identify and Characterize Stem Cells</u> .....</b>                                       | <b>9</b>  |
| 1.4.1 <i>Label Retaining Cells</i> .....   | 10        |
| 1.4.2 <i>In Vitro Morphology and Clonogenicity</i> .....   | 12        |
| 1.4.3 <i>Stem Cell Markers</i> .....   | 13        |
| 1.4.4 <i>In Vivo Lineage Tracing</i> .....   | 20        |
| <b><u>1.5 Emerging Paradigms</u> .....</b>   | <b>24</b> |
| 1.5.1 <i>The Epidermal Proliferative Unit Model</i> .....  | 24        |
| 1.5.2 <i>The Neutral Drift Model</i> .....   | 25        |
| <b><u>1.6 Stem Cells in Oral Disease</u> .....</b>   | <b>30</b> |
| <b><u>1.7 Conclusion</u> .....</b>   | <b>32</b> |
| <b>CHAPTER 2: Hierarchy and Fate of Progenitor Cells in the Oral Epithelium .....</b>                              | <b>34</b> |
| <b><u>2.1 Abstract</u> .....</b>   | <b>36</b> |

|   |           |
|---|-----------|
| <b>2.2 Introduction</b> .....   | <b>37</b> |
| <b>2.3 Materials and Methods</b> .....  | <b>38</b> |
| 2.3.1 <i>Mouse Genotypes</i> .....  | <b>38</b> |
| 2.3.2 <i>In-Situ Hybridization</i> .....  | <b>38</b> |
| 2.3.3 <i>Lineage Tracing</i> .....  | <b>39</b> |
| 2.3.4 <i>Immunofluorescence (Cryosections)</i> .....  | <b>40</b> |
| 2.3.5 <i>BrdU Pulse-Chase Experiment</i> .....  | <b>40</b> |
| 2.3.6 <i>Whole-Mount Immunofluorescence</i> .....   | <b>41</b> |
| 2.3.7 <i>KI-67 Quantification</i> .....   | <b>42</b> |
| 2.3.8 <i>Cell Cycle Calculations Using BrdU and EdU Dual Labeling</i> .....                                     | <b>43</b> |
| 2.3.9 <i>Dual BrdU and EdU Pulse/Chase Labeling</i> .....   | <b>44</b> |
| 2.3.10 <i>K5<sup>tTa</sup>;H2B<sup>GFP</sup> Label Retention Experiments</i> .....                              | <b>45</b> |
| 2.3.11 <i>Measuring Individual Cell Fluorescence Values in K5<sup>tTa</sup>;H2B<sup>GFP</sup> Samples</i> ..... | <b>46</b> |
| 2.3.12 <i>Clonal Analysis of Buccal Mucosa and Tongue Epithelium</i> .....                                      | <b>46</b> |
| 2.3.13 <i>Nuclear Density and Clonal Analysis of 5-Fluorouracil Treated Mice</i> .....                          | <b>48</b> |
| 2.3.14 <i>Mitotic Figure Quantification and Orientation Analysis</i> .....                                      | <b>49</b> |

|  |           |
|--|-----------|
| 2.3.15 <i>Buccal Mucosa Single Cell Dissociation and FACS Sorting</i> .....  | 50        |
| 2.3.16 <i>Single Cell RNAseq</i> .....   | 51        |
| 2.3.17 <i>Analysis of Single Cell RNAseq</i> .....   | 51        |
| 2.3.18 <i>Gene Ontology Analysis</i> .....   | 52        |
| 2.3.19 <i>Imaging Equipment and Software</i> .....   | 53        |
| 2.3.20 <i>Statistical Analysis</i> .....   | 53        |
| 2.3.21 <i>Antibodies</i> .....   | 53        |
| <b>2.4 Results</b> .....   | <b>55</b> |
| <b>2.5 Discussion</b> .....  | <b>78</b> |
| <b>CHAPTER 3: Characterization of X-linked Hypohidrotic Ectodermal Dysplasia (XL-HED) Hair and Sweat Gland Phenotypes Using Photomicrograph Analysis and Live Confocal Imaging</b> ..... | <b>80</b> |
| <b>3.1 Abstract</b> .....  | <b>81</b> |
| <b>3.2 Introduction</b> .....  | <b>82</b> |
| <b>3.3 Materials and Methods</b> .....   | <b>86</b> |
| 3.3.1 <i>Study Participant Recruitment and Demographics</i> .....  | 86        |
| 3.3.2 <i>Medical Questionnaire</i> .....   | 88        |
| 3.3.3 <i>Genotyping</i> .....  | 90        |

|   |                |
|---|----------------|
| 3.3.4 <i>Pilocarpine-Induced Iontophoresis</i> .....  | 90             |
| 3.3.5 <i>Live Confocal Microscopy Imaging of<br/>    Palmar Sweat Ducts</i> .....                                 | 90             |
| 3.3.6 <i>Phototrichogram Analysis</i> .....   | 91             |
| 3.3.7 <i>Statistical Methods</i> .....  | 92             |
| <b>3.4 <u>Results</u></b> .....   | <b>93</b>      |
| 3.4.1 <i>Medical Questionnaire</i> .....  | 93             |
| 3.4.2 <i>Sweat Duct Counts</i> .....  | 94             |
| 3.4.3 <i>Pilocarpine-Induced Sweat Volumes</i> .....  | 94             |
| 3.4.4 <i>Hair Counts</i> .....  | 96             |
| 3.4.5 <i>Follicular Units</i> .....   | 96             |
| 3.4.6 <i>Hair Width</i> .....   | 97             |
| 3.4.7 <i>Hair Growth</i> .....  | 97             |
| 3.4.8 <i>Genotyping of EDA1</i> .....   | 100            |
| 3.4.9 <i>Age Correlation Analysis</i> .....   | 100            |
| <b>3.5 <u>Discussion</u></b> .....  | <b>101</b>     |
| <br><b>CHAPTER 4: White lesions of the Oral Cavity: Clinical Presentation,<br/>Diagnosis, and Treatment</b> ..... | <br><b>105</b> |
| <b>4.1 <u>Abstract</u></b> .....  | <b>106</b>     |

|  |            |
|--|------------|
| <b><u>4.2 Introduction</u></b> .....                     | <b>107</b> |
| <b><u>4.3 Hereditary Lesions</u></b> .....               | <b>107</b> |
| 4.3.1 <i>Leukoedema</i> .....                            | 107        |
| 4.3.2 <i>White Sponge Nevus</i> .....                    | 110        |
| <b><u>4.4 Reactive Lesions</u></b> .....                 | <b>113</b> |
| 4.4.1 <i>Frictional Hyperkeratosis</i> .....             | 113        |
| 4.4.2 <i>Smokeless Tobacco Changes</i> .....             | 116        |
| 4.4.3 <i>Nicotine Stomatitis (Smoker's Palate)</i> ..... | 120        |
| 4.4.4 <i>Hairy Tongue</i> .....                          | 123        |
| 4.4.5 <i>Hairy Leukoplakia</i> .....                     | 126        |
| <b><u>4.5 Inflammatory Mediated Lesions</u></b> .....    | <b>129</b> |
| 4.5.1 <i>Oral Lichen Planus</i> .....                    | 129        |
| 4.5.2 <i>Oral Lichenoid Reactions</i> .....              | 133        |
| <b><u>4.6 Pre-Neoplastic/Neoplastic</u></b> .....        | <b>136</b> |
| 4.6.1 <i>Oral Leukoplakia</i> .....                      | 136        |
| 4.6.2 <i>Squamous Cell Carcinoma</i> .....               | 140        |
| <b><u>4.7 Other</u></b> .....                            | <b>143</b> |

|   |            |
|---|------------|
| 4.7.1 <i>Geographic Tongue (Benign Migratory Glossitis)</i> ..... | 143        |
| <b>4.8 Conclusion</b> .....                                       | <b>146</b> |
| <b>CHAPTER 5: Summary and Future Perspectives</b> .....           | <b>147</b> |
| <b>Literature Cited</b> .....                                     | <b>174</b> |

## LIST OF TABLES

|   |           |
|---|-----------|
| <b>Table 1.1</b> Candidate oral epithelial stem cell markers<br>in various oral sites.....                  | <b>16</b> |
| <b>Table 3.1</b> Demographic characteristics of control and<br>XL-HED subjects .....                        | <b>87</b> |
| <b>Table 3.2</b> Clinical characteristics of XL-HED subjects<br>as determined by medical questionnaire..... | <b>89</b> |

## LIST OF FIGURES

|   |     |
|---|-----|
| <b>Figure 1.1</b> Oral mucosa in <i>Mus musculus</i> .....  | 7   |
| <b>Figure 1.2</b> <i>CRE</i> recombinase technology .....   | 22  |
| <b>Figure 1.3</b> The invariant asymmetry and neutral drift models .....  | 28  |
| <b>Figure 2.1</b> <i>Bmi1</i> labels progenitor cells within the basal layer of the rapidly dividing oral mucosa .....  | 58  |
| <b>Figure 2.2</b> The buccal mucosa does not contain label retaining cells and exhibits rapid cell division rates .....   | 63  |
| <b>Figure 2.3</b> <i>Bmi1</i> -labeled OEPCs in the buccal mucosa and dorsal tongue divide via population asymmetry with neutral drift dynamics .....             | 67  |
| <b>Figure 2.4</b> 5FU has long-lasting effects on epithelial mitotic rates within the buccal mucosa and causes expansion of OEPCs .....                           | 71  |
| <b>Figure 2.5</b> Buccal mucosal epithelial basal layer keratinocytes are composed of OEPCs and maturing keratinocytes at varying stages of differentiation ..... | 76  |
| <b>Figure 3.1</b> XL-HED subjects show a decrease in palmar sweat ducts and produce little to no sweat.....   | 95  |
| <b>Figure 3.2</b> Phototrichogram analysis reveals multiple properties of XL-HED subject hair that differ significantly from controls .....                       | 98  |
| <b>Figure 4.1</b> Leukoedema on the right buccal mucosa.....  | 109 |
| <b>Figure 4.2</b> White sponge nevus on the right buccal mucosa .....   | 112 |
| <b>Figure 4.3</b> Frictional hyperkeratosis .....   | 115 |



|  |            |
|--|------------|
| <b>Figure 4.4</b> Soft tissue changes of the right mandibular buccal vestibule where the patient habitually placed his smokeless tobacco ..... | <b>119</b> |
| <b>Figure 4.5</b> Nicotine stomatitis in a habitual pipe/cigar smoker .....  | <b>122</b> |
| <b>Figure 4.6</b> Hairy tongue on the posterior two-thirds of the dorsal tongue.....   | <b>125</b> |
| <b>Figure 4.7</b> Hairy leukoplakia .....  | <b>128</b> |
| <b>Figure 4.8</b> Oral lichen planus.....  | <b>132</b> |
| <b>Figure 4.9</b> Oral lichenoid reaction.....   | <b>135</b> |
| <b>Figure 4.10</b> Oral leukoplakia.....   | <b>142</b> |
| <b>Figure 4.11</b> Geographic tongue .....   | <b>145</b> |

**LIST OF SUPPLEMENTAL TABLES**

**Supplemental Table 1** Hair characteristics of control and  
XL-HED Subjects ..... **150**

**Supplemental Table 2** *EDA-A1* genotyping results for XL-HED subjects .. **153**

## **LIST OF SUPPLEMENTAL FIGURES**

|  |            |
|--|------------|
| <b>Supplemental Figure S1</b> <i>Bmi1</i> is expressed predominantly in basal layer cells throughout the oral mucosa. ....   | <b>155</b> |
| <b>Supplemental Figure S2</b> <i>Bmi1</i> labels long-lived OEPCs in the oral mucosal epithelium .....   | <b>157</b> |
| <b>Supplemental Figure S3</b> <i>Krt14</i> labels long-lived OEPCs in the oral mucosal epithelium .....  | <b>159</b> |
| <b>Supplemental Figure S4</b> <i>Gli1</i> labels long-lived OEPCs in the oral mucosal epithelium .....   | <b>160</b> |
| <b>Supplemental Figure S5</b> <i>Sox2</i> labels long-lived OEPCs in the oral mucosal epithelium, but not in lower lip skin .....  | <b>162</b> |
| <b>Supplemental Figure S6</b> <i>Lrig1</i> labels long-lived OEPCs in most, but not all, oral mucosal sites .....  | <b>164</b> |
| <b>Supplemental Figure S7</b> Buccal mucosal basal layer keratinocytes are highly proliferative and exhibit rapid cell turnover .....  | <b>165</b> |
| <b>Supplemental Figure S8</b> <i>Bmi1</i> -labeled basal layer progenitor cells in the buccal mucosa and dorsal tongue divide via population asymmetry—not invariant asymmetry—and follow neutral drift dynamics ..... | <b>167</b> |
| <b>Supplemental Figure S9</b> Buccal epithelial basal layer keratinocytes increase both p53 expression and the number of parallel oriented mitoses in response to 5FU-induced damage.....                              | <b>169</b> |
| <b>Supplemental Figure S10</b> Gene ontology terms associated with the upregulated differentially expressed genes for clusters 0-5.....  | <b>171</b> |
| <b>Supplemental Figure S11</b> Age correlation analysis .....  | <b>173</b> |

## **CHAPTER 1**

### **Introduction to Oral Epithelial and Epidermal Stem Cells in Tissue Maintenance and Disease**

The research presented within this dissertation seeks to address several important questions as they relate to oral and epidermal epithelial progenitor and stem cell biology: 1) What role do ectodermally derived epithelial embryonic progenitor cells play in the development of craniofacial structures and what sequelae arise when these processes go awry? 2) Where are adult oral epithelial stem cells located within the oral epithelium, how are they organized hierarchically within this tissue, and how do they maintain tissue homeostasis? 3) What types of oral and maxillofacial pathologic entities may be due to aberrations in oral epithelial stem cell biology? By utilizing a holistic approach to study the various roles that epidermal and oral epithelial stem cells play in these areas, their overall importance in development, adult tissue homeostasis, and disease become increasingly evident.

In this chapter, I introduce the roles that oral epithelial stem cells play in both the development and maintenance of tissues that make up the craniofacial complex as well as their possible contribution to some pathologic states. I will also discuss stem cell paradigms in the skin that are applicable to the oral mucosa. A majority of the content contained within this chapter was published in the International Journal of Oral Science, July 2013 (K. B. Jones & Klein, 2013).

Kyle B. Jones<sup>1</sup> and Ophir D. Klein<sup>1,2,3</sup>

<sup>1</sup>Program in Craniofacial and Mesenchymal Biology, University of California, San Francisco, San Francisco, CA, USA

<sup>2</sup>Division of Medical Genetics, Department of Pediatrics, University of California, San Francisco, San Francisco, CA, USA

<sup>3</sup>Center for Craniofacial Anomalies, Department of Orofacial Sciences, University of California, San Francisco, San Francisco, CA, USA

## **1.1 ABSTRACT**

The identification and characterization of stem cells is a major focus of developmental biology and regenerative medicine. The advent of genetic inducible fate mapping techniques has made it possible to precisely label specific cell populations and to follow their progeny over time. When combined with advanced mathematical and statistical methods, stem cell division dynamics can be studied in new and exciting ways. Despite advances in a number of tissues, relatively little attention has been paid to stem cells in the oral epithelium. This chapter will focus on current knowledge about adult oral epithelial stem cells, paradigms in other epithelial stem cell systems such as the epidermis that could facilitate new discoveries in this area, and the potential roles of epithelial stem cells in oral disease.

## **1.2 INTRODUCTION**

In recent years, many labs have focused on the identification and characterization of stem cells in various embryonic and adult tissues. These efforts have led to important discoveries about the nature of stem cells and their roles in tissue maintenance and regeneration. Relatively little work has been done to identify oral epithelial stem cells (OESCs) compared with other tissue systems. This review will focus on the basic biology of the oral mucosa and epidermis, methods used thus far to identify stem cells in these and other tissues, emerging paradigms in other epithelial stem cell systems that may be important for OESC biology, and the possible role of OESCs in oral disease.

## **1.3 ORAL MUCOSAL AND EPIDERMAL DEVELOPMENT AND HISTOLOGY**

The epithelium on the inner surface of the lips, floor of the mouth, gingiva, cheeks, and hard palate is derived from embryonic ectoderm, whereas the epithelium surrounding the tongue is derived from both endoderm and ectoderm (Waitzer, 1984). The epidermis is also derived from embryonic ectoderm (Fuchs, 2007). The majority of the connective tissue elements in the head originate from neural crest cells (Martin, 1992). Although outside the scope of this dissertation, considerable efforts have been made to identify and characterize the mesenchymal stem cell populations in the connective tissue, some of which are thought to be derived directly from primitive neural crest cells (see Cutlan, Saunders, Olsen, & Fullen, 2010; Jorgenson & Levin, 1981; Timmer et al., 1997) for comprehensive reviews). During development of both the epidermis and oral mucosa, primitive ectoderm invaginates into the underlying

mesenchyme and, through a series of complex signals between both tissues, leads to the formation of various adnexal structures. These include teeth, minor salivary glands, and occasional sebaceous glands in the oral mucosa and hair follicles, sebaceous glands, and sweat glands in the skin, among others (Pispa & Thesleff, 2003).

In mammals, the oral mucosa can be broadly divided into three subtypes: masticatory (hard palate and gingiva), specialized (dorsal surface of the tongue), and lining (buccal mucosa, ventral surface of the tongue, soft palate, intraoral surfaces of the lips, and alveolar mucosa). The oral mucosa consists of an outer, stratified squamous epithelium in direct contact with an underlying, dense connective tissue called the lamina propria, which contains blood vessels, minor salivary glands, structural fibers, nerves, fibroblasts, and other cell types (see Jorgenson & Levin, 1981 for comprehensive reviews; Fig. 1.1a). In humans, the masticatory and specialized mucosae are keratinized, whereas the lining mucosa is not; however, the location of keratinized oral tissues can vary depending on the species (Fig. 1.1b) (Jorgenson & Levin, 1981). In a similar fashion, the epidermis also consists of an outer stratified squamous epithelium that contacts underlying connective tissue. The first area of connective tissue is called the papillary dermis, which consists of loosely arranged collagen bundles. Deep to the papillary dermis is the reticular dermis, which contains denser aggregations of collagen bundles along with blood vessels, nerves, sweat glands, and hair follicles. Finally, deep to the reticular dermis is the hypodermis, which consists primarily of adipose tissue and some connective tissue (Kanitakis, 2002).

Histologically in both the oral mucosa and epidermis, undulations of epithelium, called rete ridges, can be seen protruding downwards into either the lamina propria or

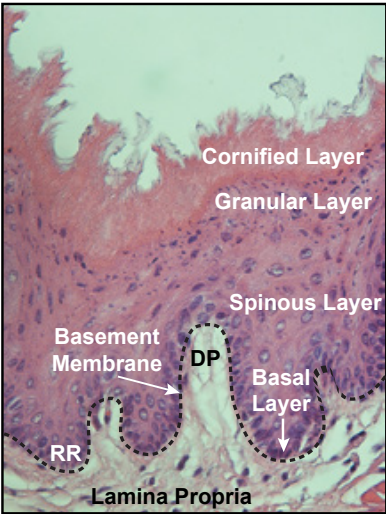


papillary dermis, respectively (Fig. 1.1a). This in turn creates corresponding finger-like upward projections of lamina propria/connective tissue, named connective tissue papillae in the oral mucosa and dermal papillae in the skin. The interdigitating rete ridges and connective tissue papillae provide increased surface area contacts that help prevent separation of the oral epithelium and epidermis from the underlying connective tissue when forces are applied to the tissue, such as during mastication (T. Wu et al., 2012).

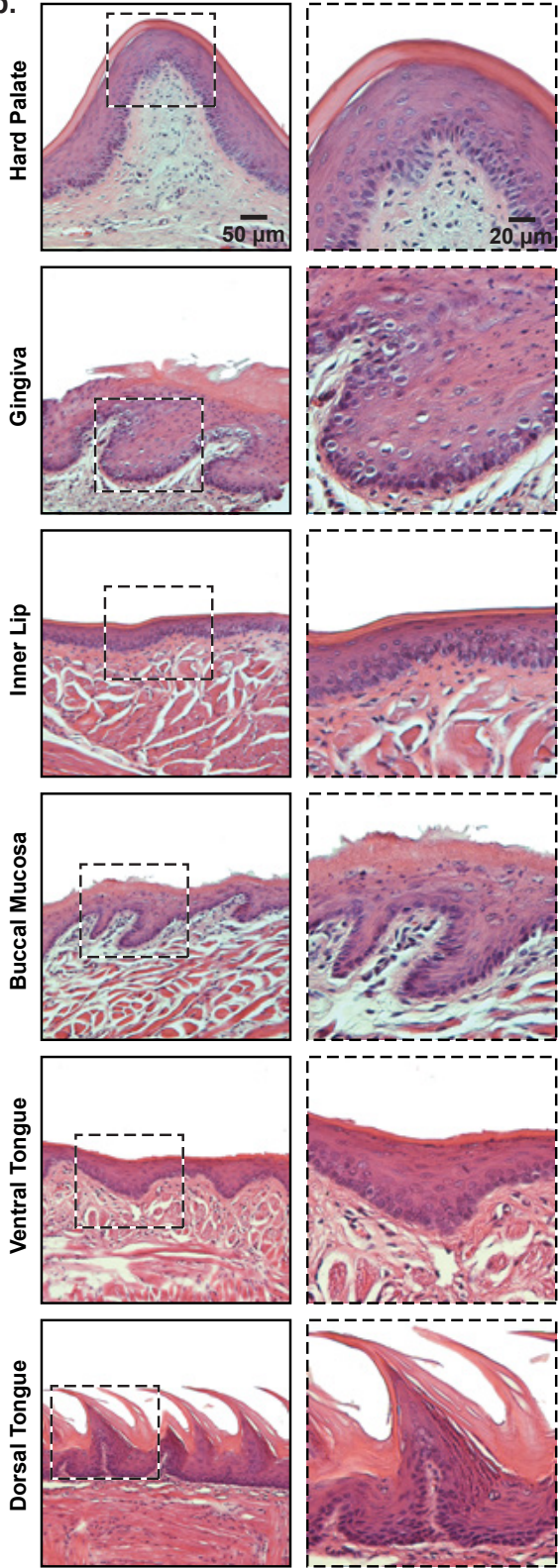
Keratinized oral epithelium and epidermis consist of basal, spinous, granular, and corneal layers within a stratified epithelium (Fig. 1.1a). Non-keratinized oral epithelium is also stratified, but consists of basal, spinous, intermediate, and superficial layers (Squier & Kremer, 2001). Cell divisions in all oral epithelium and epidermis take place exclusively in the basal layer. After dividing, committed cells undergo a differentiation process that leads to the sequential expression of various structural keratin proteins and the loss of intracellular organelles as cells move superficially, begin to flatten, and are eventually sloughed off the surface (Dale, Salonen, & Jones, 1990; Fuchs, 1995; Squier & Kremer, 2001; Winning & Townsend, 2000).

Figure 1.1

a.



b.



**Figure 1.1 Oral mucosa in *Mus musculus*.** (a) Diagram of haematoxylin and eosin (H&E) stained buccal mucosa collected from a 12-week old C57BL/6 female mouse. In this photo the basal, spinous, granular, and cornified layers are all present. Rete ridges and dermal papilla can also be identified. Unlike humans, the buccal mucosa in C57BL/6 mice is keratinized; in general, the location and type of keratinization within the oral cavity differs among mammalian species.(Barrett, Selvarajah, Franey, Wills, & Berkovitz, 1998) (b) 7µm H&E stained sections from intraoral sites. All surfaces of the oral epithelium in C57BL/6 mice, unlike humans, appear to be keratinized. DP, dermal papilla; RR, rete ridge.

## 1.4 METHODS USED TO IDENTIFY AND CHARACTERIZE STEM CELLS

Over the last few decades, several techniques have been utilized to identify stem cells. Significant progress has been made recently through the use of genetically modified mouse models, which have been used to build upon the classical techniques that were initially developed to isolate and study stem cells.

A stem cell has the ability to differentiate into some or all of the cell types required to maintain homeostasis within a particular tissue, organ system, or even an entire organism. The developmental stage at which a stem cell is isolated usually determines what types of cells it can differentiate into. For example, embryonic stem cells isolated from the inner cell mass of the blastocyst are pluripotent and can differentiate into any of the three germ layers (endoderm, mesoderm, and ectoderm). Adult stem cells found in various adult tissues, however, are typically more limited with respect to differentiation and thus are considered multi- or oligopotent (Kolios & Moodley, 2013). Along with the ability to differentiate into different cell types, stem cells are also able to self-renew, a property that ensures their ability to survive and produce the post-mitotic cells necessary for maintenance of tissue homeostasis.

The gold standards for identification of adult stem cells are genetic inducible fate mapping (GIFM) and transplantation (Joyner & Zervas, 2006; Legué & Joyner, 2010; Van Keymeulen & Blanpain, 2012). GIFM involves placing a permanent genetic mark on a putative stem cell *in vivo* (usually by genetically activating a fluorescent or colorimetric reporter) such that the cell will be “labeled” and will pass that label on genetically to all of its progeny, which will pass it on to their progeny, and so on. This technique makes it

possible to measure a cell's ability to both self-renew and to produce the various differentiated cells found in a given tissue. Transplantation assays, in contrast, test the ability of a single cell type to fully reform an entire tissue when isolated and transplanted to another animal/location.

#### **1.4.1 Label Retaining Cells**

Several decades ago, pulse-chase experiments were carried out using tritiated-thymidine ( $^3\text{H-TdR}$ ), a radio-labeled DNA nucleoside that is incorporated into proliferating cells, to determine cell turn-over rates in skin and oral mucosa (Cutright & Bauer, 1967; Potten, 1975). These experiments showed that in addition to highly proliferative cells that quickly lose their  $^3\text{H-TdR}$  label, some cells in the basal layer divided much less frequently and retained the label (label retaining cells, or LRCs). Early  $^3\text{H-TdR}$  studies identified LRCs as long as 240 days post-labeling in mouse palate and buccal mucosa and up to 69 days in hamster tongue (Bickenbach, 1981; Bickenbach & Mackenzie, 1984). More recently, work utilizing 5-bromo-2'-deoxyuridine (BrdU), another labeled DNA nucleoside, showed an increased number of LRCs in the gingiva at 45 days post-labeling compared with the ventral tongue, dorsal tongue, hard palate, buccal mucosa, and alveolar mucosa (Asaka, Akiyama, Kitagawa, & Shimizu, 2009). BrdU was also used to identify LRCs in rat buccal mucosa, tongue, and hard palate. After a 10 week chase, LRCs made up about 3-7% of cells (Y.-L. Huang, Tao, Xia, Li, & Cheng, 2009c). In all of the  $^3\text{H-TdR}$  and BrdU experiments, LRCs were restricted to the basal layer. Additionally, in thicker tissues LRCs were found predominantly at the bases of the rete ridges, whereas in thinner epithelium with few rete ridges (e.g. buccal mucosa), LRCs were found randomly distributed in the basal

layer (Asaka et al., 2009). In the tongue, LRCs were located predominantly at the boundaries of the papillary and interpapillary epithelium near the anterior and posterior columns of the filiform papillae (Bickenbach & Mackenzie, 1984; Hume & Potten, 1976).

One important caveat is that none of these studies determined if the LRCs identified within the oral mucosa were keratinocytes. Melanocytes, Langerhans cells, Merkel cells, and inflammatory cells are all known to reside within the oral mucosa (Winning & Townsend, 2000). Modern immunohistochemical techniques make it possible to co-stain LRCs for other markers that can differentiate between these various cell types, and the results of such studies will be important to obtain. A second caveat to LRC studies in general is that for a cell to incorporate a labeled nucleoside, it must go through DNA synthesis, which can make it difficult to label cells that rarely divide. Although one LRC study reported that nearly 100% of all basal cells in the oral epithelium were labeled after a 10-day continuous administration of BrdU, rare populations of slowly dividing cells may still have been missed (Asaka et al., 2009).

The *K5tTa; tetO-H2B-EGFP* system in mice provides an alternative way to label slowly cycling cells (Tumbar et al., 2004). In this system, all keratin 5 (K5) positive cells express green fluorescent protein (GFP) beginning in embryogenesis. In the adult mouse, all basal layer cells in the oral epithelium and epidermis, including presumptive stem cells, continue to express K5 (Dale et al., 1990). When doxycycline is given to the mice, the cells stop expressing GFP. In rapidly dividing cells, the GFP signal is diluted, while slowly dividing and/or post-mitotic cells remain green. This system has been successfully used in several tissues, including the skin, hair follicle, and tooth (Mascreé et al., 2012; Seidel et al., 2010; Tumbar et al., 2004). Because this method initially

labels all K5-positive cells in the mouse, including those that cycle very slowly, it could provide a more reliable quantification of LRCs in the oral mucosa. Indeed, in Chapter 2 using this system I show that oral basal layer stem/progenitor cells rapidly divide and do not retain any GFP label.

It is important to note that label retention is not necessarily a characteristic of all stem cells. For example, *Lgr6* marks a primitive epidermal stem cell in the central isthmus of the hair follicle that does not retain any BrdU label (Snippert, Haegebarth, et al., 2010a). Additionally, epithelial progenitors in the esophagus do not retain any *H2B-EGFP* label (Doupé et al., 2012).

#### **1.4.2 *In Vitro* Morphology and Clonogenicity**

One of the classical hallmarks of stem cells is their ability to self-renew through proliferation. For this reason, it has been assumed that cells with high *in vitro* growth potential represent stem cells. Several studies have used the *in vitro* morphologic and growth characteristics of isolated cell populations to assay for stemness.

In 1985, Barrandon and Green reported that cell size could predict the ability of human keratinocytes to form clones *in vitro* (Barrandon & Green, 1985). Smaller cells had, on average, greater clonogenicity (i.e. they can more efficiently form clones in culture). In a subsequent study, they found three different clone morphologies: holoclones (*holo* = entire), meroclones (*mero* = partial), and paraclones (*para* = beyond). Holoclones produced round colonies with smooth edges while meroclones produced smaller colonies with irregular edges. Fewer than 5% of the colonies formed by holoclones terminally differentiated, whereas paraclones contained cells with very

limited *in vitro* lifespans. Meroclones had growth potential intermediate to holoclones and paraclones (Barrandon & Green, 1987). Currently, it is generally accepted that holoclones consist primarily of stem cells, meroclones contain slightly more differentiated yet highly proliferative cells called transit-amplifying (TA) cells, and paraclones are comprised of committed, terminally differentiating cells. Several recent studies in the oral mucosa used morphologic and clonogenic characteristics to assert that cells isolated using putative stem cell markers were indeed stem cells (Calenic, Ishkitiev, Yaegaki, Imai, Kumazawa, et al., 2010b; Igarashi et al., 2008; Luo, Okubo, Randell, & Hogan, 2009; Nakamura, Endo, & Kinoshita, 2007).

It should be noted that *in vitro* clonogenic and morphologic experiments mainly provide indirect evidence about stem cell identity. Transplantation assays can be used in conjunction with morphologic observations and clonogenic growth assays to demonstrate that the cells in question are able to fully reform the tissue of interest. Other more advanced *in vivo* techniques to identify and study stem cell behavior (described in greater detail below) are becoming the methods of choice over classical *in vitro* techniques.

### **1.4.3 Stem Cell Markers**

The hematopoietic stem cell (HSC) system is one of the best characterized stem cell systems in humans (Bryder, Rossi, & Weissman, 2006). Numerous cell surface receptors and intracellular proteins have been identified that are differentially expressed between HSCs and their differentiated progeny. This has led not only to an increased understanding of HSC biology, but has also translated into important clinical therapies



(Bryder et al., 2006). In the oral mucosa, some progress has been made in identifying proteins that mark stem cells. Unfortunately, many of the markers identified thus far are also expressed in other basal cells and therefore only allow for the enrichment of stem cells instead of isolation of pure populations.

Many of the initial proteins used to identify and isolate OESCs were first reported as stem cell markers in the hair follicle and interfollicular epidermis (IFE). These include  $\alpha_6$  and  $\beta_1$  integrins (P. H. Jones & Watt, 1993; Kaur & Li, 2000), keratins 15 and 19 (Lyle et al., 1998; Michel et al., 1996), p63 (Pellegrini et al., 2001), and melanoma chondroitin sulphate proteoglycan (MCSP) (Legg, Jensen, Broad, Leigh, & Watt, 2003). Along with other putative stem cell markers such as  $\alpha_6\beta_4$ , oct3/4, CD44H, p75, ATP-binding cassette sub-family G member 2 (ABCG2), and K5, the epidermal markers are indeed expressed by the oral epithelium (Table 1.1) (Calenic, Ishkitiev, Yaegaki, Imai, Costache, et al., 2010a; Calenic, Ishkitiev, Yaegaki, Imai, Kumazawa, et al., 2010b; Luo et al., 2009; Mackenzie, 2005; Nakamura et al., 2007; Sen et al., 2011; Q. Tao et al., 2009; Zhou, Schuetz, & Bunting, 2001).

To test whether the stem cell markers identified in other tissues specifically label OESCs, oral epithelial cells were sorted based on the expression of putative stem cell markers and then studied *in vitro*. One study showed that  $\alpha_6\beta_4^{\text{pos}}$  CD71<sup>neg</sup> gingival keratinocytes not only had a high colony forming efficiency, but also expressed other putative stem cell markers such as p63 and K19. Moreover, these  $\alpha_6\beta_4^{\text{pos}}$  CD71<sup>neg</sup> cells were able to form oral epithelial equivalents (OEE), a fully stratified epithelium

derived from isolated oral epithelial cells that is grown *in vitro* (Calenic, Ishkitiev, Yaegaki, Imai, Costache, et al., 2010a).

Tongue epithelial cells sorted for high levels of K5 and  $\beta$ 1 integrin produced more holoclones in culture than the corresponding epithelial cells expressing lower levels of these markers. These cells could also form OEEs in culture (Luo et al., 2009). A collagen IV matrix was used in another study to enrich for buccal epithelial stem cells. The most adherent cells had the highest colony forming efficiencies *in vitro*. (Igarashi et al., 2008) Finally, cells in the buccal and gingival epithelium expressing high levels of the neurotrophin receptor p75 had greater *in vitro* proliferative capacity, were typically slowly cycling *in vivo*, and could recapitulate OEEs *ex vivo*. These cells were only present in the tips of the dermal papillae and the rete ridges, suggesting that p75 specifically labels OEEs (Nakamura et al., 2007).

Although no *in vitro* system can perfectly mimic the *in vivo* environment, together these studies suggested that the basal layer of the oral epithelium consists of a heterogeneous mixture of cells with varying proliferative capacities. The observation that only certain cells have the ability to form OEEs in culture is probably the most convincing evidence that only a subset of the basal cells are true stem cells. *In vivo* methods, such as GIFM, will be needed to confirm the results of these studies and to allow for the *in vivo* characterization of these cells.

**Table 1.1**

| Candidate OESC Markers in Normal Tissues  | Oral Site(s) Studied                                | Function  | Importance in Stem Cell Biology  |
|---|---|---|--|
| <p><b><math>\beta_1</math> integrin</b> (P. H. Jones &amp; Watt, 1993; Nakamura et al., 2007; Sen et al., 2011)</p>   | <p>Human derived buccal/gingival cultured cells</p> | <p>A component of integrin complexes; binds to molecules expressed by the BM</p>                          | <p>Functionally down regulated in epithelial cells leaving the basal layer that have committed to differentiation; expressed in basal keratinocytes where OESCs reside</p> |
| <p><b><math>\alpha_6\beta_4</math> integrin</b> (Calenic, Ishkitiev, Yaegaki, Imai, Costache, et al., 2010a; Calenic, Ishkitiev, Yaegaki, Imai, Kumazawa, et al., 2010b; Mackenzie, 2005; Watt, 2002)</p> | <p>Human gingiva and hard palate</p>                | <p>Cell adhesion receptor; part of hemidesmosome complex that binds to laminin 5 in BM</p>                | <p>Expressed exclusively on surface of basal keratinocytes where OESCs reside</p>  |
| <p><b>Collagen IV</b> (Igarashi et al., 2008; P. H. Jones &amp; Watt, 1993)</p>   | <p>Rabbit buccal mucosa</p>                         | <p>Found predominantly in BM</p>  | <p>Basal layer stem cells are thought to be more adherent to BM; shown to enrich for keratinocyte stem cells</p>   |
| <p><b>CD44H</b> (Calenic, Ishkitiev, Yaegaki, Imai, Costache, et al., 2010a; Pittenger, 1999)</p>   | <p>Human gingiva</p>                                | <p>Type 1 transmembrane glycoprotein involved in cell-cell interactions, cell adhesion, and migration</p> | <p>Cell adhesion molecule associated with stem cells; used to identify mesenchymal stem cells</p>  |
| <p><b>CD71</b> (Calenic, Ishkitiev, Yaegaki, Imai, Kumazawa, et al., 2010b; Tani, Morris, &amp; Kaur, 2000)</p>   | <p>Human gingiva</p>                                | <p>Transferrin receptor</p>   | <p>Highly expressed in actively cycling cells; expressed at low levels in slower cycling keratinocyte stem cells</p>   |
|   |   |   |  |

| <b>Candidate OESC Markers in Normal Tissues</b>  | <b>Oral Site(s) Studied</b>     | <b>Function</b>  | <b>Importance in Stem Cell Biology</b>   |
|--|---------------------------------|--|--|
| <b>CD117 aka (c-kit)</b><br><b>(not expressed)</b><br>(Calenic, Ishkitiev, Yaegaki, Imai, Costache, et al., 2010a; Okada et al., 1991) | Human gingiva                   | Cytokine stem cell growth factor receptor  | Expressed in hematopoietic stem and progenitor cells   |
| <b>MCSP</b> (Legg et al., 2003; Mackenzie, 2005)   | Human hard palate               | Cell surface proteoglycan involved in spreading, migration, and invasion of melanoma cells | May contribute to stem cell clustering by promoting cell-cell adhesion                             |
| <b>p75</b> (Nakamura et al., 2007; Okumura, Shimada, Imamura, & Yasumoto, 2003; Sen et al., 2011)                                      | Human gingiva and buccal mucosa | Low affinity neurotrophic receptor that binds NGF  | May protect stem cells from apoptosis and affect cell growth                                       |
| <b>Keratin 5</b> (Luo et al., 2009; Tumber et al., 2004)   | Mouse tongue                    | Structural intermediate filament protein expressed by all basal epithelial cells in body   | Expressed in basal keratinocytes where OESCs reside  |
| <b>Keratin 14</b> (Okubo, Clark, & Hogan, 2009; Raimondi, Molinolo, & Gutkind, 2009; Vasioukhin, Degenstein, Wise, & Fuchs, 1999)      | Mouse tongue and buccal mucosa  | Intermediate filament protein  | Expressed in basal keratinocytes where OESCs reside; shown to mark OESCs and epidermal stem cells  |
| <b>Keratin 15</b> (Liu, Lyle, Yang, & Cotsarelis, 2003; Mackenzie, 2005)   | Human hard palate               | Intermediate filament protein  | Expressed in hair follicle bulge stem cells and less differentiated keratinocytes in neonatal mice |
|  |                                 |  |  |

| <b>Candidate OESC Markers in Normal Tissues</b>  | <b>Oral Site(s) Studied</b>                 | <b>Function</b>  | <b>Importance in Stem Cell Biology</b>  |
|--|---|--|---|
| <b>Keratin 19</b> (Calenic, Ishkitiev, Yaegaki, Imai, Costache, et al., 2010a; Mackenzie, 2005; Michel et al., 1996)                                       | Human gingiva and hard palate               | Intermediate filament protein; smallest acidic keratin                       | Expressed in glabrous (non-hairy) skin stem cells   |
| <b>Nestin</b><br><b>(not expressed)</b><br>(Calenic, Ishkitiev, Yaegaki, Imai, Costache, et al., 2010a; Zimmerman et al., 1994)                            | Human gingiva                               | Class VI intermediate filament   | Expressed in developing neuroepithelial stem cells  |
| <b>p63</b> (Calenic, Ishkitiev, Yaegaki, Imai, Costache, et al., 2010a; Pellegrini et al., 2001; Sen et al., 2011; Q. Tao et al., 2009)                    | Human gingiva and buccal mucosa; rat palate | Transcription factor involved in morphogenesis, esp. in stratified epithelia | Expressed in epidermal stem cells   |
| <b>Oct 3/4</b> (Calenic, Ishkitiev, Yaegaki, Imai, Costache, et al., 2010a; Niwa, Miyazaki, & Smith, 2000)   | Human gingiva                               | Homeodomain transcription factor   | Oct 3/4 levels influence self-renewal of embryonic stem cells   |
| <b>Nanog</b><br><b>(not expressed)</b><br>(Calenic, Ishkitiev, Yaegaki, Imai, Costache, et al., 2010a; I. Chambers et al., 2003; M. Nakagawa et al., 2007) | Human gingiva                               | Homeodomain transcription factor   | One of the critical transcription factors needed for self-renewal in embryonic stem cells and iPS cells |
|  |   |  |   |

| Candidate OESC Markers in Normal Tissues                                    | Oral Site(s) Studied                | Function   | Importance in Stem Cell Biology   |
|---|-------------------------------------|--|---|
| <b>Sox2</b> (Arnold et al., 2011; Okubo et al., 2009)                       | Mouse tongue                        | Transcription factor containing high mobility group (HMG) domains  | Maintains self-renewal in embryonic stem cells; expressed in several adult stem cells |
| <b>ABCG2</b> (Ding, Wu, & Jiang, 2010; Sen et al., 2011; Zhou et al., 2001) | Human derived buccal cultured cells | Transporter that can pump a wide variety of compounds out of cells | Expressed by stem cells from several different tissues                                |

Basement membrane (BM), nerve growth factor (NGF), induced pluripotent stem cells (iPS)

#### 1.4.4 *In Vivo* Lineage Tracing

The *Cre-ER-loxP* system in mice is the principle type of GIFM used for lineage tracing, and it has significantly increased our understanding of the identity and behaviors of stem cells in numerous tissues such as the epidermis (Fig. 1.2) (Doupé et al., 2012; Seidel et al., 2010; Snippert, van der Flier, et al., 2010b; Tian et al., 2011). Use of this system has enabled researchers to specifically label cells that express a gene of interest to determine if that gene is a bona fide stem cell marker. Although cell surface markers have been used in the past to isolate and then grow putative stem cells *in vitro*, *in vivo* labeling and lineage tracing allows cells to be studied in their native environments and avoids the artificial nature of *in vitro* culture systems. Several epidermal stem cell markers have been identified in this way, including *Lgr5*, *Lgr6*, *Blimp1*, *Lrig1*, *Sox2*, and *Bmi1* (Arnold et al., 2011; Horsley et al., 2006; Jaks et al., 2008; K. B. Jensen et al., 2009; Snippert, Haegebarth, et al., 2010a; Tian et al., 2011).

To date, few studies have utilized *in vivo* lineage tracing to study adult OESCs. In one study that utilized a *K14-CreER; Rosa26-LSL-LacZ* mouse model, columns of labeled blue cells could be found on the dorsal tongue and in the buccal mucosa after a one month chase (Raimondi et al., 2009). A subsequent study used the same mouse model and provided evidence that *K14<sup>+</sup> Trp63<sup>+</sup> Sox2<sup>+</sup> K5<sup>+</sup>* cells adjacent to the taste bud represent progenitor cells that generated both taste bud receptor cells and keratinized pore cells. These researchers also posited that *K14<sup>+</sup> Trp63<sup>+</sup> Sox2<sup>low</sup> K5<sup>+</sup>* cells represent the long term progenitor cells of the filiform papillae and are located in the basal cell layer (Okubo et al., 2009). Finally, a *Sox2-Cre-ER; Rosa26-LSL-EYFP* mouse model showed that *Sox2* is expressed by basal layer stem cells for at least 10

months after labeling in the dorsal tongue (Arnold et al., 2011). Numerous Cre-ER mouse constructs are currently available for several genes shown to mark stem cell populations in other epithelial tissues such as the hair follicle, IFE, and intestinal crypt. Using these mouse models will enable the identification and characterization of novel OESCs.



Figure 1.2

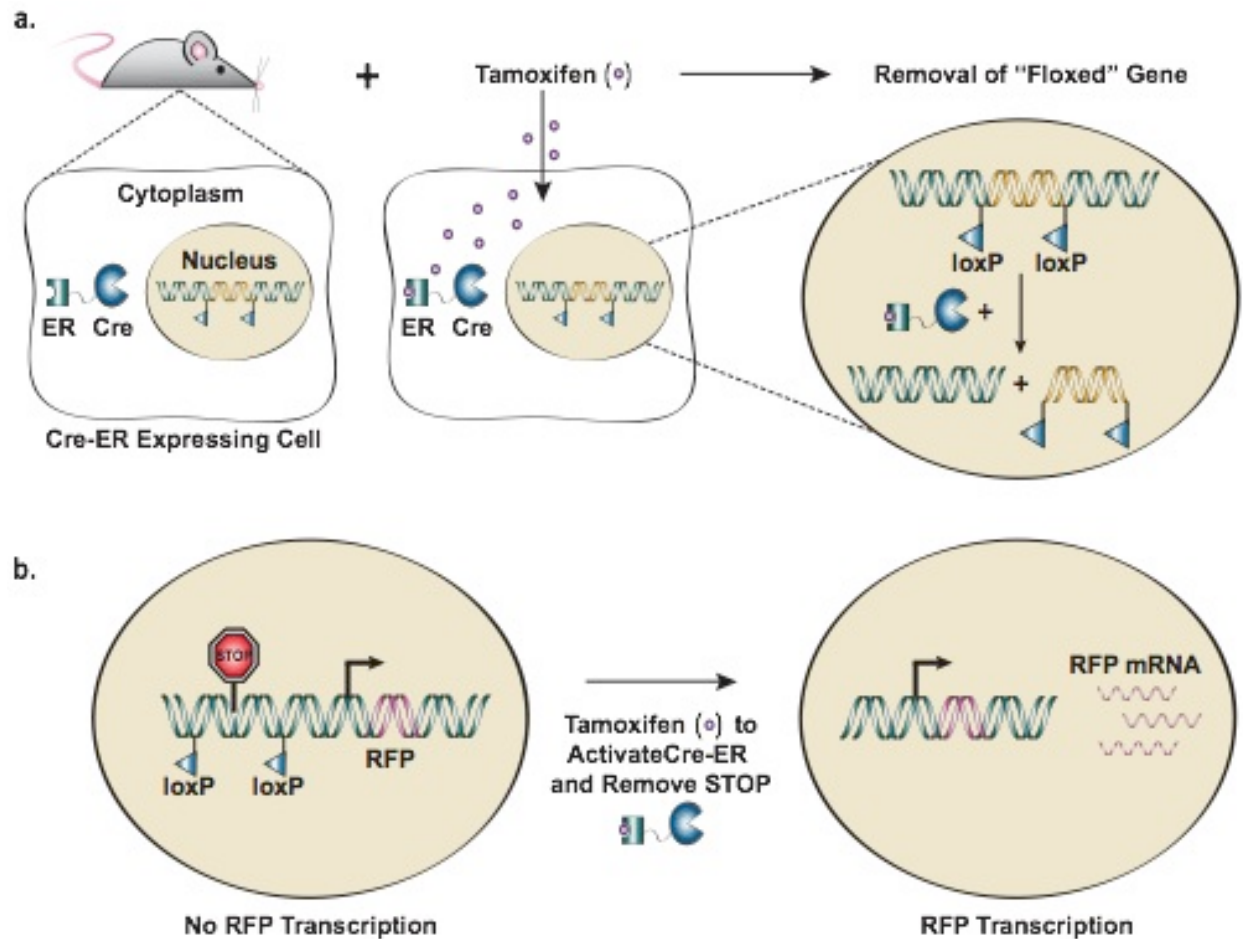


**Figure 1.2 CRE recombinase technology.** The CRE recombinase enzyme was identified in the P1 bacteriophage, where it recognizes and recombines 34 base-pair DNA sequences called *loxP* sites (Hoess, Ziese, & Sternberg, 1982; Sternberg & Hamilton, 1981). *LoxP* sites consist of two 13 base-pair palindromic DNA sequences separated by an 8 base spacer region. When two *loxP* sites are oriented in the same direction on a strand of DNA, the CRE recombinase can recombine them such that the intervening DNA will be removed from the genome. Transgenic mice have been developed that harbor genes flanked by *loxP* sites ("floxed" genes). When bred with mice that express a tissue specific CRE recombinase (i.e. a CRE whose expression is controlled by a specific promoter that is only active in a particular tissue), floxed gene expression can be completely abrogated in very specific cell populations.

Recently, newer mouse models have been created that allow for temporal control of *Cre* expression. CRE recombinases fused to mutant estrogen receptors (ER) have been developed that no longer bind endogenous estrogens at physiologic levels, but instead are only activated by binding tamoxifen or its active metabolite 4-Hydroxy-Tamoxifen (Vasioukhin et al., 1999). In the absence of tamoxifen, the *Cre-ER* construct is sequestered in the cytoplasm (**a**). When tamoxifen binds the ER domain of the fusion protein, the CRE recombinase translocates to the nucleus, where it removes floxed genes from the genome. Some transgenic fluorescent reporters are constructed such that they are inhibited from being transcribed by floxed transcriptional STOP elements (aka lox-stop-lox or LSL elements). When the *Cre-ER* construct is activated and enters the nucleus, it can remove this STOP sequence, which will allow the fluorescent reporter to be expressed, which in this example is red fluorescent protein (RFP) (**b**).

## **1.5 EMERGING PARADIGMS**

Widely accepted hypotheses regarding basic epithelial stem cell biology over the last 30 years have recently been revisited as more sophisticated tools and mathematical modeling have become available. This has led to the emergence of new paradigms for stem cell biology, as discussed below.

### **1.5.1 The Epidermal Proliferative Unit Model**

In 1974, Potten proposed the epidermal proliferative unit (EPU) hypothesis to describe the organization of cells in the epidermis (Potten, 1974). Based on  $^3\text{H}$ -TdR data and morphological evidence, the EPU model hypothesizes that groups of approximately 11 cells in the basal layer of the skin are responsible for the production of discrete, hexagonal columns of terminally differentiating cells (Potten, 1974). Additionally, the  $^3\text{H}$ -TdR labeling studies suggested that a central, slowly dividing stem cell within each EPU gave rise to peripheral, more rapidly dividing TA cells (Hume & Potten, 1979). Supporting this hypothesis, labeling of cells in the epidermis with retroviruses or mutagens resulted in labeled columns of cells emanating from the basal layer all the way to the cornified layer (Ghazizadeh & Taichman, 2001; Mackenzie, 1997; S. Ro & Rannala, 2004; 2005).

The EPU hypothesis proposes that when stem cells within the basal layer of the epidermis divide, they do so asymmetrically and give rise to a stem cell and a TA cell (Fig. 1.3a-d) (Potten, 1974). In this model, TA cells are thought to be responsible for the majority of cell divisions within the epidermis. The TA cells give rise to both additional TA cells as well as to the post-mitotic differentiated cells within the epithelium. After

multiple divisions, TA cells senesce and terminally differentiate. In this way, it is thought that stem cells protect themselves from the accumulation of random mutations that would otherwise be incurred via multiple rounds of DNA replication, thus ensuring long-term integrity of the epidermis. The EPU hypothesis is now known more broadly as the invariant asymmetry model. Since the stem cell in this model always retains its “stemness” with each division while its daughter does not (i.e. the daughter becomes a TA cell), these divisions are considered invariant and asymmetric. The model implies that there is a hierarchy of cells within the basal layer that creates a heterogeneous mixture of stem cells, TA cells, and differentiated cells.

### **1.5.2 The Neutral Drift Model**

Several studies within the last few years have called into question the invariant asymmetry hypothesis; these have used the mouse testes, epidermis, intestinal crypt, and esophagus as model systems. These studies provide strong evidence that stem cells in these tissues follow cycling dynamics best explained by the population asymmetry model, also known as the neutral drift model (Fig. 1.3e-h) (Clayton et al., 2007; Doupé et al., 2012; Doupé, Klein, Simons, & Jones, 2010; A. M. Klein, Nakagawa, Ichikawa, Yoshida, & Simons, 2010; Snippert, van der Flier, et al., 2010b). Using an *Ah-Cre-ER; Rosa26-LSL-EYFP* mouse, investigators found that the distribution of labeled basal cells in distinct clones exhibited the characteristic scaling behavior predicted by the neutral drift model (reviewed in A. M. Klein & Simons, 2011). This model posits that all basal layer cells in the epidermis are equipotent stem cells that can divide randomly in 1 of 3 ways: into 2 stem cells, into a stem cell and a cell marked for differentiation, or into 2 cells marked for differentiation (Fig. 1.3e). Although

this process is stochastic, each basal cell has the potential to remain a stem cell or to terminally differentiate. Thus, at the individual cell level, stem cells can divide symmetrically; however, at the population level, these divisions are asymmetric in that they are balanced such that homeostasis is maintained within the tissue. How this balance is maintained is not yet clear.

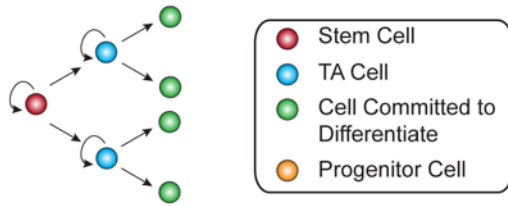
To follow up on these experiments, two mouse models (*K14-Cre-ER; Rosa26-LSL-YFP* and *Inv-Cre-ER; Rosa26-LSL-YFP*) were employed for similar lineage tracing and clonal analyses in the IFE as those described above. The authors used a wounding assay to determine whether either of these cell populations contributed differently to wound healing. Whereas *K14-Cre-ER* labeled long-lived, slowly cycling stem cells that contributed greatly to healing, *Inv-Cre-ER* targeted a more differentiated progenitor cell population that did not respond to tissue damage in the same way. In this case, progenitor cells did not have the same proliferative and/or differentiation potential as stem cells, but they could still give rise to differentiated progeny under normal homeostatic conditions. Interestingly, although the *K14-Cre-ER* labeled cells exhibited more canonical stem cell characteristics than the *Inv-Cre-ER* cells, both populations followed neutral drift dynamics (Mascré et al., 2012). Thus, even though stochastic processes seem to govern stem cell fates in the IFE, a stem cell hierarchy also appears to be present. This differs from the initial hypothesis that all basal layer cells in the IFE behave as equipotent stem cells.

Clonal analysis has not yet been used in the oral epithelium to determine whether basal layer stem cell division follows the invariant asymmetry or neutral drift models. It is unclear whether OESCs behave similarly to the IFE, since both of these

tissues are ectodermally derived, or if perhaps OESCs behave more like the endodermally derived esophageal epithelium. Unlike the IFE, there are no epithelial LRCs present in the esophagus (Doupé et al., 2012). Understanding how homeostasis in the oral epithelium is maintained as well as how it responds to perturbations, such as tissue damage, will be important for understanding how to prevent and treat oral hyper/hypoproliferative diseases and conditions. Since few lineage-tracing experiments have been performed in the oral mucosa to identify genes that label stem or progenitor cells, for now it is difficult to conduct clonal analyses to study stem cell division dynamics. Further research will be needed to identify specific genes that label stem and/or progenitor cells in the oral epithelium so that comprehensive clonal analyses may be carried out.

**Figure 1.3**

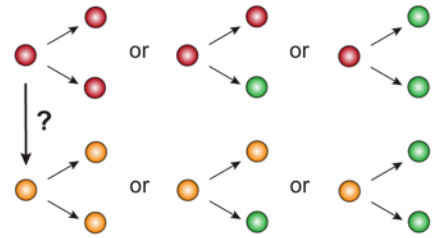
**a** Invariant Asymmetry Model



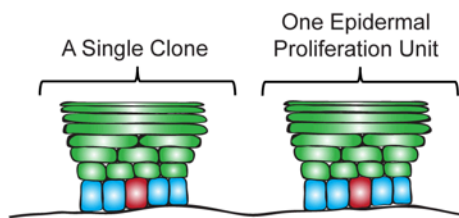
**e** Neutral Drift Model With A Single Stem Cell



Neutral Drift Model With Stem and Progenitor Cells

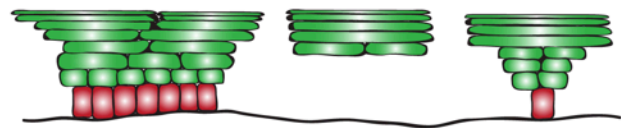


**b**



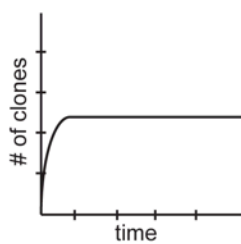
- Only one stem cell per clone
- The number of labeled clones will remain constant with time (**Fig. 1c**)
- All clones will have the same maximum number of labeled basal cells over time (**Fig. 1d**)

**f**

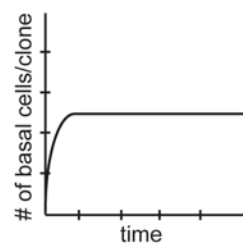


- Variable number of stem/progenitor cells per clone
- The number of labeled clones will decrease over time (**Fig. 1g**)
- The number of labeled basal cells in surviving clones will increase linearly with time (**Fig. 1h**)

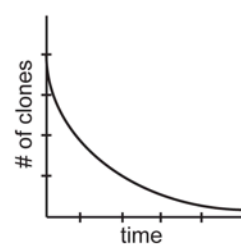
**c**



**d**



**g**



**h**

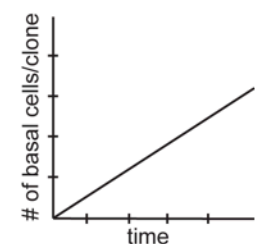


**Figure 1.3 The invariant asymmetry and neutral drift models. (a)** The invariant asymmetry model in the interfollicular epidermis proposes that a self-renewing stem cell gives rise to transit amplifying cells, which then give rise to differentiating keratinocytes in discrete cellular territories called epidermal proliferation units. If stem cells in this model are labeled using genetic inducible fate mapping (GIFM), then the overall number of clones (groups of labeled cells; **(b)**) along with the number of basal cells per

clone would be expected to reach a maximum size over time **(c, d)**. **(e)** In the neutral drift model one or more stem/progenitor cell populations may be present and cell division results in one of three outcomes: two additional stem/progenitor cells, a stem/progenitor cell and a differentiating keratinocyte, or two differentiating keratinocytes. These divisions occur in a stochastic (random) manner, and thus if these stem/progenitor cells are labeled using GIFM, then clones of various sizes will result **(f)**. However, with time, the overall number of clones will decrease due to random chance whereas the number of basal cells in surviving clones will increase linearly with time **(g, h)**. Figure modified from Klein et al. (A. M. Klein & Simons, 2011)



## 1.6 STEM CELLS IN ORAL DISEASE

The role that stem cells play in oral disease is of much interest. Most of the work to date has focused on identifying cancer stem cells (CSC) in pre-malignant oral lesions and oral squamous cell carcinomas (OSCC). Although somewhat controversial (Rosen & Jordan, 2009), CSCs are thought to make up variable portions of solid tumors, are believed to be responsible for maintaining a tumor's growth, and have been shown to be more resistant to radio- and chemotherapies than more differentiated cells within the tumor (reviewed in Bhaijee, Pepper, Pitman, & Bell, 2012; Mannelli & Gallo, 2012; Visvader & Lindeman, 2008). For these reasons, some have attributed tumor recurrence and metastasis to surviving CSC clones (D. Chen et al., 2017; Visvader & Lindeman, 2008). Because many head and neck cancers are resistant to standard radio- and chemotherapies, identifying CSCs and then creating therapies that specifically eliminate them could lead to significantly improved outcomes for patients.

CSCs are defined by their ability to form secondary tumors when isolated from a primary tumor and xenografted to immunocompromised mice. CSCs can then be re-isolated from the secondary tumor and serially transplanted to other immunocompromised mice (Visvader & Lindeman, 2008). Like normal stem cells, CSCs are able to self-renew and differentiate into various cell types; however, due to deleterious mutations, they give rise to tumors instead of normal tissues. Markers such as CD44, CD133, and aldehyde dehydrogenase (ALDH) have been found to mark OSCC cells that can be serially transplanted and reproduce differentiated, heterogeneous tumors in immunocompromised mice (Clay et al., 2010; Prince et al., 2007; Q. Zhang et al., 2010).

Some of the same markers used to identify OESCs have also been used to identify and/or better characterize CSCs in pre-neoplastic lesions and OSCC. Putative OESC markers such as  $\alpha\beta6$ , CD44, Oct-4, Nanog, CD117, ABCG2, and CK19 have all been reported to be expressed at higher levels in putative CSC populations compared to non-transformed cells (Chiou et al., 2008; Dang & Ramos, 2009; Yanamoto et al., 2011; P. Zhang, Zhang, Mao, Zhang, & Chen, 2009a). One study showed that the labeling index of p75 was similar among normal and oral leukoplakia samples, whereas increased p75 expression correlated with a worse OSCC tumor grade (Kiyosue et al., 2011). Another group showed that K15 was down-regulated in oral lichen planus while  $\alpha6$ -integrin,  $\beta1$ -integrin, and MCSP were upregulated in both oral lichen planus and hyperkeratotic oral lesions (Köse, Lalli, Kutulola, Odell, & Waseem, 2007). Others also reported that oral dysplasias had decreased expression of p63 (Takeda et al., 2006). Additionally, several studies have attempted to correlate putative CSC markers with patient prognosis and survival, showing that tumors expressing higher levels of certain CSC markers tend to have poorer outcomes (D. Chen et al., 2017; Chiou et al., 2008; Du et al., 2011; Häyry et al., 2010; Kiyosue et al., 2011; Ravindran & Devaraj, 2012; Tsai, Yu, Chang, Yu, & Chou, 2011). One caveat is that unless serial transplantation assays have shown that the stem cell markers being studied actually label CSCs, it is difficult to draw firm conclusions about the identity and function of positively staining cells within OSCCs. This is true even for stem cell markers that have already been shown to label normal OESCs, since these cells may not perform similar functions within tumors.

Key questions remain to be answered in order to better understand the relationship between OESCs and oral disease. First, identification of *bona fide* OESC markers is paramount. If specific markers can be identified, then the role of OESCs in various oral disease states can be directly studied using *in vivo* models. Second, elucidating the stem cell hierarchy and cycling dynamics of OESCs will enable a better understanding of how these processes change during disease, which could aid in the development of therapies that correct these changes. It is possible that many hyperproliferative disorders (e.g. leukoplakia, erythroleukoplakia, OSCC) as well as hypoproliferative conditions (e.g. oral mucositis due to radio-/chemotherapies) are directly caused by pathologic changes in OESCs. Given that the oral mucosa communicates directly with the external environment and is easily accessible, it is conceivable that treatments could be developed that specifically target OESCs *in situ*. A basic understanding of normal OESC biology will be needed to fully appreciate the role that stem cells play in oral disease.

## **1.7 CONCLUSION**

Some progress has been made in identifying and characterizing OESCs, but significant questions remain: are there specific genetic markers that are only expressed by OESCs? Do OESCs follow the invariant asymmetry or neutral drift model? Does a stem cell niche exist in the oral epithelium? If so, what are its effects on OESCs and what are the molecular signals that drive these effects? What role do OESCs play in oral disease? The technical and methodological advances that are now available and presented in this dissertation will help to answer these and other questions related to

stem cell biology. A clearer understanding of OESC biology will hopefully lead to novel therapies for oral diseases that will significantly improve patients' lives.

## CHAPTER 2

### Hierarchy and Fate of Progenitor Cells in the Oral Epithelium

In this chapter, I use multiple methods to identify oral epithelial stem cells as well as to study their organization and cell division kinetics, which confirm that the oral mucosa is one of the most rapidly dividing tissues within the body. I also investigate the response of oral epithelial progenitor cells to chemotherapy-induced damage, yielding possible insights into the pathophysiology of oral mucositis, a common side-effect of this type of therapy. Finally, I perform a single cell analysis of oral epithelial basal layer cells via single cell RNA-sequencing to show that the basal layer is comprised of broadly distributed oral epithelial progenitor cells along with keratinocytes fated for differentiation at various stages of maturation. These results challenge previous reports regarding oral mucosal stem cell biology and instead align with existing stem cell paradigms in the interfollicular epidermis and other epithelial tissues.

Kyle B. Jones<sup>1</sup>, Sachiko Furukawa<sup>1,2\*</sup>, Hongfang Ma<sup>1,3\*</sup>, Pauline Marangoni<sup>1</sup>, Henry Pinkard<sup>4,5,6</sup>, Rebecca D'Urso<sup>1</sup>, Allon M. Klein<sup>7</sup>, and Ophir D. Klein<sup>1,8\*\*</sup>

<sup>1</sup>Program in Craniofacial Biology and Department of Orofacial Sciences, University of California, San Francisco, San Francisco, CA, USA

<sup>2</sup>Section of Oral and Maxillofacial Oncology, Division of Maxillofacial Diagnostic and Surgical Sciences, Faculty of Dental Science, Kyushu University, Fukuoka, Japan

<sup>3</sup>Department of Plastic and Reconstructive Surgery, Sir Run Run Shaw Hospital, Zhejiang University School of Medicine, China

<sup>4</sup>Department of Pathology, University of California, San Francisco, San Francisco, CA, USA

<sup>5</sup>Biological Imaging Development Center, University of California, San Francisco, San Francisco, CA, USA

<sup>6</sup>Computational Biology Graduate Group, University of California, San Francisco, San Francisco, CA USA

<sup>7</sup>Department of Systems Biology, Harvard Medical School, Boston, MA, USA

<sup>8</sup>Department of Pediatrics and Institute for Human Genetics, University of California, San Francisco, San Francisco, CA, USA

\* Equal contribution

## 2.1 ABSTRACT

The oral mucosa is one of the most rapidly dividing tissues in the body and serves as a barrier to repeated physical and chemical insults from mastication, food, and bacteria (K. B. Jones & Klein, 2013). Breakdown of this barrier due to disease or trauma such as radio or chemotherapy can lead to significant morbidity and potentially life-threatening infections for patients (Cinausero et al., 2017; Lalla, Sonis, & Peterson, 2008). Determining the identity and organization of oral epithelial progenitor cells (OEPCs) is therefore paramount to understanding their roles in tissue homeostasis and in diseases such as oral squamous cell carcinoma. Here, we show via lineage tracing and label retention experiments that rapidly-dividing OEPCs, which are labeled by *Bmi1*, are located broadly within the basal layer of the mucosa in diverse regions of the oral cavity. Through quantitative clonal analysis, we demonstrate that OEPCs undergo population asymmetrical divisions following neutral drift dynamics and that they respond to chemotherapy-induced damage by altering their daughter cell fates. Finally, using a single cell RNAseq strategy, we establish a lineage hierarchy and propose a model that defines the organization of OEPCs within the basal layer.

## 2.2 INTRODUCTION

For several decades, the epidermal proliferative unit (EPU) hypothesis, also known as the invariant asymmetry model, was used to describe the organization of stem cells within the epidermis and oral mucosa (Potten, 1974). In this model, single stem cells within the basal layer divide slowly and asymmetrically, always resulting in a stem cell and a daughter transit amplifying (TA) cell, which remain closely associated with one another and are organized in stem cell/TA territories, or progenitor units (Ghazizadeh & Taichman, 2001; Hume & Potten, 1979; Mackenzie, 1997; S. Ro & Rannala, 2004; 2005). More recently, studies in several epithelial tissues such as the epidermis and esophagus support an alternative called the population asymmetry model, in which basal layer keratinocytes comprise a pool of equipotent, actively dividing stem cells that, following mitosis, give rise to varying combinations of stem and differentiated cell progeny in proportions necessary to maintain tissue homeostasis (Fig. S1a,b) (Clayton et al., 2007; Doupé et al., 2010; 2012; A. M. Klein et al., 2010; A. M. Klein & Simons, 2011; Snippert, van der Flier, et al., 2010b). Although work in the tongue epithelium supported the invariant asymmetry stem cell model, based in part on the presence of solitary stem cells expressing high levels of *Bmi1* within the dorsal tongue epithelium (Tanaka et al., 2013), quantitative clonal analysis to confirm this finding has not yet been performed. In this study, we sought to identify and characterize OEPCs in all oral mucosal sites, determine how OEPCs are organized, and resolve which model – invariant asymmetry or population asymmetry – best explains their division kinetics and clonal growth patterns.



## 2.3 MATERIALS AND METHODS

### 2.3.1 Mouse Genotypes

Mice were housed in accordance with University of California San Francisco Institutional Animal Care and Use Committee (IACUC) guidelines. The following mouse lines were obtained from The Jackson Laboratory: *Bmi1*<sup>tm1(cre/ESR1)Mrc</sup> (referred to as *Bmi1*<sup>CreER</sup>), *Sox2*<sup>tm1(cre/ERT2)Hoch</sup> (referred to as *Sox2*<sup>CreER</sup>), *Gli1*<sup>tm3(cre/ERT2)Alj</sup> (referred to as *Gli1*<sup>CreER</sup>), *Lrig1*<sup>tm1.1(cre/ERT2)Rjc</sup> (referred to as *Lrig1*<sup>CreER</sup>), *Tg(KRT14-cre/ERT)20Efu* (referred to as *K14*<sup>CreER</sup>), *Gt(ROSA)26Sor*<sup>tm14(CAG-tdTomato)Hze</sup> (referred to as *R26*<sup>tdTomato</sup>), and *Tg(tetO-HIST1H2BJ/GFP)47Efu* (referred to as *H2B*<sup>GFP</sup>). *Tg(KRT5-tTA)1216Glk/Nci* mice (referred to as *K5*<sup>tTa</sup>) were obtained from the National Cancer Institute Mouse Repository. Homozygous *Bmi1*<sup>CreER</sup>, *Sox2*<sup>CreER</sup>, *Gli1*<sup>CreER</sup>, *Lrig1*<sup>CreER</sup>, and *K14*<sup>CreER</sup> mice were crossed with homozygous *R26*<sup>tdTomato</sup> mice to generate heterozygotes for each allele, which were then used for lineage tracing and clonal analysis experiments. *K5*<sup>tTa</sup> heterozygous mice were crossed with *H2B*<sup>GFP</sup> heterozygous mice to generate *K5*<sup>tTa</sup>; *H2B*<sup>GFP</sup> heterozygotes, which were used in label retaining experiments.

### 2.3.2 In-Situ Hybridization

RNAscope 2.0 and 2.5 HD Red (ACD, 310036, 322350) and RNAscope 2.5 HD Duplex (ACD, 322430) detection kits were used following the manufacturer's instructions. 2-3 month old C57BL/6 male and female mice (n=6 mice, repeated 3 times) were euthanized and their oral mucosa/tongue tissues removed and placed into 10% neutral buffered formalin solution at room temperature for ~20 hours. Tissues were then washed 3x5 minutes in phosphate buffered saline (PBS), submitted for paraffin

processing, and embedded in paraffin blocks. 5µm sections were used for all experiments. Sections were boiled in the target retrieval solution at ~100°C for 15 minutes and incubated in the protease plus solution at 40°C for 15 minutes. *Bmi1*, *K14*, and *Krt14* probes specific for *Mus musculus* were purchased from ACD. DapB (purchased from ACD) was used as a negative control along with appropriate positive controls in each experiment. Negative controls consistently showed little to no background staining. RNA in-situ hybridization was performed in 2-3 month old C57BL/6 male and female mice (n=3 mice, repeated 3 times) using an anti-Sox2 digoxigenin-labeled probe on frozen tissue sections using standard protocols.

### 2.3.3 Lineage Tracing

Adult male and female mice (n≥2 for each time point) greater than 2 months old were given a single intraperitoneal injection of tamoxifen or corn oil (for negative controls) and then euthanized at various times post-treatment (see main text for exact chase time points). Mice were dosed as follows:

| <b>Genotype</b>  | <b>Tamoxifen Dose Range</b> |
|--|-----------------------------|
| <i>Bmi1</i> <sup>CreER</sup> ; <i>R26</i> <sup>tdTomato</sup>  | 1-5mg/25g                   |
| <i>Gli1</i> <sup>CreER</sup> ; <i>R26</i> <sup>tdTomato</sup>  | 3mg/25g                     |
| <i>Lrig1</i> <sup>CreER</sup> ; <i>R26</i> <sup>tdTomato</sup> | 3mg/25g                     |
| <i>Sox2</i> <sup>CreER</sup> ; <i>R26</i> <sup>tdTomato</sup>  | 0.3-1mg/25g                 |
| <i>K14</i> <sup>CreER</sup> ; <i>R26</i> <sup>tdTomato</sup>   | 0.04mg/25g                  |

Following euthanization, each mouse was perfused with cold 4% paraformaldehyde (PFA) dissolved in PBS. Oral mucosa, tongue, and skin were then removed and incubated in 4% PBS at 4°C on a shaker for about 2-3 hours. The tissues were then washed 3x5 minutes in PBS and incubated overnight in a 30% (w/v) sucrose-PBS solution at 4°C. The following day, the tissues were embedded and frozen in optimal cutting temperature (OCT) medium.

### **2.3.4 Immunofluorescence (Cryosections)**

7µm cryosections were cut and air dried onto glass slides, washed 3x5 minutes in PBS with 0.1% (v/v) Tween 20 (PBS-T) to remove residual OCT medium, blocked in an animal-free blocking solution (Vector Laboratories, SP-5030) for 1 hour at room temperature, incubated overnight at 4°C with a primary antibody, washed 3x10 minutes with PBS-T, incubated with a secondary antibody at room temperature for one hour, washed 2x5 minutes with PBS, stained with 4,6-diamidino-2-phenylindole (DAPI) dissolved in PBS for 30 minutes at room temperature (5µg/mL, Sigma, D9564-10MG), washed with PBS, mounted with Vectashield Antifade Mounting Medium (Vector Laboratories, H-1000), and sealed with clear nail polish.

### **2.3.5 BrdU Pulse-Chase Experiment**

3 month old wildtype C57BL/6 male and female mice (n≥2 for each time point) were given an intraperitoneal injection of 1mg of 5-bromo-2'-deoxyuridine (BrdU) dissolved in PBS and then euthanized at various time points post-treatment (see main text for exact chase time points). After being euthanized, each mouse was perfused with cold 4% PFA dissolved in PBS. The oral mucosa and tongue were then removed and

incubated in 4% PFA overnight at 4°C. The next day, the tissues were washed 3x5 minutes in PBS, submitted for paraffin processing, and then embedded in paraffin blocks. 5µm sections were used for the subsequent BrdU immunohistochemistry experiments following standard protocols. Briefly, slides were deparaffinized, an antigen retrieval step was performed using a citrate buffer (Vector Unmasking Solution, Vector Laboratories, H-3300) in a pressure cooker for 15 minutes, washed 4x5 minutes in distilled water, washed in PBS for 5 minutes, incubated in 3% (v/v) hydrogen peroxide diluted in PBS for 30 minutes at room temperature, washed in PBS for 5 minutes, incubated in 0.2N hydrochloric acid for 45 minutes at 37°C, washed again in PBS for 5 minutes, washed for 5 minutes in PBS-T, blocked in blocking buffer (5% bovine serum albumin, 5% bovine serum, 0.1% Triton-X dissolved in PBS) for 1 hour at room temperature, incubated with an anti-BrdU primary antibody overnight at 4°C, washed 3x10 minutes in PBS-T, incubated with a biotinylated rabbit anti-rat secondary antibody at room temperature, and washed 3x10 minutes in PBS. The Vectastain Elite ABC HRP Kit (Vector Laboratories, PK-6100) was used to develop the slides following the manufacturer's protocol. Appropriate positive and negative controls were run during each experiment.

### **2.3.6 Whole-Mount Immunofluorescence**

Mice were euthanized and the buccal mucosa and tongue quickly removed, rinsed in PBS without magnesium or calcium, and placed in a pre-warmed (37°C) solution of 20mM ethylenediaminetetraacetic acid (EDTA) dissolved in PBS without magnesium or calcium. The buccal mucosa was incubated for 2 hours and the tongue for 4 hours at 37°C. Following incubation, the epithelium was peeled and separated

from the underlying connective tissue, rinsed in PBS, fixed for one hour at room temperature or overnight at 4°C in 4% PFA, washed 3x5 minutes in PBS, and stored in PBS with 0.02% sodium azide at 4°C. For immunofluorescence staining, the separated epithelial sheets were incubated in whole-mount blocking/permeabilization buffer (1% bovine serum albumin, 5% horse serum, 0.8% Triton-X) for 1-3 hours at room temperature, incubated with a primary antibody diluted in the blocking buffer overnight at 4°C, washed 3x15 minutes in PBS-T, incubated with a secondary antibody for one hour at room temperature or overnight at 4°C, washed 2x15 minutes in PBS-T, stained with DAPI dissolved in PBS for 30 minutes at room temperature, washed 2x5 minutes in PBS, and mounted basal layer side up (i.e. touching the coverslip) onto a glass slide using Vectashield Antifade Mounting Medium (Vector Laboratories, H-1000), and sealed with clear nail polish. Multiple sections of tissue from each mouse described in the main text/methods were used in each staining experiment.

### **2.3.7 KI-67 Quantification**

10 week old male and female C57BL/6 mice (n=5 mice, 6123 cells) referred to as “young mice” in main text) were used to quantify the percentage of Ki-67 positive basal layer keratinocytes in the buccal mucosal epithelium for the experiments described in Fig. 2. 18-19 month old male *Bmi1<sup>CreER</sup>;R26<sup>tdTomato</sup>* mice (n=3 mice, 5154 cells) referred to as “old mice” in the main text) were used to quantify the percentage of Ki-67 positive basal layer keratinocytes in the buccal mucosal epithelium for the experiments described in Fig. 3. In both instances, separated epithelial sheets were stained for CD45 and Ki-67 and mounted as already described. In order to accurately count the number of keratinocytes present, CD45 (expressed on all mature hematopoietic cells except for

mature erythrocytes), was used to highlight resident immune cells so that they would be excluded from the analysis. The number of Ki-67 positive cells as a percentage of the total number of cells was quantified manually using FIJI. A nonparametric Wilcoxon rank-sum two-tailed test with a significance level of 0.05 was used to compare the percentages of Ki-67 positive basal layer keratinocytes found in the “young mouse” (10 week old) samples with the percentages obtained from the “old mouse” (18-19 month old) samples. Multiple imaged areas from each sample were evaluated for this analysis.

### **2.3.8 Cell Cycle Calculations Using BrdU and EdU Dual Labeling**

8 week old female mice (n=4 mice) were used to calculate the average lengths of both the S-phase (3121 cells) and overall cell cycle times (40726 cells) using a dual BrdU/EdU labeling technique described comprehensively previously (Martynoga, Morrison, Price, & Mason, 2005). Briefly, mice were first given an intraperitoneal injection with 0.75 mg/25g of 5-ethynyl-2'-deoxyuridine (EdU), followed 1.5 hours later by an intraperitoneal injection with 0.75mg/25 of BrdU. Mice were then euthanized 30 minutes later, 2 hours from the first injection with EdU (see Fig. 2.2c). Epithelial sheets were prepared from the buccal mucosa of each mouse as already described. Buccal mucosal epithelium was then blocked for 3 hours in whole-mount blocking/permeabilization buffer, incubated in 1N hydrochloric acid diluted in water for 20 minutes at 37°C, washed 4x5 minutes in PBS-T, and stained for EdU using the Click-iT EdU Alexa Fluor 647 kit following the manufacturer's instructions (ThermoFisher, C10340). Following staining, the samples were washed 3x10 minutes in PBS-T, incubated overnight at 4°C in a specific anti-BrdU antibody that does not cross-react with EdU, washed 3x15 minutes in PBS-T, incubated with a secondary antibody for one

hour at room temperature, washed 3x15 minutes in PBS-T, stained with DAPI for 30 minutes at room temperature, washed 1x5 minutes in PBS, mounted onto glass slides as already described, and sealed with clear nail polish. Following injection with EdU and BrdU, cells that have exited the S-phase prior to euthanasia will only label with EdU whereas cells still within the S-phase when the mouse is euthanized will be labeled with both EdU and BrdU (see Fig. 2f). For the calculations, it was assumed that EdU and BrdU did not reach detectable levels within tissues for 30 minutes following injection into the mouse. Using the formulas below as previously described by Martynoga et al., the average length of S-phase was calculated first, which was then used to calculate the average overall cell cycle length. The average percent of Ki-67 positive keratinocytes calculated in Fig. 2c (95.05%) was used to estimate the number of cycling cells in each area ( $P_{\text{cells}}$ ) imaged/analyzed when calculating the average cell cycle time.

|   |   |
|---|---|
| $\frac{\text{Time during which cells can incorporate EdU but not BrdU } (T_i)}{\text{Length of S-Phase } (T_s)} = \frac{\text{Number of cells that leave S-phase during experiment (EdU+/BrdU-)} (L_{\text{cells}})}{\text{Number of cells still in S-phase at the end of the experiment (EdU+/BrdU+)} (S_{\text{cells}})}$ | $\therefore T_s = T_i \left( \frac{S_{\text{cells}}}{L_{\text{cells}}} \right)$ |
| $\frac{\text{Length of S-phase } (T_s)}{\text{Length of cell cycle } (T_c)} = \frac{\text{Number of cells still in S-phase at the end of the experiment (EdU+/BrdU+)} (S_{\text{cells}})}{\text{Number of proliferating cells in area sampled (Ki67+)} (P_{\text{cells}})}$   | $\therefore T_c = T_s \left( \frac{P_{\text{cells}}}{S_{\text{cells}}} \right)$ |

### 2.3.9 Dual BrdU and EdU Pulse/Chase Labeling

3 month old male and female C57BL/6 mice (n=3 mice) were injected with BrdU for 48 hours and with EdU 3 hours prior to euthanasia. The buccal mucosa was

isolated, epithelium separated from the underlying connective tissue, and probed for BrdU and EdU expression as already described.

### **2.3.10 $K5^{tTa};H2B^{GFP}$ Label Retention Experiments**

2 to 4 month old male and female  $K5^{tTa};H2B^{GFP}$  mice were used (n≥3 mice per chase time point). To inhibit expression of the  $H2B^{GFP}$  allele, mice were initially given an intraperitoneal injection of doxycycline (0.4mg, Enzo Life Sciences, ALX-380-273-G005) and were then maintained on mouse chow that contained doxycycline (200mg/kg, BioServ, S3888). Mice were subsequently euthanized at 0 days (baseline), 3 days, 7 days, 21 days, 6 weeks, and 3 months after doxycycline treatment. The buccal mucosa in each mouse was removed, the epithelium separated from the underlying connective tissue, stained with DAPI in PBS for 30 minutes at room temperature, rinsed 2x5 minutes in PBS, and mounted onto glass slides as already described. Tissues were imaged in two ways. First, confocal microscope settings (e.g. laser power, exposure time, binning, gain, etc.) were adjusted to maximize the EGFP signal in the baseline  $K5^{tTa};H2B^{GFP}$  samples (i.e. did not receive any doxycycline), without over-exposing them and over-saturating the microscope camera. These same microscopic imaging parameters were then used to image the remaining  $K5^{tTa};H2B^{GFP}$  samples in order to determine the relative differences in fluorescence between them. Next, optimized confocal settings were adjusted for each sample to maximize EGFP expression in order to detect any rare, label retaining cells at later chase time points.



### 2.3.11 Measuring Individual Cell Fluorescence Values in $K5^{tTa};H2B^{GFP}$ Samples

Using the confocal images taken with identical imaging parameters for each  $K5^{tTa};H2B^{GFP}$  sample, the total relative fluorescence values for individual basal layer keratinocytes were calculated in FIJI (baseline: n=2 mice, 2173 cells; 3 day chase: n=6 mice, 4797 cells; 7 day chase: n=3 mice, 3030 cells). Relative fluorescence values were calculated by manually tracing individual cell nuclei (the location of the GFP signal) and then measuring the IntDen output under the analyze menu in FIJI. The IntDen function multiplies the mean fluorescence (i.e. mean pixel intensity) within a specified region of interest by its area (i.e. number of pixels). In this way, the total relative fluorescence takes into account both nuclear size and mean pixel intensity. Background subtraction was also applied to each sample to control for low levels of background fluorescence.

### 2.3.12 Clonal Analysis of Buccal Mucosa and Tongue Epithelium

2 to 3 month old (“young”) or 15 to 19 month old (“old”) male and female  $Bmi1^{CreER};R26^{tdTomato}$  mice (n≥3 mice per chase time point) were given a single intraperitoneal injection of tamoxifen (1mg/25g for clonal analyses in the buccal mucosa and 2mg/25g for clonal analyses in the tongue) to label single basal layer keratinocytes sufficiently far enough apart so that clonal collisions would be avoided. “Young” mice analyzed for clones within the buccal mucosa were euthanized at 3 days, 5 days, 14 days, 21 days, 28 days, 6 weeks, 3 months, 6 months, and 9.8 months following injection with tamoxifen. “Old” mice analyzed for clones within the buccal mucosa were euthanized at 3 days, 7 days, 14 days, 21 days, 6 weeks, and 3 months following injection with tamoxifen. “Young” mice analyzed for clones within the dorsal tongue

epithelium were euthanized at 3 days, 7 days, 21 days, 6 weeks, and 4 months following tamoxifen injection. The buccal mucosa and tongue were then removed and epithelial sheets separated, incubated with an anti- $\beta$ 4-integrin primary antibody and appropriate secondary antibody, and mounted on glass slides as already described. A large grid of overlapping confocal stack tiles (each measuring either 512x512 pixels or 996x996 pixels) was then imaged for each sample with z-stack spacing of 1 $\mu$ m. Tiles were stitched together using the Imaris MicroMagellan Compiler plugin for FIJI (freely available at [http://biomicroscopy.ucsf.edu/mediawiki/index.php?title=Analysis\\_Software\\_Repository](http://biomicroscopy.ucsf.edu/mediawiki/index.php?title=Analysis_Software_Repository)) and clones analyzed in FIJI. Representative groups of tiles from each sample were then selected and the total number of clones as well as the total number of basal layer keratinocytes per clone quantified. For Figs. 2.3d,e,g,h, asymptotic fits of a neutral drift model were performed as described previously (A. M. Klein, Doupé, Jones, & Simons, 2007; X. Lim et al., 2013). In brief, the average clone size,  $\langle n(t) \rangle$ , is predicted to grow linearly,  $\langle n(t) \rangle = 1/\rho + (r\lambda/\rho)*t$ , where  $\rho$  is the fraction of basal cells that divide,  $\lambda$  is the cell cycle rate, and  $2r$  is the fraction of divisions that give rise to daughter cells with a symmetric fate (both dividing or both differentiating). The density of clones in the basal layer,  $N_C(t)$ , is predicted to drop in a reciprocal manner,  $N_C(t) = N_C(0)/(1 + r\lambda*t)$ . Numerical fits of the data to these curves were carried out in Microsoft Excel. Statistical significance of the fits is given in the main text. Parameter values are not important to establish the general signature of neutral drift, but are provided for completeness: for the younger adult *Bmi1<sup>CreER</sup>;R26<sup>tdTomato</sup>* mouse labeled clones in the buccal mucosa, we found  $r\lambda/\rho=1.7$ cells/week (Fig. 3d), and  $r\lambda/N_C(0)=0.22$ clones/tile/week (Fig. 2.3e). With

$N_c(0)=3.9\pm 0.6$  clones/tile (mean $\pm$ SEM), and  $\lambda=2$  days (estimated from H2B-GFP dilution and from EdU/BrdU double-labeling), this gives an estimate of  $r\approx 0.23$ ,  $\rho\approx 0.47$ . For the aged *Bmi1*<sup>CreER</sup>;*R26*<sup>tdTomato</sup> mice (Fig. 2.3i, Supplemental Fig. S8e), the slope values for the average basal layer footprint were  $r\lambda/\rho=0.85$  cells/week. Finally, for dorsal tongue basal layer keratinocytes in the *Bmi1*<sup>CreER</sup>;*R26*<sup>tdTomato</sup> mice, the slope values for the average basal layer footprint were  $r\lambda/\rho=2.8$  cells/week.

### 2.3.13 Nuclear Density and Clonal Analysis of 5-Fluorouracil Treated Mice

5-Fluorouracil (5FU) powder (Sigma, F6627-5G) was dissolved in sterile 0.85% saline at a concentration of 6.25mg/mL, incubated at 60°C for 45 minutes with intermittent vortexing in order to ensure complete dissolution of the powder into solution, and pH adjusted to 9.2. Aliquots were then frozen at -20°C and thawed only once prior to injection into mice. 8-9 month old male and female *Bmi1*<sup>CreER</sup>;*R26*<sup>tdTomato</sup> mice (n=3 mice per chase time point) were first given an intraperitoneal injection with tamoxifen (1mg/25g) on day 0, and then given 3 sequential intraperitoneal injections of either 0.85% normal saline or 5FU (50mg/kg) on days 1, 2, and 3. Mice were euthanized at days 1, 3, 7, 14, and 21 days following the last dose of saline or 5FU (see Fig. 2.4a). Buccal mucosa was removed, epithelial sheets separated, incubated with anti- $\beta 4$ -integrin/secondary antibodies, and mounted on glass slides as described above. Samples were then imaged and clones analyzed as already described. Additionally, clone size distributions were analyzed in mice at the 1 day chase (control: n=2 mice, 203 clones; 5FU-treated: n=3 mice, 507 clones) and at the 3 day chase (control: n=3 mice, 367 clones; 5FU-treated: n=3 mice, 292 clones) time points. The number of RFP-labeled suprabasal layer keratinocytes was also quantified at the 1 day chase (control:

n=2 mice, 691 cells; 5FU-treated: n=3 mice, 1458 cells) and 3 day chase (control: n=3 mice, 1465 cells; 5FU-treated: n=3 mice, 1281 cells) time points. Finally, the number of nuclei in the basal layer was quantified at the 1 day chase in control (n=3 mice, 4021 nuclei) and 5FU-treated mice (n=3 mice, 3551 nuclei). A two-tailed Fisher's exact test with a significance level of 0.05 was used for statistical analyses.

### **2.3.14 Mitotic Figure Quantification and Orientation Analysis**

Using the whole-mount clonal analysis imaging data collected from the saline or 5FU treated *Bmi1<sup>CreER</sup>;R26<sup>tdTomato</sup>* mice, mitotic figures were identified via histomorphology and their overall number quantified and orientation assessed. Only a portion of the total mitotic figures identified were at a suitable stage of division such that their mitotic orientations could be reliably evaluated. To do this, orthogonal views were created in FIJI for images containing mitotic figures, which permitted the evaluation of each mitotic figure in multiple planes of section in order to establish its proper orientation. Mitotic figures were grouped into one of 5 categories based on the relationship of the dividing cells to the underlying basement membrane (BM), represented by  $\beta$ 4-integrin staining, as well as to one another. The categories were as follows: parallel (both mitotic figures touch the BM), oblique (one mitotic figure touches the BM while the other has lifted off at an approximately 45° angle to the remaining mitotic figure), perpendicular (one mitotic figure touches the BM while the other is directly above the underlying mitotic figure), intermediate (one mitotic figure touches the BM while the second is barely touching the BM and appears to be in the process of lifting off), and suprabasal (both mitotic figures have simultaneously lifted off the BM and are no longer touching it). See Fig. 2.4 for examples. Mitotic figures whose orientations

could be accurately determined were analyzed in control mice (n=11 mice, 533 mitotic figures) and 5FU-treated mice (n=14 mice, 440 mitotic figures). A two-tailed Fisher's exact test with a significance level of 0.05 was used to compare the number of parallel-orientated mitotic figures in the saline treated mice with those in the 5FU treated mice. In order to maximize the sample size for the 5FU treated mice, the mitotic orientation counts from each chase time point were pooled. A nonparametric two-tailed Wilcoxon rank-sum test with a significance level of 0.05 was used to compare the overall number of mitotic figures per field (tile) imaged in the saline treated *Bmi1<sup>CreER</sup>;R26<sup>tdTomato</sup>* mice (n=11 mice, 1224 mitotic figures [MFs]) with the total number of mitotic figures identified at each of the chase time points in the 5FU treated mice (1 day chase: n=2 mice, 89 MFs; 3 day chase: n=3 mice, 159 MFs; 7 day chase: n=3 mice, 257 MFs; 14 day chase: n=3 mice, 238 MFs; 21 day chase: n=3 mice, 383 MFs).

### **2.3.15 Buccal Mucosa Single Cell Dissociation and FACS Sorting**

Freshly dissected buccal mucosae from 12 week old female C57BL/6 mice (n=10 mice) were incubated in EDTA (20mM) and PBS without calcium or magnesium for 90 min at 37°C, and the epithelium peeled away from the connective tissues. The epithelial sheets were minced into small pieces and incubated in DMEM/F12 (Gibco, 11039-021) with 1% penicillin/streptomycin (Gibco, 15140-122), 30ug/ml DNase I (Worthington, LS002007), 1mg/ml collagenase/dispase (Roche, 10269638001) for 30 min at 37°C with intermittent shaking to help dissociate the cells. Cells were then filtered through a 40µm filter (Falcon, 352340) into FACS buffer (DMEM/F12 medium with 5% fetal bovine serum, 10mM HEPES, and 2.5mM EDTA), spun down at 4°C, and resuspended in FACS buffer with Fluorescein isothiocyanate (FITC) labeled anti-mouse CD104 (β4-

integrin) antibodies and incubated for 30 minutes on ice in the dark. Cells were then spun down at 4°C, resuspended in FACS buffer, and sorted on a FACSAria II cell sorter (Becton Dickinson). Prior to sorting, dead cells and debris were stained with DAPI (0.5ug/mL) and excluded. An appropriate antibody isotype control was also used.

### **2.3.16 Single Cell RNAseq**

Sorted, individual cells positive for high levels of  $\beta$ 4-integrin expression were run on the Chromium Controller (10X Genomics) using the Chromium Single Cell Library Kit Version 1 (10X Genomics, PN-120232) according to the manufacturer's instructions. The resulting cDNA library was then sequenced on an Illumina HiSeq 2500 (Illumina) using the HiSeq 2500 Rapid Run with SBS Kit v2 (Illumina, FC-402-4021). 605 cells were sequenced with a mean of 261,423 sequencing reads per cell.

### **2.3.17 Analysis of Single Cell RNAseq Data**

Transcriptional clustering from FACS sorted basal layer cells was performed using the Seurat package (Macosko et al., 2015; Satija, Farrell, Gennert, Schier, & Regev, 2015). Only genes expressed in a minimum of 3 cells and cells expressing at least 200 genes were kept in the analysis. Following mitochondrial gene removal, cells displaying a unique gene count over 3,200 were filtered out. Principal component analysis coupled with permutation tests revealed that ten significant principal components recapitulated the variation across the entire sample. Graph-based clustering of the cells revealed six clusters whose biological identity was assessed by characterizing specific markers. Sets of significantly overexpressed and underexpressed genes unique to each cell cluster when compared with all other

clusters simultaneously were identified using this analysis strategy. Additionally, pairwise comparisons between individual cell clusters (e.g. cluster 0 vs. cluster 1) were performed and yielded additional sets of significantly overexpressed and underexpressed genes. These pairwise comparisons enabled the identification of relative differences in gene expression important to keratinocyte maturation, as detailed in Fig. 2.5c.

### **2.3.18 Gene Ontology Analysis**

Using the differentially expressed genes identified in the single cell RNAseq analysis pipeline, gene functional annotation clustering and functional classification analyses using the database for annotation, visualization, and integrated discovery (DAVID) were performed (D. W. Huang, Sherman, & Lempicki, 2009b; 2009a). Medium classification stringency thresholds and DAVID recommended default settings were used for all analyses. In both the gene functional annotation clustering and functional classification analyses, group enrichment scores were created, which represent the log-transformed geometric means of the EASE scores (p-values) for each enriched term. Enrichment scores of 1.5 or greater were considered significant. In the gene functional annotation clustering analysis, gene ontology terms with p-values less than 0.01 within clusters with enrichment scores of 1.5 or greater were identified and processed through REVIGO using the medium similarity threshold (Supek, Bošnjak, Škunca, & Šmuc, 2011). REVIGO is an online tool that summarizes long lists of gene ontology terms by eliminating redundant terms. This analysis yielded condensed lists of gene ontology terms, which were further curated to remove any remaining redundancies.

### 2.3.19 Imaging Equipment and Software

Whole-mount tissues and cryosections were imaged at room temperature on one of two microscopes: an inverted Zeiss confocal microscope with a Yokogawa CSU-10 spinning disc and Andor iXon EMCCD camera using a Zeiss Plan-NeoFluar 40x (NA: 1.3) 1022-818 oil immersion objective or with an inverted Zeiss Spinning Disc with a Yokogawa CSU-X1 spinning disc and Axiocam 506 CCD camera using a Zeiss 40x (NA: 1.1) LD C-Apochromat water immersion objective. FFPE sections were imaged on an upright Leica DM5000B microscope with a Leica DFC 500 camera and using 40x (NA: 0.75) HCX PL S-APO air objective or a 63x (NA: 1.3) HCX PL APO oil objective. All image analysis was performed using FIJI (Schindelin et al., 2012; Schindelin, Rueden, Hiner, & Eliceiri, 2015). Figures were created using Adobe Illustrator CS6.

### 2.3.20 Statistical Analysis

All statistical analyses were run using Stata/SE, version 11.2 (StatCorp). Nonparametric two-tailed Wilcoxon rank sum and Fisher's exact tests were used with a significance level set at  $\alpha=0.05$ . Error bars represent either the standard deviation or 95% confidence interval, as detailed within the text.

### 2.3.21 Antibodies

| Primary Antibody  | Secondary Antibody   | Application                  |
|---|--|------------------------------|
| Rat anti-mouse $\beta$ 4-integrin (1:100, 346-11A clone, BD Bioscience, 553745) | Goat anti-rat IgG Alexa Fluor-488 (1:400, Invitrogen, A-11006) | Cryosections and whole-mount |
|   |  |                              |



| <b>Primary Antibody</b>   | <b>Secondary Antibody</b>  | <b>Application</b>                       |
|---|--|--|
| Rabbit anti-mouse Ki-67 (1:100, SP6 clone, ThermoScientific, RM-9106-S1)                            | Goat anti-rabbit IgG Alexa Fluor-568 (1:400, Invitrogen, A-11011)      | Whole-mount                              |
| Mouse anti-mouse p53 (1:50, PAb-122 clone, Invitrogen, MA5-12453)                                   | Goat anti-mouse IgG Alexa Fluor-488 (1:400, Invitrogen, A-11001)       | Whole-mount                              |
| Rabbit anti- mouse Keratin 14 (1:500, Poly19053 clone, Biolegend, 905304)                           | Goat anti-rabbit IgG Alexa Fluor-633 (1:400, Invitrogen, A-21070)      | Whole-mount                              |
| Rat anti-mouse CD45 (1:100, 30-F11 clone, Biolegend, 103101)  | Rabbit anti-rat IgG Alexa Fluor-488 (1:400, Invitrogen, A-21210)       | Whole-mount                              |
| Mouse anti-BrdU (1:300, MOBU-1 clone, Invitrogen, B35128)   | Goat anti-mouse IgG Alexa Fluor-488 (1:400, Invitrogen, A-11001)       | Whole-mount (for dual EdU/BrdU staining) |
| Rat anti-BrdU (1:500, BU1/75 [ICR1] clone, Abcam, ab6326)   | Biotinylated Rabbit anti-rat IgG (1:500, Vector Laboratories, BA-4001) | FFPE sections                            |
| FITC conjugated Rat anti-mouse CD104 ( $\beta$ 4-integrin, 1:100, 346-11A clone, Biolegend, 123605) |  | Single cell sorting via FACS             |
| Rat IgG2a kappa FITC Isotype Control (1:100, RTK2758 clone, Biolegend, 400505)                      |  | Single cell sorting via FACS             |

## 2.4 RESULTS

For several decades, the epidermal proliferative unit (EPU) hypothesis, also known as the invariant asymmetry model, was used to describe the organization of stem cells within the epidermis and oral mucosa (Potten, 1974). In this model, single stem cells within the basal layer divide slowly and asymmetrically, always resulting in a stem cell and a daughter transit amplifying (TA) cell, which remain closely associated with one another and are organized in stem cell/TA territories, or progenitor units (Ghazizadeh & Taichman, 2001; Hume & Potten, 1979; Mackenzie, 1997; S. Ro & Rannala, 2004; 2005). More recently, studies in several epithelial tissues such as the epidermis and esophagus support an alternative called the population asymmetry model, in which basal layer keratinocytes comprise a pool of equipotent, actively dividing stem cells that, following mitosis, give rise to varying combinations of stem and differentiated cell progeny in proportions necessary to maintain tissue homeostasis (Supplemental Fig. S1a,b) (Clayton et al., 2007; Doupé et al., 2010; 2012; A. M. Klein et al., 2010; A. M. Klein & Simons, 2011; Snippert, van der Flier, et al., 2010b). Although work in the tongue epithelium supported the invariant asymmetry stem cell model, based in part on the presence of solitary stem cells expressing high levels of *Bmi1* within the dorsal tongue epithelium (Tanaka et al., 2013), quantitative clonal analysis to confirm this finding has not yet been performed. In this study, we sought to identify and characterize OEPCs in all oral mucosal sites, determine how OEPCs are organized, and resolve which model – invariant asymmetry or population asymmetry – best explains their division kinetics and clonal growth patterns.

*Bmi1* is expressed in various adult somatic stem cell and cancer stem cell populations (D. Chen et al., 2017; Siddique & Saleem, 2012). A prior study in keratinocytes within the dorsal tongue epithelium using *in situ* hybridization (ISH) and lineage tracing techniques reported that *Bmi1* is expressed at high levels by rare, solitary stem cells in the interpapillary pits (Tanaka et al., 2013). Therefore, we initially set out to determine if *Bmi1* labeled rare OEPCs at other oral mucosal sites by using RNAscope, a sensitive and specific ISH method. Surprisingly, we found that *Bmi1* expression was present at low levels in most basal and some suprabasal layer keratinocytes throughout the oral mucosa, including the dorsal tongue (Fig. 2.1a,b; Supplemental Fig. S1c-h), in marked contrast to what had been previously reported. We next used lineage tracing in a *Bmi1*<sup>CreER</sup>;*R26*<sup>tdTomato</sup> mouse to verify that *Bmi1*-expressing keratinocytes were located primarily within the basal layer and to determine if *Bmi1* also labeled OEPCs. Following a single dose of tamoxifen and 24-hour chase, labeled keratinocytes were found almost exclusively in the basal layer throughout the oral mucosa, confirming the location of *Bmi1*-expressing cells identified in the RNAscope ISH assay (Fig. 2.1c; Supplemental Fig. S1i; Supplemental Fig. S2). Furthermore, in contrast to the previous report that single *Bmi1*-expressing keratinocytes reside within each dorsal tongue interpapillary pit (Tanaka et al., 2013), multiple *Bmi1*-expressing keratinocytes were identified, often in close proximity to one another (Fig. 2.1c). Labeling throughout the oral mucosa persisted for up to 13 months, confirming that *Bmi1* labeled long-lived OEPCs. We also used other *CreER* mouse lines driven by *Krt14*, *Gli1*, *Sox2*, and *Lrig1* with the same Tamoxifen administration protocol and found that, similar to *Bmi1*, these drivers also labeled OEPCs in the basal layer and

showed labeling that persisted for at least 3 to 6 months (Supplemental Fig. S3-S6). Additionally, we used an *Lgr6-GFP-CreER* mouse line that, unlike the other *CreER* mouse lines, showed sparse labeling in basal layer keratinocytes (results not shown). Short-term lineage traces of up to 2 weeks showed suprabasal layer cell labeling originating from the underlying labeled basal layer cells, implying that *Lgr6* is expressed by OEPCs, at least in the short term. Interestingly, when an antibody against GFP was used, discrete clusters of *Lgr6* positive basal layer cells were identified. Whether these *Lgr6* positive cells represent a discrete cell population within the basal layer remains to be elucidated in future studies. Take together, these findings strongly suggest that OEPCs are located within the basal layer of the oral mucosa, and not in the suprabasal layer, as had been previously suggested (Tanaka et al., 2013). Further studies will be necessary to determine the biological role that each of the genes driving *CreER* expression, i.e. *Krt14*, *Gli1*, *Sox2*, *Lrig1*, and *Lgr6*, have within OEPCs.

Figure 2.1

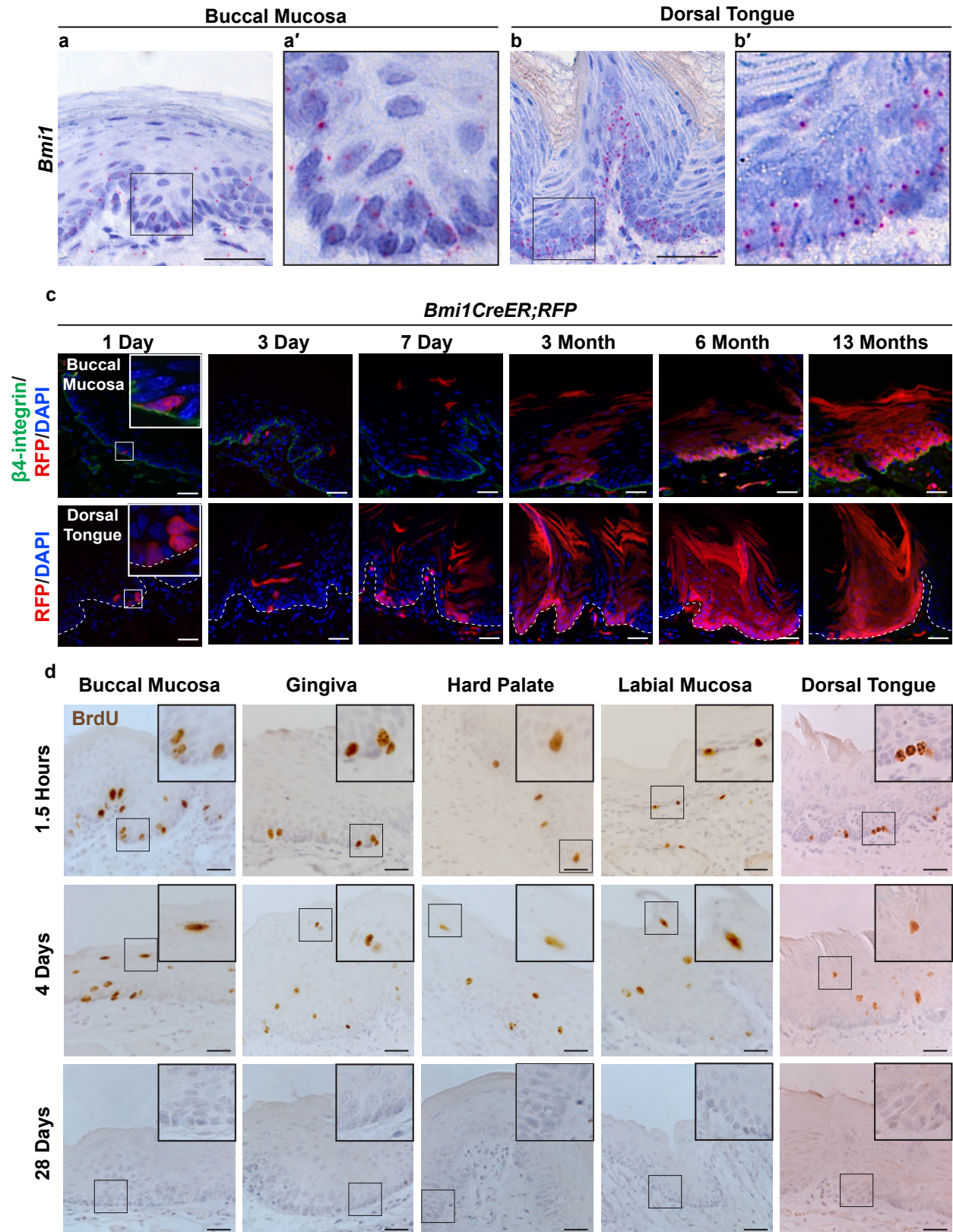


**Figure 2.1 *Bmi1* labels progenitor cells within the basal layer of the rapidly dividing oral mucosa.**

**(a,b)** Representative images from RNAscope in-situ hybridization experiments show that *Bmi1* (individual transcripts are represented by red dots) is expressed predominantly by basal layer keratinocytes in the buccal mucosa and dorsal tongue. Keratinocytes expressing high levels of *Bmi1* in either the basal or suprabasal layers were not identified. Scale bars, 30µm. **(c)** 1 day chase in *Bmi1*<sup>CreER</sup>;*R26*<sup>tdTomato</sup> mice following administration of a single low dose of tamoxifen shows that labeling occurs almost exclusively in basal layer keratinocytes, consistent with the in-situ experiment results (a,b). Labeling in these cells gives rise to large clones that persist for at least 13 months. Scale bars, 30µm. Dashed white line represents epithelial/connective tissue interface. **(d)** Mice injected with BrdU and euthanized 1.5 hours later show labeling almost exclusively in basal layer keratinocytes, confirming that actively dividing cells are located within the basal layer. BrdU-labeled keratinocytes reach the stratum corneum by as early as 4 days post-treatment. By day 28, label retaining basal layer keratinocytes are rarely seen. Scale bars, 30µm. DAPI, 4,6-diamidino-2-phenylindole; RFP, red fluorescent protein; BrdU, 5-bromo-2'-deoxyuridine.

To determine the division kinetics of basal layer keratinocytes, we injected wild-type mice with a single dose of BrdU and euthanized them at various time points (Fig. 2.1d). 1.5 hours post-injection, BrdU-labeled keratinocytes were detected predominantly in the basal layer, confirming this layer as the primary site of cell division within the oral mucosa. By day 4, BrdU-labeled keratinocytes were present in the stratum corneum, consistent with the rapid turnover rate of the oral mucosa. By day 28, almost no BrdU label remained except for in a few rare cells, indicating that the vast majority of basal layer keratinocytes were mitotically active (Supplemental Fig. S1j). In light of the similar rates of turnover in the various regions of the oral mucosa, we focused our analysis on the buccal epithelium, which provides a large expanse of tissue to study. To account for the rapid loss of BrdU, we assessed Ki-67 expression in the buccal mucosal epithelium of wild-type mice via whole-mount immunofluorescence. Approximately 95% of basal layer keratinocytes expressed Ki-67, underscoring the high proliferative index of the oral mucosa (Fig. 2.2a,b; Supplemental Fig. S7a-c).

Classically, label retention was considered a hallmark of adult stem cells, and *Bmi1*-positive keratinocytes in the dorsal tongue epithelium have been reported to be relatively slow cycling (Tanaka et al., 2013). However, it is now clear that many adult stem cell populations are proliferative as opposed to quiescent (Doupe et al., 2012; L. Li & Clevers, 2010). We therefore assessed whether label-retaining cells (LRCs) reside in the buccal mucosal epithelium. We used the *K5tTa;tetO-H2B-EGFP* system (Tumbar et al., 2004), in which mice constitutively produce EGFP in *Krt5*-expressing basal layer keratinocytes, and EGFP transcription is shut off by treatment with doxycycline. Following treatment with doxycycline, the amount of EGFP per cell is halved with each

cell division, enabling the identification of slowly dividing cells that retain EGFP (i.e. LRCs). If the same imaging parameters, such as exposure time and laser intensity, are used between samples, the relative differences in fluorescence can be measured. Mice were euthanized at various time points following treatment with doxycycline and epithelium from the buccal mucosa imaged, which revealed a near complete loss of EGFP signal by day 21 (Fig. 2.2c). When imaging parameters were optimized to detect EGFP at each chase time point, extremely rare EGFP-positive keratinocytes were present at the 6-week and 3-month chases (Fig. 2.2d). These cells were randomly distributed and not arranged in any regular pattern, in contrast to what would be expected with the EPU hypothesis. Furthermore, the fluorescence intensity values for these cells fell below the 1<sup>st</sup> percentile values measured in baseline keratinocytes (i.e. no doxycycline treatment), leading us to conclude that they had divided multiple times and were not true LRCs. Indeed, we measured the individual mean fluorescence values of several thousand basal layer keratinocytes in the baseline, 3-day, and 7-day chase samples and did not observe any cells at the 7-day chase with mean fluorescence values greater than the 1<sup>st</sup> percentile fluorescence values measured in the baseline samples (Supplemental File S1).

To analyze the division kinetics further, we used dual BrdU/EdU labeling (Martynoga et al., 2005) to calculate the average lengths of the S-phase and cell cycle in basal layer keratinocytes, which were 2.5 and 49 hours, respectively (Fig. 2.2e,f; Supplemental Fig. S7d-f); S-phase lengths as brief as 1.8 hours have been reported in other mammalian cells, such as mouse neural progenitor cells (Arai et al., 2011). To measure how often basal layer keratinocytes entered the cell cycle, we calculated the



fluorescence decay rates between the baseline, 3-day, and 7-day *K5tTa;tetO-H2B-EGFP* samples (Fig. 2.2g,h; Supplemental Fig. S7g). The average fluorescence decay rate correlated with a division rate of approximately once every 45 hours, similar to the cell cycle length of 49 hours. To confirm this, wild-type mice were injected with BrdU at baseline, with EdU at 48 hours, and then euthanized 3 hours later at 51 hours (Fig. 2.2i). Several keratinocytes in the buccal mucosal epithelium showed dual staining for both BrdU and EdU, confirming their reentry into the cell cycle within 48 hours. These findings support a model in which the majority of basal layer keratinocytes continually and rapidly enter the cell cycle, on average about once every 2 days. This rapid turnover of basal layer keratinocytes results in a lack of LRCs, which does not support the invariant asymmetry model.

**Figure 2.2**

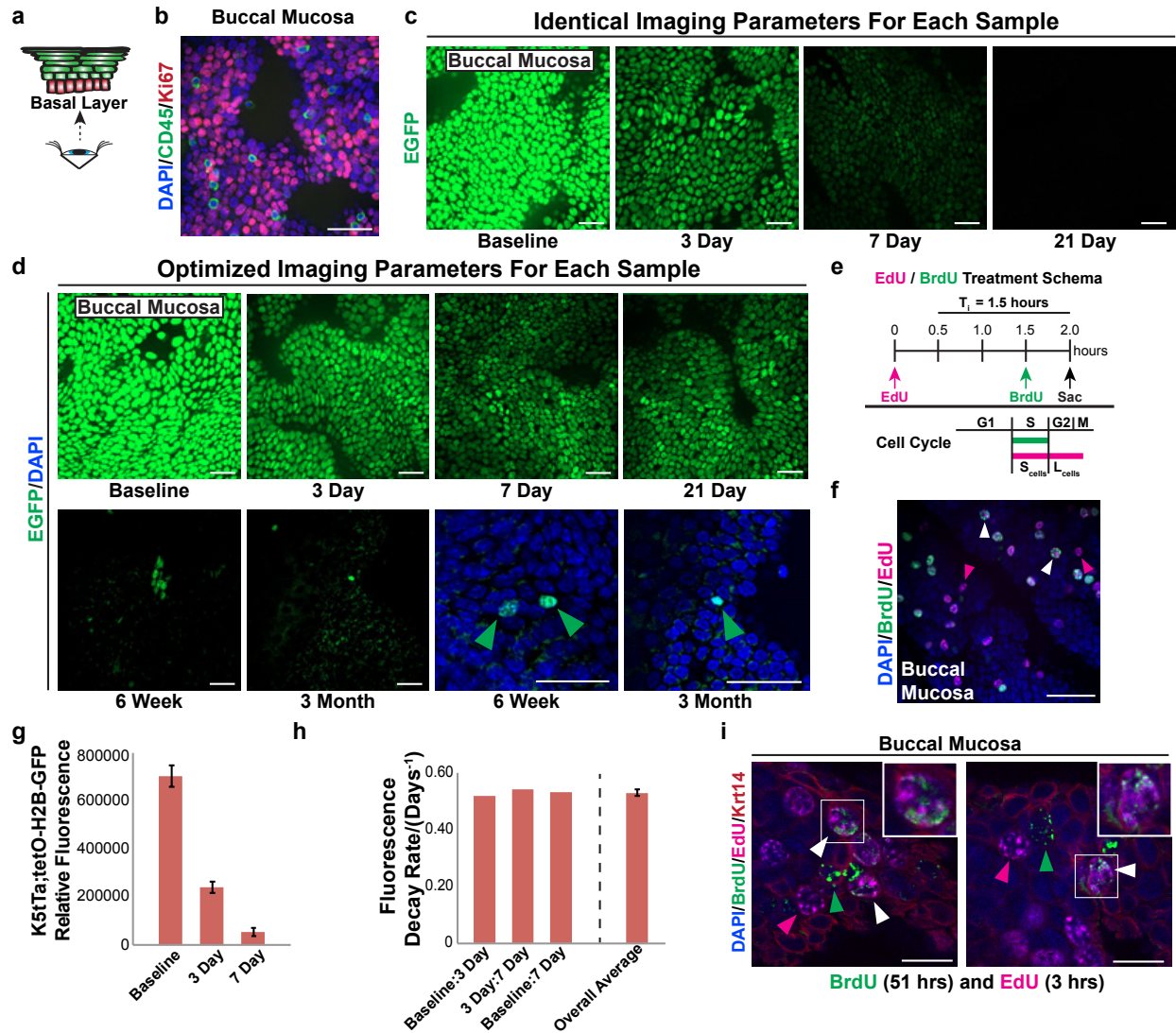


**Figure 2.2** The buccal mucosa does not contain label retaining cells and exhibits rapid cell division rates. **(a,b)** Whole-mount imaging reveals that the majority of buccal mucosal basal layer keratinocytes in 10-week-old C57BL/6 mice express Ki-67. CD45+ immune cells were excluded from the analysis. Scale bars, 30µm. **(c)** Whole-mount imaging of buccal epithelium from *K5Tta; tetO-H2B-EGFP* mice following administration of food containing doxycycline to shut off H2B-EGFP expression shows rapid and nearly complete loss of EGFP signal by 21 days when the same imaging parameters (e.g. laser power, exposure time, etc.) are applied to each sample. **(d)** Using optimized imaging parameters to maximize the detectable EGFP signal within the same samples from (c), the vast majority of basal layer

keratinocytes lose measurable EGFP expression by 6 weeks. Extremely rare, faintly EGFP positive keratinocytes are present at the 6 week and 3 month chases; however, they likely do not represent stem cells due to their random distribution within the tissue. Scale bars, 30 $\mu$ m. **(e,f)** Using temporally spaced pulses of EdU and BrdU along with whole-mount imaging, the average S-phase and total cell cycle times were calculated for buccal mucosal basal layer keratinocytes. Following injection with EdU and BrdU, keratinocytes that have exited the S-phase prior to euthanasia will only label with EdU (pink arrow heads), whereas keratinocytes still within the S-phase when the mouse is euthanized will be labeled with both EdU and BrdU (white arrow heads); see text for further details. Scale bar, 30 $\mu$ m. **(g,h)** The total relative fluorescence of individual keratinocytes from the *K5tTa; tetO-H2B-EGFP* buccal mucosal samples imaged in (c) were measured and the fluorescence decay rates calculated. Bar graphs represent average cell fluorescence values  $\pm$  SD at each chase time point (g), fluorescence decay rates calculated between all time points, and the overall average decay rate  $\pm$  SD (h), which corresponds to an average division rate of about once every 2 days. **(i)** Whole-mount imaging of buccal epithelium after a 48-hour pulse with BrdU followed by a three-hour pulse with EdU shows BrdU/EdU dual labeled keratinocytes (white arrowheads) along with keratinocytes that are labeled with only BrdU (green arrowheads) or EdU (red arrowheads), showing that basal layer keratinocytes can reenter the cell cycle within 2 days from their last division. Scale bars, 10 $\mu$ m. SD, standard deviation; BrdU, 5-bromo-2'-deoxyuridine; EGFP, enhanced green fluorescent protein; EdU, 5-ethynyl-2'-deoxyuridine; DAPI, 4,6-diamidino-2-phenylindole.

We next used quantitative clonal analysis to determine if OEPCs divided via invariant or population asymmetry. 3 month old *Bmi1<sup>CreER</sup>;R26<sup>tdTomato</sup>* mice were injected with a low dose of tamoxifen to induce sparse labeling, euthanized at various time points, and clones within the buccal and dorsal tongue epithelium analyzed via whole-mount imaging (Fig 2.3a-c,f; Supplemental Fig. S8a). Labeled clones (i.e. any group of basal/suprabasal labeled keratinocytes with at least one labeled cell in the basal layer) as well as the total number of labeled basal layer keratinocytes within each clone were quantified. We found that the overall number of clones in both the buccal and dorsal tongue epithelia decreased over time while the number of labeled basal layer keratinocytes within surviving clones increased linearly with time, consistent with the population asymmetry model (Fig. 2.3d,e,g,h).

It is well-established that damaged oral mucosa regenerates more rapidly in younger patients than it does in older patients (Engeland, Bosch, Cacioppo, & Marucha, 2006). To understand what role OEPCs might have in this process, we performed the same quantitative clonal analysis in the buccal mucosa of 15 to 19 month old *Bmi1<sup>CreER</sup>;R26<sup>tdTomato</sup>* mice (Fig. S8b). Interestingly, although we found similar clonal labeling patterns as those seen in younger mice (i.e. clone sizes grew linearly with time), average clone sizes in older mice tended to be smaller with an approximately 50% reduction in the average number of labeled basal layer keratinocytes per clone, although this did not reach statistical significance ( $p=0.24$ ) (Fig. 2.3i; Supplemental Fig. S8c,d). To investigate this further, we analyzed Ki-67 expression in the buccal epithelium of 18-19 month old mice and found that only 63% of basal layer keratinocytes expressed Ki-67, compared with 95% in younger mice, a significant

decrease ( $p < 0.00001$ , Fig. 2.3j,k; Supplemental Fig. S8e). These results indicate that, as mice age, the number and/or proliferative capacity of OEPCs decreases, which could explain why oral mucosal damage in older human patients takes longer to heal.

Figure 2.3

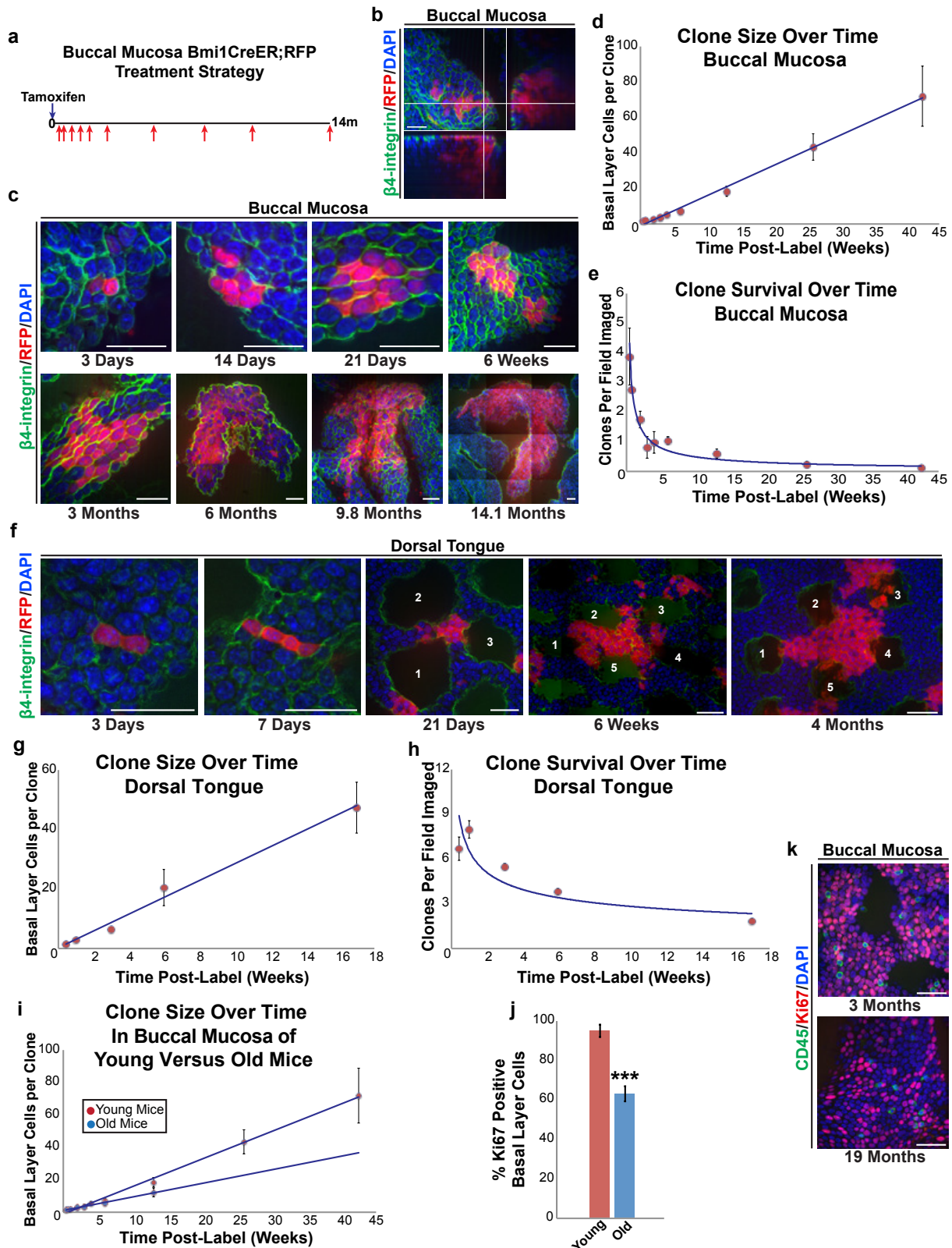


**Figure 2.3 *Bmi1*-labeled OEPCs in the buccal mucosa and dorsal tongue divide via population asymmetry with neutral drift dynamics.** (a) 2-3 month old *Bmi1*<sup>CreER</sup>;*R26*<sup>tdTomato</sup> mice were given a single dose of tamoxifen and chased up to 14 months. (b,c) Whole-mount imaging of buccal mucosal epithelial sheets; the number of clones containing at least one labeled basal layer keratinocyte were quantified along with the number of labeled basal layer keratinocytes present within each clone. Scale bars, 20µm. (d,e) As predicted by the population asymmetry model with neutral drift dynamics, the number of labeled basal layer keratinocytes per clone increased over time (d, 1.7 cells/week ± 0.08 SE) while the overall number of clones decreased (e, 0.22 clones/tile/week ± 0.03 SE). Data points represent mean values ± SD. Solid curves show neutral drift predictions of linear growth of the average (d) and inverse-linear decay of the labeling density (e) (A. M. Klein et al., 2007; A. M. Klein & Simons, 2011). (f) Similar clonal labeling patterns were observed in the dorsal tongue epithelium of *Bmi1*<sup>CreER</sup>;*R26*<sup>tdTomato</sup> mice. Many clones at early chase time points were associated with up to three dorsal tongue papillae (21 day chase, papillae numbered 1-3) while at later time points they were associated with as many as 5 dorsal tongue papillae (6 week and 4 month chases, papillae numbered 1-5). Scale bars, 20µm. (g,h) Dorsal tongue clone size (g, increase of 2.8 cells/week ± 0.20 SE) and clone survival patterns over time (h, loss of 0.03 clones/tile/week ± 0.0009 SE) were similar to those found in the buccal mucosa. Data points represent mean values ± SD. Solid curves show neutral drift predictions for growth within clones and clone survival over time. (i) Clonal analysis of the buccal mucosa from 15 month old *Bmi1*<sup>CreER</sup>;*R26*<sup>tdTomato</sup> mice showed similar clonal growth patterns over time as seen in the 2-3 month old mice; however, the OEPC competition rate in the older mice was halved compared with the younger mice (increase of 0.85 cells/week ± 0.06 SE vs. 1.7 cells/week ± 0.08 SE). Data points represent mean values ± SD. Solid lines represent the neutral drift predictions for clonal growth. (j, k) Whole-mount imaging of buccal mucosa from old and young mice revealed that older mice had significantly fewer Ki-67+ cells (Wilcoxon rank-sum test, p<0.00001). Bar graphs represent the average percent of basal layer keratinocytes that were Ki-67 positive ± SD. Scale bars, 30µm. OEPC, oral epithelial progenitor cell; SE, standard error; SD, standard deviation; DAPI, 4,6-diamidino-2-phenylindole; RFP, red fluorescent protein.

With an understanding of how OEPCs behave under normal steady state conditions, we next addressed their response to cytotoxic damage. We injected mice with 5-fluorouracil (5FU), a cytostatic pyrimidine analogue used to treat cancer that induces oral mucositis in humans (Mustafa Baydar, 2005). 5FU acts primarily by irreversibly inhibiting thymidylate synthase and may also be incorporated into nascent DNA and RNA, which can cause DNA strand breaks and severe RNA dysfunction. Together, these effects lead to cell cycle arrest or apoptosis via other effectors such as p53 (Longley, Harkin, & Johnston, 2003). *Bmi1<sup>CreER</sup>;R26<sup>tdTomato</sup>* mice were first injected with tamoxifen to label OEPCs, treated with either saline or 5FU once daily for 3 consecutive days, euthanized at various time points, and clones analyzed (Fig. 2.4a). Within the buccal mucosa, at 1 day post-5FU we detected a significant decrease in basal cell layer density ( $p=0.0002$ ) and a significant drop in mitotic activity ( $p=0.03$ ; Fig. 2.4b-d). There was also an increase in p53 protein levels over several days, confirming that the 5FU had caused DNA damage within the basal layer (Supplemental Fig. S9a). Surprisingly, basal layer keratinocytes never switched to a hyper-proliferative state following 5FU-induced damage, but instead slowly returned to normal mitotic activity between 14 and 21 days after treatment (Fig. 2.4d). Despite their slow mitotic recovery, by 3 days post-5FU, treated mice showed significantly increased average clone sizes compared with controls, which persisted through day 21 of the experiment ( $p<0.001$ ; Fig. 2.4e,f).

We next addressed the seemingly paradoxical observation that 5FU-treated mice had a decreased mitotic index yet still produced clones with increased numbers of labeled basal layer keratinocytes. One potential scenario consistent with this



observation would be that 5FU damage caused OEPCs to preferentially self-renew in order to replace damaged basal layer keratinocytes instead of creating daughter cells fated for differentiation. To test this, we measured the percentage of labeled suprabasal keratinocytes in control and 5FU-treated mice and found that, by 3 days post-5FU, treated mice had significantly fewer labeled suprabasal cells ( $p < 0.001$ , Fig. 2.4g). Further supporting this hypothesis, 5FU-treated mice exhibited a small but significant increase in the number of parallel oriented mitotic figures (i.e. both daughter cells remained in the basal layer) compared with controls ( $p = 0.01$ , Supplemental Fig. S9b-d). These results demonstrate that OEPCs compensate for tissue damage within the basal layer by altering their daughter cell fates accordingly.

**Figure 2.4**

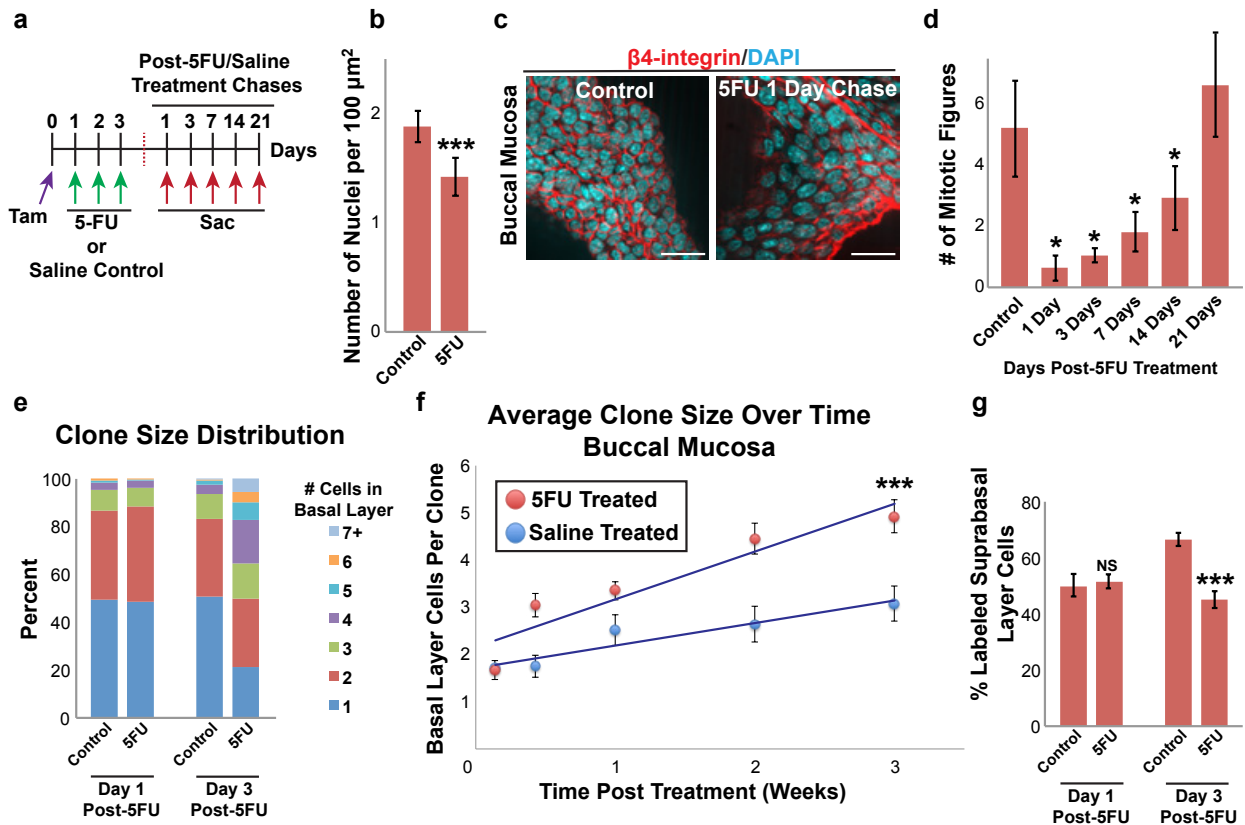


**Figure 2.4 5FU has long-lasting effects on epithelial mitotic rates within the buccal mucosa and causes expansion of OEPCs.** (a) 5FU treatment schema of *Bmi1<sup>CreER</sup>;R26<sup>tdTomato</sup>* mice. (b,c) 5FU causes a significant decrease in the buccal mucosal basal layer nuclear density in treated mice. Bar graphs represent the average number of nuclei per  $100\mu\text{m}^2 \pm \text{SD}$  in mice treated with saline or 5FU following a 1 Day chase (Fisher's exact test,  $p=0.0002$ ). Scale bars,  $20\mu\text{m}$ . (d) Following treatment with 5FU, the average number of mitotic figures decreased significantly and then slowly returned to pre-treatment levels by 21 days post-5FU exposure. Bar graphs represent the average number of mitotic figures per area imaged  $\pm \text{SD}$  (each time point was compared with control mice using the Wilcoxon rank-sum test. p-values are as follows for the 5FU chases: 1 day:  $p=0.03$ ; 3 days:  $p=0.01$ ; 7 days:  $p=0.01$ ; 14 days:  $p=0.04$ ; 21 days: not significant). (e) 3 days after the last dose of 5FU, treated mice showed an expansion in clone size distribution compared with controls. (f) Overall average clone sizes  $\pm \text{SD}$  in mice treated with 5FU are larger than those in control mice. The competition rate of basal layer progenitor cells

in 5FU treated mice is approximately double compared with controls (1.01 cells/week  $\pm$  0.12 SE vs. 0.47 cells/week  $\pm$  0.08 SE, respectively). Multivariate linear regression analysis showed that both the treatment type (control vs. 5FU,  $p < 0.001$ ) and time post-treatment ( $p < 0.001$ ) correlated strongly with clone size and accounted for 80% ( $R^2 = 0.80$ ) of the variance observed in the clone size distribution. Solid lines represent the neutral drift predictions for clonal growth. **(g)** In addition to the increase in average clone size, 5FU treated mice also show a significant decrease in the percentage of labeled suprabasal layer keratinocytes. Bar graphs represent the percentage of labeled suprabasal layer keratinocytes in control and 5FU treated mice at 1 and 3 days post-5FU treatment (error bars represent the 95% confidence interval; Fisher's exact test,  $p < 0.001$ ). 5FU, 5-fluorouracil; OEPC, oral epithelial progenitor cell; SD, standard deviation; SE, standard error; NS, not significant; DAPI, 4,6-diamidino-2-phenylindole; RFP, red fluorescent protein.

Finally, we used an unbiased single cell RNAseq approach to determine the overall diversity of cell types residing within the oral mucosal basal layer and to infer lineage relationships. We sorted buccal mucosal basal layer keratinocytes ( $\beta$ 4-integrin/CD104<sup>hi</sup>) and sequenced approximately 600 cells, which revealed 6 distinct cell clusters, each marked by a unique set of differentially expressed genes (Fig. 2.5a,b). Cells in clusters 0-4 all demonstrated keratin gene expression and exhibited transcriptional profiles consistent with keratinocytes. Cluster 5 cells, however, expressed several major histocompatibility class II genes important for antigen presentation along with CD207 (langerin) consistent with Langerhans cells, an antigen presenting dendritic cell present within the epidermis and oral mucosa. A closer examination of the various keratinocyte-associated genes expressed within clusters 0-4 revealed transcriptional profiles of keratinocytes at various stages of maturation (Fig. 2.5c). Cluster 1 expressed the highest levels of keratins and other factors associated with basal layer keratinocytes (*Krt5*, *Krt14*, *Krt15*) (Moll, Divo, & Langbein, 2008) and likely represented OEPCs. This cluster also showed upregulated expression of *Wnt4*, *Wnt10a*, and *Krt15*; until now, *Wnt4* and *Wnt10a*, which are required for maintaining the proliferative state of epidermal interfollicular stem cells (X. Lim et al., 2013), have not been reported in OEPCs. *Krt15* was also recently shown to label basal layer progenitor cells in the esophageal epithelium that were molecularly distinct from *Krt15*-negative cells (Giroux et al., 2017). Interestingly, cluster 1 did not represent a rare subpopulation of keratinocytes – rather, it comprised approximately 20% of those sequenced in the analysis. Cluster 0 cells had a similar keratin expression profile as cluster 1 and additionally expressed numerous genes associated with the G2/M phase of the cell

cycle, likely representing actively dividing OEPCs. Conversely, clusters 2, 3, and 4 showed a stepwise downregulation of OEPC markers with simultaneous upregulation of keratinocyte maturation markers, demonstrating for the first time the transcriptional transitions that occur during differentiation of the oral epithelium.

To confirm the presence of keratinocytes at various stages of maturation within the basal layer, we performed duplex RNAscope ISH with probes against *Krt14* (a basal layer/OEPC marker) and *KrtDap* (a differentiated keratinocyte marker). As predicted by the single cell RNAseq analysis, basal layer keratinocytes expressed variable combinations of each gene, likely representing the coexistence of OEPCs with keratinocytes fated for differentiation at various stages of maturation (Fig. 2.5d,e). Gene functional clustering/ontology analyses were performed using DAVID and Revigo (Supplemental Fig. S10; Supplemental Files S2-S5) (D. W. Huang, Sherman, & Lempicki, 2009a; 2009b; Supek et al., 2011). Cluster 0 was enriched for functional gene groups associated with the G2/M cell cycle checkpoint, further supporting their identity as actively dividing keratinocytes. Cluster 1 showed strong enrichment for genes encoding RNA-splicing factors, ribosomes, and translation initiation factors, possibly to prepare OEPCs for entry into the cell cycle or to begin differentiating. Cluster 2 showed enrichment for oxidative phosphorylation genes and could represent keratinocytes at the first stage of differentiation, with increased energy demands secondary to transcription and synthesis of numerous differentiation related proteins. Clusters 3 and 4 appeared to represent more mature keratinocytes and showed gene enrichment for protein metabolism/cross-linking, glutathione/redox homeostasis, and keratinocyte differentiation. Taken together, our results show that the basal layer in the buccal

mucosa is heterogeneous and comprised primarily of OEPCs along with other keratinocytes at more advanced stages of differentiation (Fig. 2.5f).

Figure 2.5

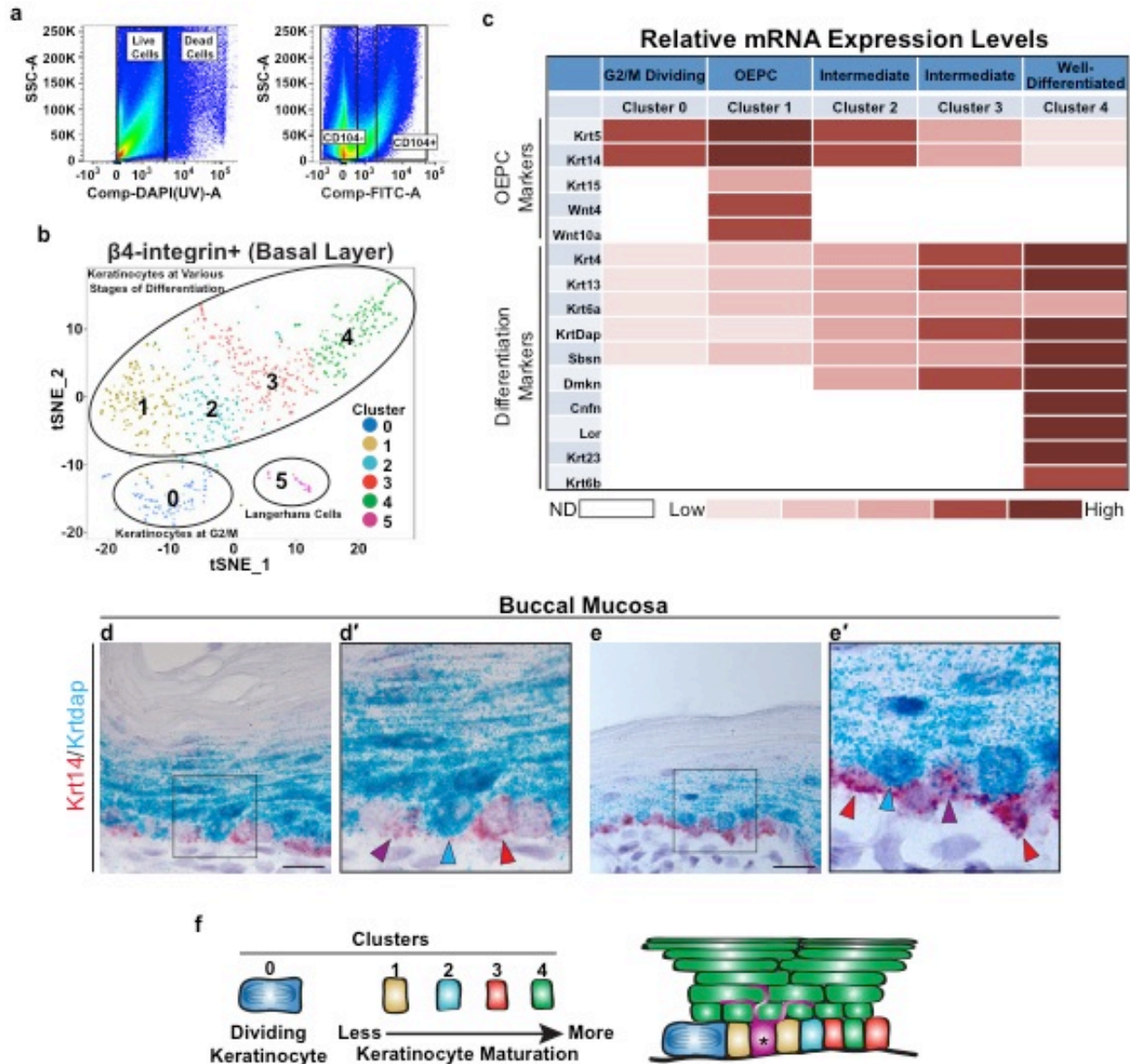


Figure 2.5 Buccal mucosal epithelial basal layer keratinocytes are composed of OEPCs and maturing keratinocytes at varying stages of differentiation. (a) FACS sorting schema for isolating live,  $\beta$ 4-integrin (CD104) high expressing cells used for single cell RNAseq analysis. (b) t-SNE plot showing the number of unique cell clusters identified during analysis. (c) Relative mRNA expression levels for keratins and other factors associated with keratinocyte differentiation within each of the clusters. (d,e) Duplex RNAscope assay using probes for *Krt14* (red dots) and *KrtDap* (blue dots). Some

keratinocytes predominantly only express *Krt14* (red arrowheads), *Krtdap* (blue arrowheads), or a combination of both (purple arrowheads). These expression patterns likely represent keratinocytes at various stages of maturation, as predicted by the single cell RNAseq analysis. **(f)** Proposed model depicting the different keratinocyte populations present within the basal cell layer of the buccal mucosa and their corresponding cluster designations identified via the single cell RNAseq analysis from (b). The asterisk (\*) labels a Langerhans cell population corresponding to cluster 5 from (b). OEPC, oral epithelial progenitor cell; FACS, fluorescent activated cell sorting; ND, not able to determine.



In conclusion, our data show that *Bmi1*-labeled OEPCs are ubiquitously distributed throughout the oral mucosal basal layer, and that within the buccal and dorsal tongue epithelia they rapidly divide and follow the population asymmetry model with neutral drift dynamics. These results differ substantially from the current oral mucosa stem cell paradigm and challenge our understanding of the role that OEPCs play in the context of tissue homeostasis, regeneration, and disease. The differences between our findings and an earlier report in the tongue (Tanaka et al., 2013) are likely due in part to differences in labeling efficiency of the mouse reporter constructs used as well as to the high sensitivity and specificity of the RNAscope ISH technique (Tanaka et al., 2013).

We also demonstrate that the effects of 5FU on OEPCs are unexpectedly long-lasting, despite the drug's rapid plasma half-life. In one study, 5FU was detected in patients' plasma 9 days following treatment with a large 5FU bolus (Tamura et al., 2011). Since mice in our study were given 3 large boluses of 5FU, it is possible that 5FU levels remained elevated within the plasma for an extended period of time, which could explain why mitotic levels within the buccal mucosa slowly increased back to normal instead of transitioning rapidly to a hyperproliferative state. Additionally, the post-chemotherapy treatment effects of 5FU (e.g. irreversible inhibition of thymidylate synthase and incorporation within DNA and RNA molecules) could lead to continued cell cycle arrest even after 5FU levels significantly drop in the plasma. These extended effects on OEPCs, in addition to the complex milieu of signaling factors at the sites of mucosal damage, could help explain why oral mucositis, a common side-effect of

chemotherapy, can take as many as 2-4 weeks to resolve following the last dose of chemotherapy (Lalla et al., 2008).

Lastly, the mitotic figure orientation and single cell RNAseq analyses support a model in which most OEPCs divide into two daughter cells that initially remain within the basal layer. Through currently unknown intrinsic and/or extrinsic signals, each cell then either retains its identity as an OEPC or begins to terminally differentiate and eventually delaminate from the basal layer. It is not clear if commitment to differentiation is an irreversible step or if there still remains some plasticity to return to an OEPC state, possibly as a response to damage within the basal layer. Future work to identify the signals that drive OEPC daughter cell fate behavior will be crucial to understanding how overall tissue homeostasis is maintained and how OEPCs contribute to oral disease.

## CHAPTER 3

### Characterization of X-linked Hypohidrotic Ectodermal Dysplasia (XL-HED)

#### Hair and Sweat Gland Phenotypes Using Phototrichogram Analysis and Live Confocal Imaging

In this chapter, I use novel techniques to characterize the hair and sweat gland phenotypes that result from defective ectodysplasin signaling within ectodermally derived epidermal progenitor cells during development. The novel non-invasive techniques described here could be used to assess changes in these phenotypes in future clinical trials. The results of this chapter were published in the American Journal of Medical Genetics Part A, July 2013 (K. B. Jones et al., 2013).

Kyle B. Jones<sup>1,+</sup>, Alice F. Goodwin<sup>1,+</sup>, Maya Landan<sup>1</sup>, Kerstin Seidel<sup>1</sup>, Dong-Kha Tran<sup>1</sup>, Jacob Hogue<sup>2</sup>, Miquella Chavez<sup>1</sup>, Mary Fete<sup>3</sup>, Wenli Yu<sup>1</sup>, Tarek Hussein<sup>1</sup>, Ramsey Johnson<sup>4</sup>, Kenneth Huttner<sup>4</sup>, Andrew H. Jheon<sup>1</sup>, and Ophir D. Klein<sup>1,2,5</sup>

<sup>1</sup>Program in Craniofacial and Mesenchymal Biology, University of California, San Francisco, San Francisco, CA, USA

<sup>2</sup>Division of Medical Genetics, Department of Pediatrics, University of California, San Francisco, San Francisco, CA, USA

<sup>3</sup>National Foundation for Ectodermal Dysplasias, Mascoutah, IL, USA

<sup>4</sup>Edimer Pharmaceuticals Inc, Cambridge, Massachusetts, USA

<sup>5</sup>Center for Craniofacial Anomalies, Department of Orofacial Sciences, University of California, San Francisco, San Francisco, CA, USA

<sup>+</sup> Equal contribution

### 3.1 ABSTRACT

Hypohidrotic ectodermal dysplasia (HED) is the most common type of ectodermal dysplasia (ED), which encompasses a large group of syndromes that share several phenotypic features such as missing or malformed ectodermal structures, including skin, hair, sweat glands, and teeth. X-linked hypohidrotic ectodermal dysplasia (XL-HED) is associated with mutations in ectodysplasin (*EDA1*). Hypohidrosis due to hypoplastic sweat glands and thin, sparse hair are phenotypic features that significantly affect the daily lives of XL-HED individuals and therefore require systematic analysis. We set out to determine the quality of life of individuals with XL-HED and to quantify sweat duct and hair phenotypes using confocal imaging, pilocarpine iontophoresis, and phototrichogram analysis. Using these highly sensitive and non-invasive techniques, we demonstrated that 11/12 XL-HED individuals presented with a complete absence of sweat ducts and that none produced sweat. We determined that the thin hair phenotype observed in XL-HED was due to multiple factors, such as fewer terminal hairs with decreased thickness and slower growth rate, as well as fewer follicular units and fewer hairs per unit. The precise characterization of XL-HED phenotypes using sensitive and non-invasive techniques presented in our study will improve upon larger genotype-phenotype studies and in the assessment of future therapies in XL-HED.

### 3.2 INTRODUCTION

Ectodermal dysplasia (ED) describes a large group of syndromes characterized by missing or malformed ectodermal structures, including skin, hair, sweat glands, and teeth (reviewed in Mikkola, 2009). Hypohidrotic ectodermal dysplasia (HED) is the most prevalent type of ED and is inherited in an X-linked (XL), autosomal recessive (AR), or autosomal dominant (AD) manner. The incidence of XL-HED is estimated at 1 in 100,000 live male births, and the carrier incidence is around 17.3 in 100,000 women. The clinical features of XL-HED include severe hypohidrosis, sparse hair and eyebrows, periorbital wrinkling, dry skin, missing and malformed teeth, increased susceptibility to respiratory infections, as well as hypoplasia of sweat, sebaceous, meibomian, lacrimal, and mammary glands (Clarke, Phillips, Brown, & Harper, 1987; Clauss et al., 2008). XL-HED is caused by mutations in the gene encoding ectodysplasin (*EDA1*), a ligand in the tumor necrosis factor (TNF) superfamily. AR-HED and AD-HED are caused by mutations in the EDA receptor (EDAR), or the cytosolic, EDAR-specific adaptor molecule called EDAR-associated death domain (EDARADD) (Mikkola & Thesleff, 2003; Trzeciak & Koczorowski, 2016).

A major cause of mortality and morbidity in infants with XL-HED is hyperthermia due to sweat gland hypoplasia and hypohidrosis. The mortality rate of XL-HED individuals in the first year of life is estimated to be 2.1% (Blüschke, Nüsken, & Schneider, 2010). Additionally, the majority of XL-HED individuals experience fevers early in life. It has been suggested that acute episodes of severe hyperthermia, which can lead to febrile seizures, may be associated with developmental abnormalities (Blüschke et al., 2010). Heat intolerance later in life continues to affect those with XL-

HED, limiting their ability to perform many daily activities, especially exercise (Hammersen, Neukam, Nüsken, & Schneider, 2011). Sparse hair can also significantly impact XL-HED individuals beginning in young adulthood, due to its negative psychosocial consequences. Therefore, novel or improved therapies for sweat gland hypoplasia and sparse hair may dramatically improve the lives of XL-HED individuals.

A great deal is known about the role of the EDA pathway in ectoderm-derived tissue and organ development based on data from mice and humans. Mice with spontaneous mutations that phenocopy characteristics of HED were found to carry mutations in *Eda*, *Edar* or *Edaradd* (Reviewed in Courtney, Blackburn, & Sharpe, 2005). *Eda*, *Edar*, and *Edaradd* are expressed in the ectoderm of the skin and become restricted to the placode during development (Cui & Schlessinger, 2006). The EDA pathway is activated in the ectoderm by inductive Wnt/ $\beta$ catenin signals from the underlying mesenchyme (Y. Zhang et al., 2009b), and in turn, activates the NF- $\kappa$ B pathway and downstream targets including Shh, Wnt and BMP. Interestingly, in humans, a non-synonymous single nucleotide polymorphism (SNP) in *EDAR* (1540T/C) common in East Asian populations enhanced EDA signaling and contributed to the thick and straight hair, opposite to the thin, sparse hair observed in HED (Fujimoto et al., 2008; Mou et al., 2008).

Potential molecular therapies are in development to treat XL-HED patients, largely based on knowledge gained from studies in animal models. Pre- and peri-natal treatment of mice carrying *Eda* mutations with recombinant human EDA1 alleviated many of the XL-HED-associated phenotypes involving hair, sweat gland, and 3<sup>rd</sup> molars (Gaide & Schneider, 2003). Indeed, a complete rescue of hair and 3<sup>rd</sup> molar phenotypes

was possible when EDA1 was administered prior to birth, whereas sweat gland hypoplasia was rescued in the immediate postnatal period with EDA1 administration (Gaide & Schneider, 2003). Thus, there appears to be a therapeutic window during which EDA1 administration is most effective. Furthermore, multiple characteristics of XL-HED were recognized in a German shepherd dog, including symmetrical hairlessness, missing and conical shaped teeth, an inability to sweat, and an increased rate of pulmonary infections. These features were later linked to a mutation in the canine *EDA* gene (Casal, Scheidt, Rhodes, Henthorn, & Werner, 2005). Most XL-HED dogs treated post-natally with recombinant human EDA1 developed a permanent dentition similar to controls, had significantly improved sweat response, and decreased incidence of respiratory infections. However, the hair phenotype was not rescued, likely due to the fact that hair follicles in dogs normally form *in utero* prior to when EDA1 was administered (Casal et al., 2007; Mauldin, Gaide, Schneider, & Casal, 2009). Although EDA1 therapy did not fully rescue the dental, hair, and sweat phenotypes associated with XL-HED in the dog model, it did alleviate the morbidities associated with these phenotypes. These examples underscore the potentially significant therapeutic effects that EDA1 replacement therapy might have in the treatment of human XL-HED.

As progress is made towards initiating clinical trials to treat XL-HED subjects, it is critical that clinical features characterizing XL-HED phenotypes are more specifically defined. Quantitative, reproducible, and non-invasive methods to measure XL-HED phenotypes will enable researchers to accurately assess treatment efficacy. In this study, we analyzed and quantified sweat gland hypoplasia and sparse hair phenotypes

using a novel application of confocal imaging, pilocarpine iontophoresis, and phototrichograms in a cohort of 12 XL-HED affected and 13 unaffected control males.



### **3.3 MATERIALS AND METHODS**

#### **3.3.1 Study Participant Recruitment and Demographics**

This study was approved by the University of California, San Francisco Institutional Review Board. Primary objectives of the study were to quantitatively assess the number of sweat ducts present in the palm of the hand, sweat production, and hair characteristics. All study subjects, or their legal guardians if subjects were under 18 years of age, provided written informed consent prior to participation in the study. To participate in the study, subjects must never have used pharmacologic treatment for thinning hair and must have been at least 10 years of age. A total of 13 healthy male control subjects with no family history of XL-HED and 12 male case subjects previously diagnosed clinically with XL-HED participated in the study. XLHED subjects were recruited from a National Foundation for Ectodermal Dysplasias (NFED) family conference. A convenience sample of control subjects was used, therefore, controls were not age or ethnicity matched with XL-HED subjects. The 12 XL-HED subjects consisted of 2 pairs of brothers and 8 unrelated individuals representing 10 distinct families. Control subjects were all unrelated. The majority of subjects in both control and XL-HED cohorts were Caucasian (53.9% and 83.3%, respectively; Table 2.1). The ages of the control cohort participants ranged from 19 to 29 years while the XL-HED cohort ages ranged from 11 to 29 years (Table 2.1). The median age for both groups was approximately 25 years.

**Table 3.1 Demographic Characteristics of Control and XL-HED Subjects**

|   | Control (N=13)     |    | XL-HED (N=12)      |    | p-value <sup>1</sup> |
|---|--------------------|----|--------------------|----|----------------------|
| <b>Demographic Characteristic</b>         |                    |    |                    |    |                      |
| Age (in years, median (IQR))              | 25.5 (24.3 - 27.4) |    | 25.5 (15.7 - 28.2) |    | 0.51                 |
| Age Range (in years)                      | 19 – 29            |    | 11 – 29            |    |                      |
| BMI (in kg/m <sup>2</sup> , median (IQR)) | 23.7 (22.8 - 25.8) |    | 21.7 (18.6 - 24.3) |    | 0.10                 |
| Race                                      | <i>n</i>           | %  | <i>n</i>           | %  |                      |
| Asian                                     | 3                  | 23 | 0                  | 0  |                      |
| Black                                     | 0                  | 0  | 1                  | 8  |                      |
| White                                     | 7                  | 54 | 10                 | 84 |                      |
| Other                                     | 3                  | 23 | 1                  | 8  |                      |

<sup>1</sup>p-values were calculated using the Wilcoxon rank-sum test

### **3.3.2 Medical Questionnaire**

Participants were interviewed and a detailed medical history was collected. The medical questionnaire, completed in part by control subjects and in total by XL-HED subjects, included questions pertaining to sweating, hair, skin, and quality of life (Table 2.2).

**Table 3.2 Clinical Characteristics of XL-HED Subjects as Determined by Medical Questionnaire**

| Clinical Characteristic                   | XL-HED (N=12) |     | Controls (N=13)  |   |
|---|---------------|-----|------------------|---|
|   | n             | %   | n                | % |
| Heat intolerance                          | 12            | 100 | 0                | 0 |
| Exercise limited by heat intolerance      | 10            | 83  | 0                | 0 |
| Decreased sweating                        | 12            | 100 | 1                | 8 |
| Unexplained fevers                        | 2             | 17  | 0                | 0 |
| Dry skin/eczema                           | 12            | 100 | n/a <sup>1</sup> |   |
| Experienced thinning hair and/or eyebrows | 8             | 67  | n/a              |   |
| Fingernails/toenails appear normal        | 9             | 75  | n/a              |   |
| Chronic childhood nasal drainage/blockage | 11            | 92  | n/a              |   |
| Respiratory related problems as a child   | 8             | 67  | n/a              |   |
| Asthma                                    | 5             | 42  | n/a              |   |
| Dry mouth                                 | 7             | 58  | n/a              |   |
| Dry eyes                                  | 5             | 42  | n/a              |   |
| Hoarseness of voice                       | 10            | 83  | n/a              |   |
| Nose bleeds as a child                    | 10            | 83  | n/a              |   |

<sup>1</sup> n/a Data not available. Control subjects not asked question on medical questionnaire.

### **3.3.3 Genotyping**

Eleven of the affected subjects underwent genotyping for *EDA1* mutations to confirm a diagnosis of XL-HED. Previous genotyping for the *EDA1* gene confirmed a mutation at this locus for one subject (#23).

### **3.3.4 Pilocarpine-Induced Iontophoresis**

Pilocarpine-induced iontophoresis was performed using the Wescor 3700 device (Wescor Biomedical Systems, Logan, UT). Two electrodes containing Pilogel® Iontophoretic Discs (solid agar consisting of 96% water and 0.5% pilocarpine nitrate; Wescor) were placed on the forearms of study participants. 1.5 mA of current was run for 5 minutes through the electrodes, after which time they were removed and a Macroduct Sweat Collector (Wescor) was placed over the site of pilocarpine iontophoresis. Sweat was collected for 30 minutes from a 57 mm<sup>2</sup> surface area. The maximum volume of sweat that can be collected with the Macroduct Sweat Collector is 93 µl, as estimated by weight.

### **3.3.5 Live Confocal Microscopy Imaging of Palmar Sweat Ducts**

Sweat duct density (number/cm<sup>2</sup>) in the thenar (thumb) region of the palm of each subject was determined through analysis of images collected by direct visualization with an FDA 510(k) device, the Lucid VivaScope 1500 ([www.lucid-tech.com](http://www.lucid-tech.com)). The Lucid VivaScope is a live confocal imaging device that enables live imaging of epithelial tissues and structures, including the visualization of sweat ducts (Rajadhyaksha, González, Zavislan, Anderson, & Webb, 1999). The maximum depth of imaging is approximately 300 µm; however, in this, study images were taken near the

surface of the epidermis in order to visualize sweat ducts. An adhesive ring was placed on the subject's palm to which the VivaScope was attached via a magnetic lock. A series of photographs were taken of an area approximately 6mm X 6mm. An individual (R.J., included as an author) trained in the use of this device was involved in the acquisition of all images. Two independent observers blinded to subject XL-HED status quantified the sweat ducts in the images obtained by the VivaScope.

### **3.3.6 Phototrichogram Analysis**

Total and anagen hair counts in the scalp were determined from color macrophotographs of clipped hair on the occipital scalp in a 1 cm<sup>2</sup> circular target area centered by a cosmetic ink dot, if necessary (Canfield, 1996; Van Neste & Fuh, 2001). Hair in the target area was clipped to approximately a 1 mm length for determination of preliminary total hair count, and then clipped to the scalp to monitor hair growth over the 2 to 3 day period between visits. At Study Visit 2, a macrophotograph of the target area was taken for the determination of anagen and telogen hair counts, based on the number of hairs that had lengthened over the intervening time period. Macrophotographs were taken using a Nikon D90 digital camera at fixed focus, distance, and exposure with the use of a Nikon 60 mm lens and EpiFlash from Canfield Scientific, Inc. (Fairfield, NJ). All digital images were provided to Canfield Scientific who served as the central photography reader for quality assurance and hair counting/analysis. Digital macrophotographs were analyzed by trained technicians who were blinded to subject XL-HED status. Hair analysis was performed by means of Canfield's proprietary computer-based imaging software. Study Visit 1 images were used to visually identify the number of follicular units as well as the number of vellus and

terminally differentiated hairs that appeared to emerge from each follicular unit. If a hair shaft was obstructed by a gel bubble, tattoo ink, or other artifact then the follicular unit was omitted from the analysis. Each follicular unit was manually tagged with parameters set for 2 hairs per unit, 3 hairs per unit, or 4+ hairs per unit. Hair thickness and growth rate were also directly measured with the assistance of the analysis software. Alignment of images was possible for all subjects except subjects #11 (control) and #4 (XL-HED) because each had hair too light in color for optimal analysis. For this reason, subjects #11 and #4 were excluded from this analysis.

### **3.3.7 Statistical Methods**

All statistical analyses were performed using Stata/SE 11.1 for Mac (StataCorp, College Station, TX). During data analysis, several variables did not follow normal distributions. For this reason, the more conservative non-parametric Wilcoxon Rank-Sum test was used to analyze all continuous data. Summary statistics for continuous variables are reported as the median and interquartile range (IQR). Categorical variables were analyzed using Fisher's Exact Test. Findings were considered statistically significant if  $p < 0.05$ .

## 3.4 RESULTS

### 3.4.1 Medical Questionnaire

12 XL-HED affected males and 13 unaffected control males between the ages of 11 and 29 were recruited for the study. Control subjects were asked a portion of questions on the medical questionnaire, while XL-HED subjects completed these along with additional questions pertaining to their hair and sweat phenotypes. The data collected from the medical questionnaire is summarized in Table 2.2. As previously reported, XL-HED subjects reported increased heat intolerance (12/12;  $p < 0.0001$ ), limitations in exercise due to heat intolerance (10/12;  $p < 0.0001$ ), and decreased sweating (12/12;  $p < 0.0001$ ) compared with controls. Only 17% of XL-HED subjects reported experiencing unexplained fevers during childhood ( $p = 0.22$ ) and no seizures were associated with these fevers. None in the control cohort reported any unexplained fevers.

The remainder of the medical history questionnaire information was obtained from XL-HED subjects only. All XL-HED subjects were asked detailed questions about how decreased sweating affected their lifestyle. The most common positive responses (i.e., lifestyle was affected by decreased sweating) included involvement in outdoors sports (11/12), daily life (10/12), choice of occupation (8/12), choice of vacation destination (8/12), and decision to live in a cooler climate (6/12). Of the 7/12 XL-HED subjects that reported suffering from dry mouth and the 5/12 from dry eyes, only 4 subjects reported suffering from both. Lastly, 10/12 subjects reported experiencing chronic nosebleeds as children, with most recalling onset of nosebleeds under the age



of 5 (7/10). 8/10 subjects reported suffering from chronic nosebleeds as adults with a range of 3 to 75 nosebleeds per year.

### **3.4.2 Sweat Duct Counts**

Live confocal microscopic imaging (Fig. 3.1a,b) revealed that control subjects had a median of 115 palmar sweat ducts per 36 mm<sup>2</sup> (IQR (intermediate quartile range): 97.5 – 119.5), whereas XL-HED subjects had a median of 0 (IQR: 0 – 0; p<0.0001; Fig. 3.1c).

### **3.4.3 Pilocarpine-Induced Sweat Volumes**

Using pilocarpine iontophoresis, control subjects had a median sweat volume of 52 µl (IQR: 33 – 63), whereas all XL-HED subjects produced no sweat (IQR: 0 – 0; p<0.0001; Fig. 3.1d). Interestingly, one of these XL-HED subjects (#8) presented with sweat ducts, but only half as many as the control subject with the fewest sweat ducts. One control subject (#16), whose sweat ducts were in the normal range and who did not report decreased sweating or heat intolerance, had pilocarpine-induced sweat volume that was minimal (i.e., 3 µl).

**Figure 3.1**

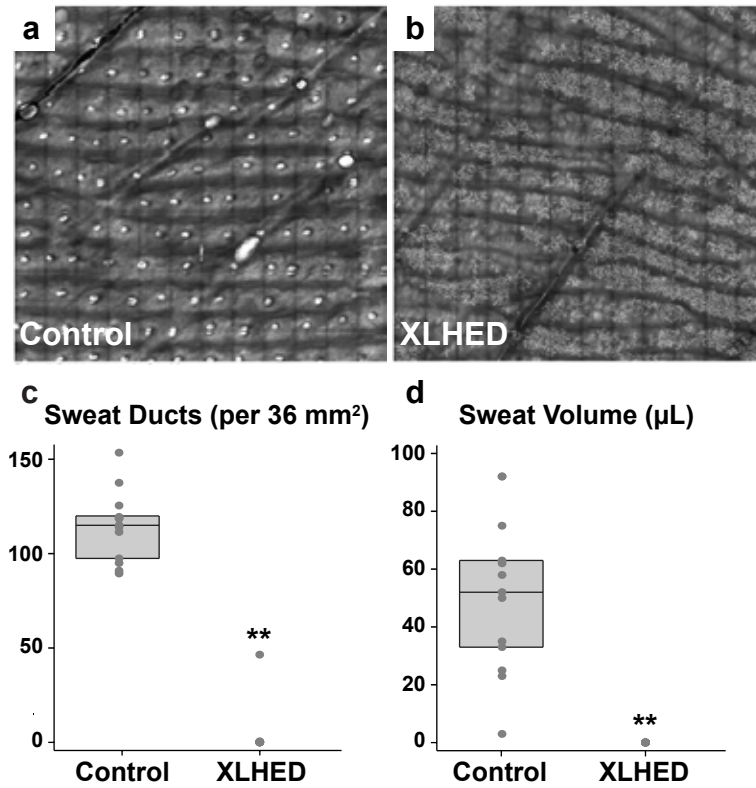


**Figure 3.1 XL-HED subjects show a decrease in palmar sweat ducts and produce little to no sweat.** (a,b) Live confocal imaging of a 36 mm<sup>2</sup> area of the palm shows an absence of sweat ducts in the XL-HED subject compared to control. Sweat ducts appear as small, round, white dots in the control subject. Note: spindly, white projections seen in the XL-HED subject (b) may be dendritic cells and were seen in both XL-HED and control subjects. (c) Quantification of the number of palmar sweat ducts shows that XL-HED subjects have few sweat ducts compared to control subjects. (d) Graph of the sweat volumes collected over 30 minutes using pilocarpine iontophoresis shows XL-HED subjects produced little to no sweat. Note that in (c) and (d), each circle corresponds to a measurement for an individual subject. The upper, middle, and lower horizontal lines in the rectangular box behind the circles represent the 75<sup>th</sup>, 50<sup>th</sup> (median), and 25<sup>th</sup> percentiles, respectively. \*\* p<0.0001.

### 3.4.4 Hair Counts

All hair counts and subsequent hair analyses were calculated from a surface area of 1 cm<sup>2</sup> (Fig. 3.2a-d; Supplemental Table 1). Total hair counts were significantly different between groups, with control subjects having a median of 212 total hairs (IQR: 195.5 – 296.5) and XL-HED subjects having a median count of 93 (IQR: 80 – 134; p=0.0001). Further analysis revealed that this large disparity was due primarily to a difference in terminal (i.e. thick) hair counts as opposed to vellus (i.e., thin, non-terminal) hairs. Control subjects had a median of 197.5 terminal hairs (IQR: 176.5 – 268) compared with XL-HED subjects that had a median of 84 terminal hairs (IQR: 64 – 97; p<0.0001; Fig. 3.2e). Vellus hair counts were similar between control and XL-HED subjects (Fig. 3.2e). The ratio of terminal to vellus hairs in control subjects had a median ratio of 8.7 (IQR: 6.4 – 11.1), whereas XL-HED subjects had a median ratio of 3.2 (IQR: 2.4 – 14.5; p=0.30). A terminal to vellus hair ratio of <4 typically denotes hair thinning (Sinclair & Dawber, 2001).

### 3.4.5 Follicular Units

XL-HED and control subjects differed significantly with respect to various follicular unit (FU) characteristics (Fig. 3.2f). Controls presented with significantly more FUs per cm<sup>2</sup> with a median of 135.5 (IQR: 121 – 180.5) compared with XL-HED subjects who had a median of 88 FUs (IQR: 78 – 118; p=0.0021; Fig. 3.2f). Controls also possessed a higher average number of hairs per FU with a median of 1.6 (IQR: 1.4 – 1.8), whereas XL-HED subjects had a median of 1 (IQR: 1 – 1.1; p=0.0003).

We next analyzed the number of FUs in each group that had 1, 2, 3, and 4 or

more hairs (FUs with more than 4 hairs were scarce, and it was difficult to determine the exact number of hairs present; thus, FUs with 4 or more hairs were grouped together). Since control subjects had significantly more FUs compared to XL-HED subjects, we calculated the percentages of FUs that had 1, 2, 3, or 4 hairs. Strikingly, 97.2% (IQR: 90.6% – 100%) of FUs in XL-HED subjects had only 1 hair, whereas only 50.5% (IQR: 44.5% – 59.5%;  $p < 0.0001$ ) of FUs in control subjects had 1 hair (Fig. 3.2g). There were also significant differences between control and XL-HED subjects in the number of FUs with 2, 3, and 4 or more hairs (Fig. 3.2g).

### **3.4.6 Hair Width**

The width of terminal hairs in control subjects was significantly larger compared to XL-HED subjects. Controls had a median terminal hair width of 71  $\mu\text{m}$  (IQR: 59 – 76.3), whereas XL-HED subjects had a median width of 50.5  $\mu\text{m}$  (IQR: 44.5 – 56.2;  $p = 0.0007$ ; Fig. 3.2h). There was no significant difference in the width of vellus hairs.

### **3.4.7 Hair Growth**

We calculated the percent of terminal hairs that were in anagen (i.e., growth phase). Surprisingly, controls had a median of 89.5% of terminal hairs in anagen (IQR: 85.9% – 92.5%), and XL-HED subjects had a similar median of 86.3% (IQR: 80.5% – 97.9%;  $p = 0.81$ ; Fig. 3.2i). The percentage of vellus hairs in anagen was also similar between groups ( $p = 0.31$ ). Control subjects had faster growing terminal hairs with a median growth rate of 16.2  $\mu\text{m}/\text{hour}$  (IQR: 14.6 – 18) compared with XL-HED subjects who had a median growth rate of 10.1  $\mu\text{m}/\text{hour}$  (IQR: 9.6 – 12;  $p = 0.0001$ ; Fig. 3.2j).

Figure 3.2

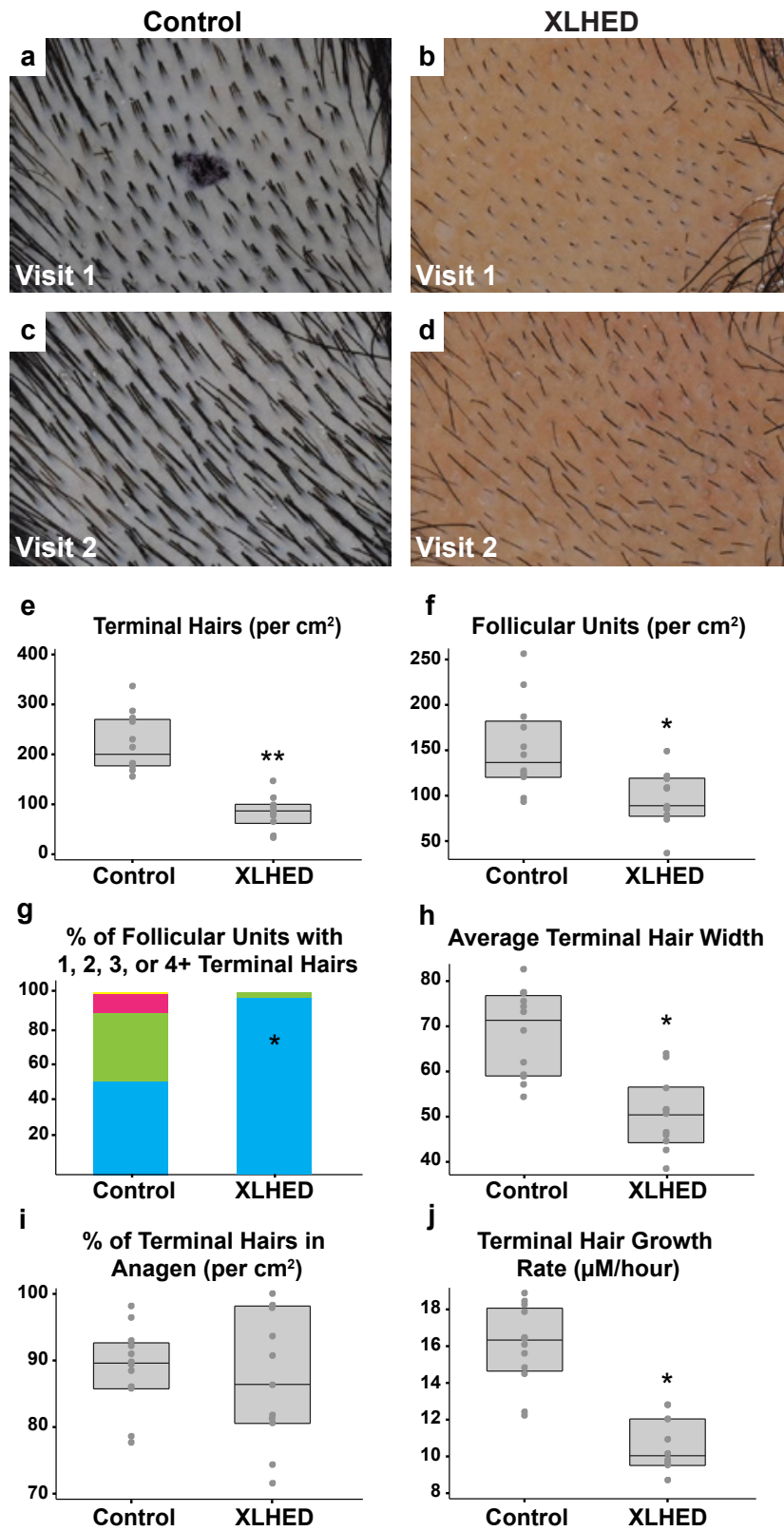


**Figure 3.2 Phototrichogram analysis reveals multiple properties of XL-HED subject hair that differ significantly from controls. (a-d)** Photographs of the shaved scalp in control and XL-HED subjects during study visit 1 **(a,b)** and again 2-3 days later **(visit 2; c,d)**. Such images were utilized for phototrichogram analysis. Note: the small, circular black mark in **(a)** is a temporary ink tattoo used to help identify the subject's shaved area during study visit 2. In the control subject, the tattoo washed off by the time the second photograph was taken. **(e-j)** Graphs representing measurements of various hair properties obtained after completion of the phototrichogram analysis in all study subjects. Note in **(g)**, blue bar represents the % of follicular units with 1 hair, green is two hairs, pink is 3 hairs and yellow is 4+ hairs. \* $p < 0.0005$ ; \*\* $p < 0.0001$

### **3.4.8 Genotyping of *EDA1***

Genotyping was performed on subjects (one per family) to confirm mutations in *EDA1* and to establish a definitive diagnosis of XL-HED (subject #23 was previously confirmed for XL-HED). Both previously reported and novel mutations were identified (Supplemental Table 2). Mutations were comprised mainly of missense mutations (n=9; 75%), and affected the TNF (n=5; 42%), furin (n=3; 25%), transmembrane (n=2; 17%), collagen (n=1; 8%), and extracellular (n=1; 8%) domains of the *EDA1* protein (Supplemental Table 2).

### **3.4.9 Age Correlation Analysis**

Although the median age for subjects in both groups was approximately 25 years old, 5/12 XL-HED subjects were under 18 years of age compared with none of the controls. Given that XL-HED subjects tended to be younger than the controls, we wanted to ensure that differences in hair properties between both groups were not due to differences in age. To analyze this, we conducted a Pearson correlation analysis comparing age with the ratio of terminal to vellus hairs, the percentage of terminal hairs in anagen, and the number of FUs per cm<sup>2</sup> (Supplemental Fig. S11). Age did not correlate with the differences we found in hair and FU properties between groups.

### 3.5 DISCUSSION

To develop treatments for XL-HED, it is critical that the medical genetics community identify and fully characterize the XL-HED-associated phenotypes targeted for intervention. The non-invasive collection of reproducible, quantifiable, and specific parameters will aid in the assessment of treatment efficacy. In this study, we used novel applications of non-invasive methods to precisely quantify sweat duct hypoplasia and sparse hair phenotypes, traits that significantly affect the daily lives of individuals with XL-HED.

A major morbidity associated with XL-HED is heat intolerance due to hypoplastic or absent sweat glands. Our study, similar to others (H. Schneider et al., 2011), found that all XL-HED subjects reported heat intolerance, a trait that limited their ability to exercise and participate in outdoor activities. It also influenced their choice of career, place to live, and travel destinations. Previous studies have utilized methods such as graphite prints (H. Schneider et al., 2011) and impressions of the fingertips with light body impression material (Clarke et al., 1987) to measure sweat ducts. However, these methods are not sensitive or readily reproducible. Another study used punch biopsies of the palm or scalp (Rouse, Siegfried, Breer, & Nahass, 2004) to analyze all sweat gland structures. Although more sensitive at detecting sweat glands and ducts, this technique is highly invasive. Our method of using confocal imaging of the palm to measure sweat ducts is sensitive, reproducible, and non-invasive. We determined that XL-HED subjects presented with no or few sweat ducts compared to controls. We noted that all XL-HED subjects showed a complete absence of sweat determined using pilocarpine iontophoresis, a standard, inexpensive, and non-invasive method to measure sweat



production (H. Schneider et al., 2011). These data confirm that individuals with XL-HED lack normally functioning sweat ducts and glands, and further support the role of the *EDA1* gene in the formation of sweat ducts and glands during early development (Cui & Schlessinger, 2006; Cui, Kunisada, Esibizione, Douglass, & Schlessinger, 2009).

This study is the first to use phototrichogram analysis to quantify the hair phenotype of XL-HED subjects. Overall, we found that the thin hair phenotype observed in XL-HED subjects was due to multiple factors such as fewer terminal hairs with decreased thickness and slower growth rate, fewer FUs, and fewer hairs per FU. Interestingly, the percentage of terminal hairs in anagen did not differ between control and XL-HED groups. This observation suggests that a different mechanism is involved in the XL-HED-associated hair phenotype compared to androgenetic alopecia (i.e., male or female pattern baldness), where a decreased percentage of hairs in anagen has been reported, and drug therapies have been developed such as finasteride that target the anagen phase (Boyapati & Sinclair, 2013; Van Neste & Fuh, 2001). However, therapies that may be effective in XL-HED may also offer new approaches to treating androgenetic alopecia and other disorders of hair loss such as targeting hair thickness, number of FUs, and number of hairs per FU.

To date, clear correlations between genotype and phenotype have not been determined in XL-HED. We attempted to identify genotype-phenotype correlations using regression analysis to determine relationships between the type of mutation (missense, nonsense, or deletion) or the region of *EDA1* affected (TNF, furin, transmembrane, collagen, or extracellular domains) with the various parameters of the sweat duct and hair phenotypes. Our analysis did not reveal any clear genotype-phenotype correlations

due primarily to the small sample size. Interestingly, we did observe several XL-HED individuals with unique phenotypes that may further reveal the roles that distinct *EDA1* domains play in hair and sweat gland development. XL-HED subject #8, the only subject with an in-frame deletion of 36 base pairs within the collagen domain of *EDA1*, presented with hypomorphic phenotypic features that were quite different from the other XL-HED subjects. These included the presence of residual sweat ducts in conjunction with completely nonfunctional sweat glands, and hair characteristics that were similar to control subjects in hair numbers (i.e., total hairs, total anagen hairs, FUs, and hairs per FU), but abnormal hair width and growth rate. These data suggest that the type of mutation and the protein domain(s) affected in *EDA1* may modulate the severity of the XL-HED phenotype. In contrast, XL-HED-affected brothers #5 and #6, who both harbored the same missense mutation in the furin cleavage domain of *EDA*, differed markedly from one another in hair number, percentage of terminal hairs in anagen, FU number, and rate of hair growth. However, the brothers possessed similar hair widths and hairs per FU. These results suggest that in addition to the type and location of mutations in the *EDA1* gene, other genetic and/or environmental factors may play a role in modulating various aspects of the XL-HED phenotype.

Recently, an XL-HED family was described with a highly variable clinical phenotype, and it was found that some family members carried a mutation in *EDAR* (370A) that attenuated the phenotype (Cluzeau et al., 2012). Thus, differences in XL-HED phenotype may also be due to additional mutations in the same pathway. The application of our highly quantitative methods to larger XL-HED cohorts may help to identify genotype-phenotype correlations. Although a great deal is known about the role

of EDA in the development of ectodermal appendages (Mikkola & Thesleff, 2003), genotype-phenotype correlations could further our understanding of the mechanism by which EDA initiates and maintains hair follicles and sweat glands.

Our study establishes highly quantitative, reproducible, and non-invasive measures to determine hair and sweat duct phenotypes associated with XL-HED, a prerequisite for the assessment of novel and improved therapies in the treatment of XL-HED.

## CHAPTER 4

### **White Lesions in the Oral Cavity: Clinical Presentation, Diagnosis, and Treatment**

In this chapter, I discuss several pathologic conditions associated with the oral epithelium, most of which likely involve dysfunction in oral epithelial stem cells. Understanding the role that oral epithelial stem cells play in these disease processes could some day lead to the development of improved therapies for patients. The majority of this chapter was published in *Seminars in Cutaneous Medicine and Surgery*, December 2015 (K. B. Jones & Jordan, 2015).

Kyle Burke Jones, DDS<sup>1</sup> and Richard C.K. Jordan, DDS, PhD, FRCPATH<sup>1,2,3,4</sup>

<sup>1</sup> Department of Orofacial Sciences, University of California, San Francisco, California

<sup>2</sup> Department of Radiation Oncology, University of California, San Francisco, California

<sup>3</sup> Helen Diller Comprehensive Cancer Center, University of California, San Francisco, California

<sup>4</sup> Department of Pathology, University of California, San Francisco, California

## **4.1 ABSTRACT**

White lesions in the oral cavity are common and have multiple etiologies, some of which are also associated with dermatological disease. All of these lesions likely involve dysfunction of oral epithelial progenitor cells. While most intraoral white lesions are benign, some are pre-malignant and/or malignant at the time of clinical presentation, making it extremely important to accurately identify and appropriately manage these lesions. Due to their similar clinical appearances, it may be difficult to differentiate benign white lesions from their pre-malignant/malignant counterparts. This chapter will discuss many of the most common intraoral white lesions including their clinical presentation, how to make an accurate diagnosis, and effective treatment and management strategies.

## **4.2 INTRODUCTION**

White lesions of the oral cavity are common and may have multiple etiologies. Often, due to their similar clinical appearances, a biopsy is necessary to establish the diagnosis. This chapter will focus on some of the more common intraoral white lesions with emphasis placed on clinical presentation, how to establish the diagnosis, treatment, and long-term management.

## **4.3 HEREDITARY LESIONS**

### **4.3.1 Leukoedema**

Leukoedema is a common, benign, asymptomatic intraoral condition found within several populations such as those of Indian, Caucasian, Mexican, and African American descent (Fig. 4.1) (Bouquot & Gorlin, 1986; Castellanos & Díaz-Guzmán, 2008; Martin, 1992). Clinically, it appears as a thin, grey-white, wrinkled film that cannot be wiped off and usually appears bilaterally on the buccal mucosa; however, other sites may be affected including the floor of mouth, larynx, labial, and vaginal mucosa. Presentation can occur at any age and its severity may increase with time (Waitzer, 1984). Leukoedema often disappears upon stretching of the affected area, a helpful sign that can be used to distinguish it from other white lesions. Factors such as smoking, poor oral hygiene, and the use of highly spiced foods have been suggested as potential etiologic factors; however, no definitive cause-and-effect relationships have been established (Martin, 1992). Given the high prevalence of leukoedema in several demographic groups, it is now accepted as a variation of normal. No treatment is

necessary because it is not associated with any other disease process and has no potential for malignant transformation or patient morbidity.

**Figure 4.1**

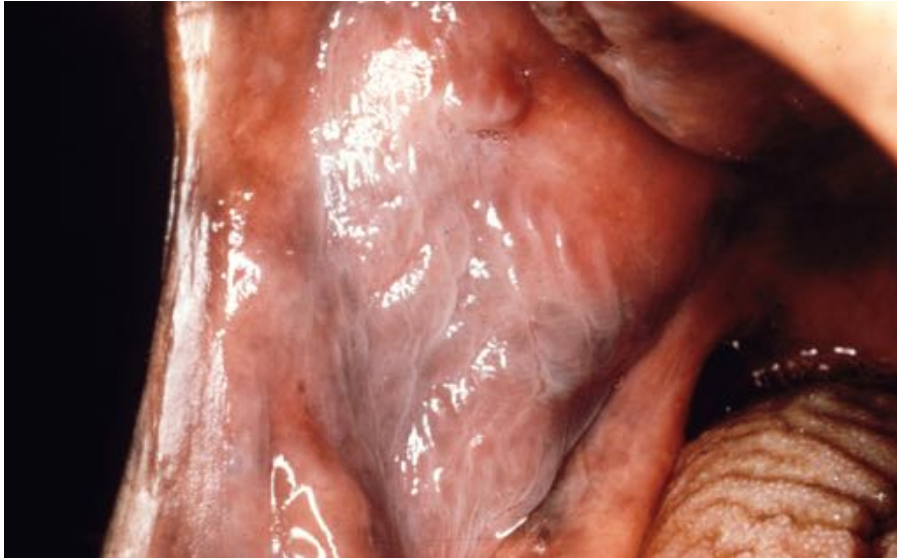


**Figure 4.1** Leukoedema on the right buccal mucosa. When affected areas are physically stretched, the lesions often disappear.



### 4.3.2 White Sponge Nevus

Inherited in an autosomal dominant fashion, white sponge nevus (WSN) is characterized by the presence of asymptomatic, thick, spongy, white plaques located primarily within the oral cavity (Fig. 4.2). Rarely, other mucous membrane sites may be affected including those of the nose, penis, anus, vagina, and esophagus (Cutlan et al., 2010; Jorgenson & Levin, 1981; Timmer et al., 1997). Within the mouth WSN is most common on the buccal mucosa followed by the labial mucosa, alveolar ridges, and floor of mouth (Jorgenson & Levin, 1981). The severity and extent of the plaques vary and may wax and wane over time within each affected patient. In a majority of cases, lesions are first noted during childhood and appear to affect males and females equally (Jorgenson & Levin, 1981).

WSN is caused by mutations in either the keratin 4 (*KRT4*) or keratin 13 (*KRT13*) genes (Richard, De Laurenzi, Didona, Bale, & Compton, 1995; Rugg et al., 1995). These mutations lead to an abnormal perinuclear accumulation of keratin tonofilaments, intracellular edema, acanthosis, and hyperparakeratosis of the epithelium. In general, WSN has not been linked to any long-term diseases such as dysplasia or cancer. The vast majority of patients require no management; however, for rare symptomatic cases (i.e. pain, sensitivity) several empirical approaches have been suggested. These include bland warm water mouth rinses of baking soda, tetracycline, penicillin, or chlorhexidine with the goal of reducing local microbial overgrowth that occasionally occurs on WSN plaques and can cause local irritation (Jorgenson & Levin, 1981; J. Lim & Ng, 1992; Marrelli, Tatullo, Dipalma, & Inchingolo, 2012; MCDONAGH, GAWKRODGER, &

WALKER, 1990; Otobe, de Sousa, Matthews, & Migliari, 2007; SATRIANO, ERICHETTI, & BARONI, 2012).

**Figure 4.2**



**Figure 4.2 White sponge nevus on the right buccal mucosa.** The characteristic thick, spongy, white plaques seen here are typically asymptomatic.

## 4.4 REACTIVE LESIONS

### 4.4.1 Frictional Hyperkeratosis

As the name implies, frictional hyperkeratosis (FH) on intraoral surfaces is caused by chronic trauma such as an ill-fitting denture, excessive tooth brushing, food impaction, or via a factitial injury (Fig. 4.3). The term *morsicatio mucosae oris* is also sometimes used to describe FH (Kang, Lee, Ro, & Lee, 2012; Woo & Lin, 2009). Regardless of the source of irritation, the oral epithelium reacts to chronic trauma via increased cellular turnover and keratin production, often with accompanying acanthosis and little to no inflammatory response of the underlying connective tissue (Chi et al., 2007; Woo & Lin, 2009).

FH lesions may be found on any intraoral surface, but most commonly affect the retromolar pad (area posterior to the last mandibular molar), the edentulous alveolar ridge, and the lateral tongue. FH lesions are discrete, non-ulcerated, non-erythematous, white papules or plaques with a rough to corrugated surface that cannot be wiped off (Natarajan & Woo, 2008). Histologically, a majority of cases are associated with benign epithelial hyperplasia along with significant surface bacterial colonization without any appreciable underlying inflammation (Woo & Lin, 2009). The location and clinical appearance of these lesions usually make their identification relatively straightforward.

FH has no known malignant potential and thus can be managed by treating the source of tissue irritation. Many patients may not consciously be aware of a causative oral habit, making it challenging to identify and modify the behavior. Occasionally, lesions may also be secondarily infected with opportunistic fungal organisms

necessitating the use of antifungal medications. Once the source of irritation has been removed along with any underlying infection, these lesions often completely resolve (Kang et al., 2012).

**Figure 4.3**

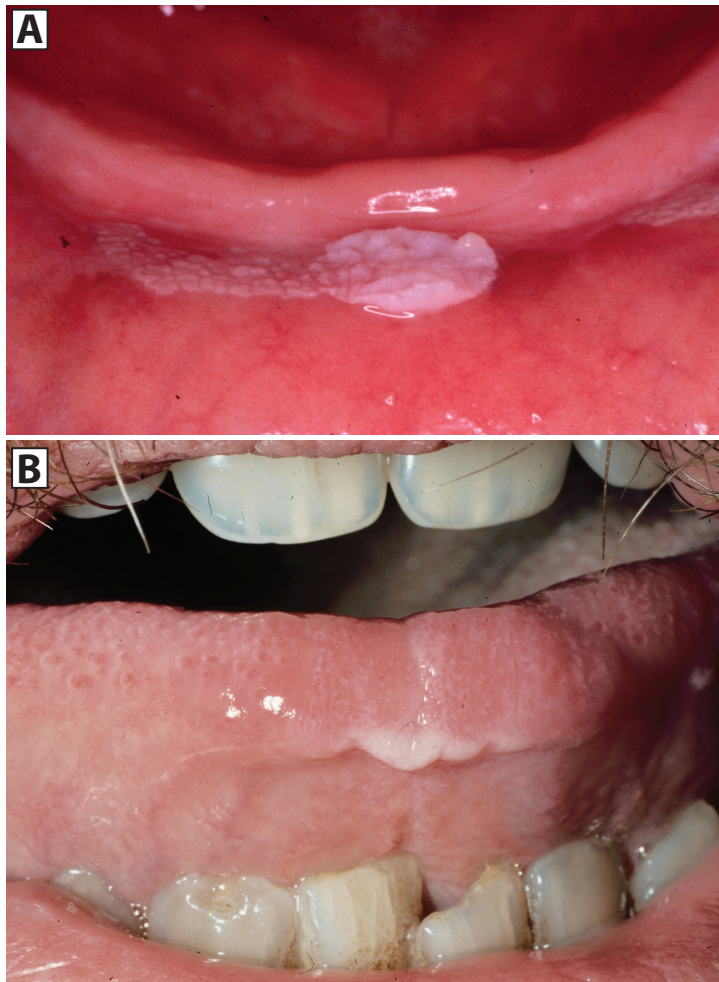


**Figure 4.3 Frictional hyperkeratosis. (A)** Frictional hyperkeratosis on the mandibular gingiva underneath an ill-fitting denture. **(B)** Frictional hyperkeratosis on the anterior tip of the tongue, likely due to chronic rubbing of the fractured lower incisor directly below the lesion.

#### **4.4.2 Smokeless Tobacco Changes**

Smokeless tobacco (ST) is used predominantly in one of three forms in the United States: a coarsely cut type known as chewing tobacco, a finely ground dry form known as snuff, and a finely ground moist form known as dipping tobacco. Placing the ST between the lip/cheek and the gingiva, typically in the lower vestibule, is seen in all three types. The use of ST has historically predominated in specific geographic regions of the US such as in the South and Midwest and within certain groups such as professional baseball players (Severson, Klein, Lichtensein, Kaufman, & Orleans, 2005; Tomar, 2003). From 2000 to 2010, the rate of ST use, specifically snuff, was on the rise in young, non-Hispanic white males (Bhattacharyya, 2012).

In addition to smokeless tobacco, since 2006 the use of electronic cigarettes (a.k.a. e-cigarettes) has been on the rise. These devices contain a metal heating element that vaporizes a solution containing nicotine and other chemicals into a vapor, which is then inhaled/exhaled by the user. Little is known about the long-term effects of e-cigarette use on the oral mucosa or any associations it may have with the development of oral cancer and periodontal disease. Further studies are needed to determine the role that e-cigarettes play, if any, in the development of oral mucosal lesions.

ST products have been known for decades to cause white changes in the oral mucosa adjacent to the area in which the tobacco is held. These mucosal changes are known as snuff dipper's lesion, tobacco pouch keratosis, or smokeless tobacco keratosis (Taybos, 2003). The lesional mucosa is painless and may show a white and

wrinkled, almost leathery appearance with or without erythema (Fig. 4.4). The lesion cannot be wiped away nor does it disappear upon stretching of the surrounding tissue. Up to 60% of individuals that use ST will develop some type of mucosal tissue change, especially those who use dipping tobacco and snuff (Allen, Vigneswaran, Tilashalski, Rodu, & Cole, 1995; "DCCPS: Behavioral Research Program: TCRB: Smoking and Tobacco Control Monographs," 1992; Grady et al., 1990; J. F. Smith, Mincer, Hopkins, & Bell, 1970; Taybos, 2003). There is a direct correlation between the amount and type of ST used and the degree of white changes seen clinically (Grady et al., 1990). If ST use is discontinued, these changes normally resolve completely within a matter of weeks, regardless of the length of time that ST was used. Interestingly, when ST lesions are biopsied, the vast majority typically only show hyperkeratosis and acanthosis of the epithelium, with minimal dysplasia (Allen et al., 1995; "DCCPS: Behavioral Research Program: TCRB: Smoking and Tobacco Control Monographs," 1992; Grady et al., 1990; J. F. Smith, 1975; J. F. Smith et al., 1970; Taybos, 2003). If cell atypia is present, it rarely rises above the level of mild dysplasia. More clinically problematic are the extensive periodontal defects found adjacent to areas of ST use, such as severe gingival recession and/or tooth abrasion (Chu, Tatakis, & Wee, 2010; "DCCPS: Behavioral Research Program: TCRB: Smoking and Tobacco Control Monographs," 1992; Taybos, 2003). Given that ST lesions rarely display dysplasia histologically, there has been considerable debate as to the role that ST plays in the development of oral cancer. Several studies using large longitudinal cohorts have shown that the progression to cancer from ST induced white lesions is negligible, leading many to now conclude that ST use, in the absence of other concurrent tobacco habits, contributes



only minimally to the risk of developing oral cancer (Roosaar, Johansson, Sandborgh-Englund, Nyrén, & Axéll, 2006; J. F. Smith, 1975; J. F. Smith et al., 1970).

After cessation of ST, any red and/or white changes that do not resolve within several weeks should be biopsied. For those who continue using ST, it is recommended that any suspicious red changes or ulcerations be biopsied immediately. Otherwise, ongoing clinical follow-up of ST lesions is recommended.

**Figure 4.4**



**Figure 4.4** Soft tissue changes of the right mandibular buccal vestibule where the patient habitually placed his smokeless tobacco. Note the significant occlusal wear of the last molar, which is often seen in conjunction with smokeless tobacco soft tissue lesions.

#### **4.4.3 Nicotine Stomatitis (Smoker's Palate)**

Nicotine stomatitis (NS), also known as smoker's palate, presents initially as erythema of the hard palate followed by the development of diffuse white papules and plaques, whose clinical appearance has been likened to that of a "dry riverbed" (Fig. 4.5). Punctuating the white plaques are red dots representing inflamed minor salivary gland ducts. NS is generally observed in those who smoke pipes/cigars, which is prevalent in men over the age of 45, or in those who engage in reverse smoking (smoking with the lit end of the cigarette inside the oral cavity) (Regezi, Sciubba, & Jordan, 2012; Taybos, 2003). It is believed that the combination of intense heat and carcinogens in the smoke irritates the tissue, resulting in NS. This hypothesis is supported by the observation that pipe/cigar smokers who wear a complete upper denture covering the hard palate while they smoke do not present with signs of NS (Ramulu, Raju, Venkatarathnam, & Reddy, n.d.). Histologically, there is hyperkeratosis, epithelial hyperplasia, and squamous metaplasia of the minor salivary gland ducts along with some inflammation of the glands themselves. These reactive changes usually resolve upon cessation of smoking (Regezi et al., 2012; Taybos, 2003).

NS palatal lesions in pipe/cigar smokers only occasionally exhibit mild dysplasia, thus they are not at high risk for malignant transformation. NS is, however, an indication of a heavy smoking habit and for this reason patients with NS should be thoroughly examined for other pre-neoplastic/neoplastic lesions elsewhere within the oral cavity (Regezi et al., 2012). Unlike pipe/cigar smokers, reverse smokers are much more likely to have substantial cellular atypia in NS lesions and have a significantly higher risk of developing squamous cell carcinoma of the hard palate (Ramulu et al., n.d.). Like

smokeless tobacco users, patients should be advised to discontinue using all tobacco products and any lesions that do not resolve after two to three weeks should be biopsied. For those who continue smoking, routine clinical follow-up is advised along with biopsies of any ulcerated or other suspicious areas. Special attention should be given to known reverse smokers since they are at a much higher risk of developing malignant neoplasms of the hard palate than pipe/cigar smokers.

**Figure 4.5**



**Figure 4.5 Nicotine stomatitis in a habitual pipe/cigar smoker.** Note the white cobblestone appearance of the hard palate and numerous red puncta representing inflamed minor salivary gland ducts.

#### 4.4.4 Hairy Tongue

Hairy tongue (HT) normally occurs on the posterior third to two thirds of the dorsal tongue. It is caused by an abnormal increase in the length of the filiform papillae along with a simultaneous decrease in their rate of desquamation. This leads to an accumulation of chromogenic bacteria, fungi, and debris that impart a variety of colors including black, green, yellow, tan, and white (Fig. 4.6) (Thompson & Kessler, 2010; WINER, 1958). There are many proposed causes including tobacco, alcohol, xerostomia, poor oral hygiene, oxidizing mouthwashes, antibiotics, and xerostomia inducing drugs (Korber & Dissemond, 2006; Thompson & Kessler, 2010). In one review, antibiotics were the causative agents in 18 (82%) of the 22 HT cases. Xerostomia inducing drugs, such as antipsychotics, were also strongly associated with HT (Thompson & Kessler, 2010). The lesion can present at any age, but is typically found in men over the age of 40, especially in those who smoke (Korber & Dissemond, 2006; Körber & Voshege, 2012; Thompson & Kessler, 2010). It is normally asymptomatic, however, for some patients the increased numbers of papillae can cause halitosis, dysgeusia, gagging, and nausea (Korber & Dissemond, 2006).

Patients with HT should be reassured that the changes are part of a completely benign process. Conservative treatments include abstention from smoking, alcohol, and drugs that may cause or exacerbate HT. An emphasis on excellent oral hygiene and gentle scraping of the dorsum of the tongue with a tongue scraper can also help aid in reducing the film on the tongue. While mechanical debridement remains the most widely used and effective therapy, several pharmacologic approaches have been various reported such as the use of gentian violet (an antifungal), topical triamcinolone

acetone, topical 40% urea solution, salicylic acid, podophyllin, and topical oral retinoids (Thompson & Kessler, 2010; WINER, 1958). While good oral hygiene is important in all patients, treatment is not necessary unless patients are symptomatic or find the condition cosmetically objectionable.

**Figure 4.6**



**Figure 4.6 Hairy tongue on the posterior two-thirds of the dorsal tongue.** Elongated filiform papillae with brown discoloration associated with a buildup of chromogenic bacteria, fungi, and/or debris can be seen.



#### 4.4.5 Hairy Leukoplakia

Hairy leukoplakia (HL) was first described in 1984 as a white lesion seen in young HIV positive homosexual men, who subsequently went on to develop AIDS. (D. Greenspan et al., 1984) Although it can be found on any intraoral site, HL predominantly presents on the lateral borders of the tongue, often bilaterally, and has slightly raised, ill-defined borders with a shaggy or corrugated surface (Fig. 4.7A) (Brasileiro, Abreu, & Mesquita, 2014; J. S. Greenspan et al., 1985). The Epstein Barr Virus (EBV) can be detected within affected cells of HL lesions and is now recognized as the causative etiologic factor (J. S. Greenspan et al., 1985; Brasileiro et al., 2014; J. S. Greenspan & Greenspan, 1989).

Histologically, HL shows hyperparakeratosis, acanthosis, and usually no dysplasia. Suprabasal, edematous, balloon-cells show EBV cytopathic changes such as a perinuclear halo and intranuclear peripheral condensation of chromatin (Fig. 4.7B-D). About half of these lesions are also secondarily infected with *Candida* species of fungi (J. S. Greenspan & Greenspan, 1989; Schiødt, Greenspan, Daniels, & Greenspan, 1987). It is not well understood why HL occurs predominantly on the lateral border of the tongue. Some studies have shown that Langerhans cells, a type of antigen presenting cell, are essentially absent in the epithelium of HL lesions (Daniels et al., 1987). Moreover, parts of the dorsal and lateral tongue naturally contain lower levels of Langerhans cells, which could predispose these areas to EBV infection or latent EBV reactivation in immunocompromised patients (Daniels, 1984; Daniels et al., 1987).

HIV infection along with other causes of local or systemic immunosuppression should be assessed in all cases of HL (A. E. Chambers et al., 2015; Epstein, Sherlock, & Greenspan, 1991). Treatment of HL should focus first on restoring a normal functioning immune system, when possible, since local treatments offer only a temporary resolution. In one study, bone marrow transplant patients with HL-like lesions following bone marrow ablation had no clinical signs of HL six months after bone marrow transplantation, suggesting that reconstitution of the immune system was sufficient to clear these lesions (Epstein, Sherlock, & Wolber, 1993). Systemic treatments with acyclovir as well as the topical use of gentian violet, retinoids, podophyllin, and acyclovir have been reported (Brasileiro et al., 2014; J. S. Greenspan & Greenspan, 1989). Good but temporary results have been reported with the use of combined acyclovir and podophyllin topical therapy (Brasileiro et al., 2014). Because fungal infections of HL lesions are present in about 50% of cases, it may be advisable to also treat these lesions concurrently with antifungal therapy.

**Figure 4.7**

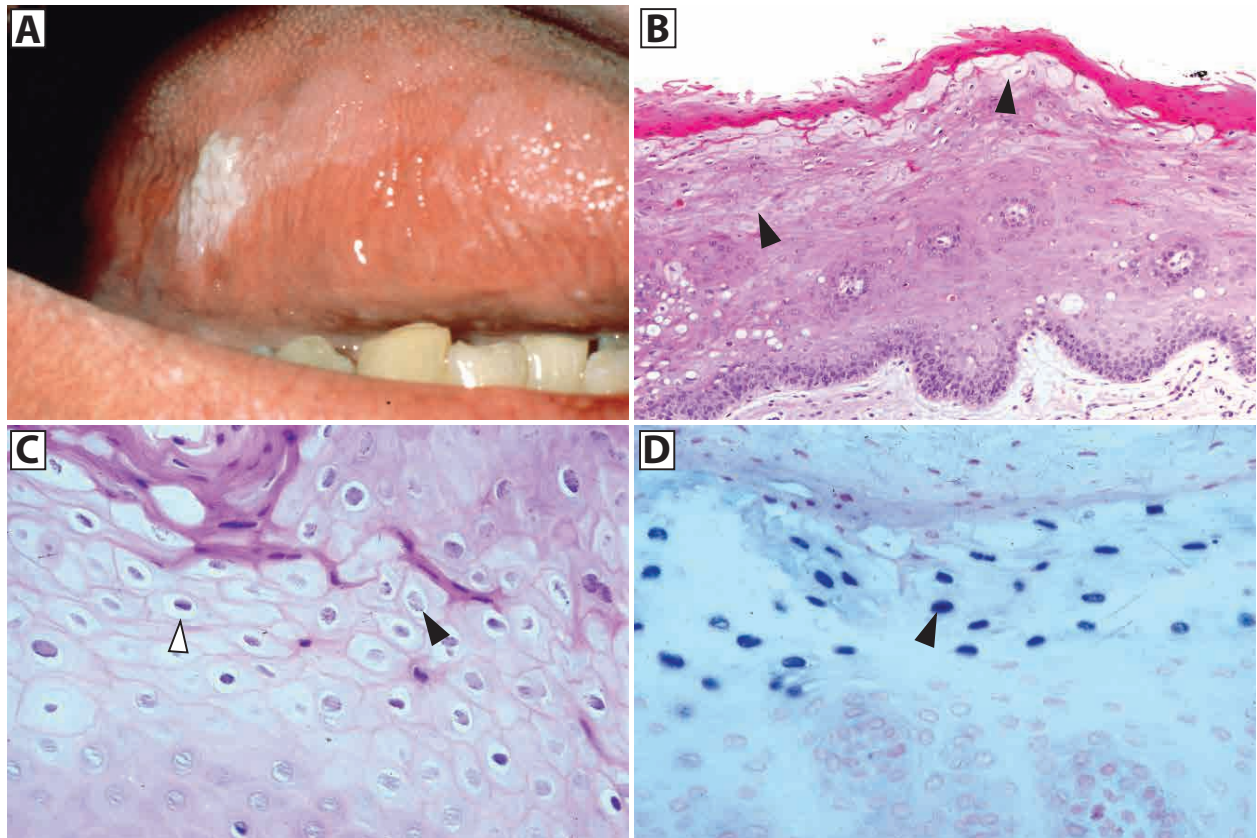


**Figure 4.7 Hairy leukoplakia. (A)** Hairy leukoplakia on the right lateral surface of the tongue. **(B)** Biopsy shows normal basal layer cells, acanthosis, hyperkeratosis, and cellular ballooning in the suprabasal layers (black arrowheads). **(C)** At higher magnification EBV cytopathic effects such as perinuclear halos (white arrowhead) and intranuclear peripheral condensation of chromatin (black arrowhead) can be seen. **(D)** In-Situ hybridization with an anti-EBV probe (EBER) shows positive cells in dark blue (black arrowhead). *EBV*, Epstein Barr Virus

## 4.5 INFLAMMATORY MEDIATED LESIONS

### 4.5.1 Oral Lichen Planus

Lichen planus is a well-known mucocutaneous disorder of presumptive autoimmune origin that may affect numerous sites including the skin, oral cavity, genitals, esophagus, nails, and scalp (Eisen, 1999). In contrast to the cutaneous form, oral lichen planus (OLP) tends to persist over time with less spontaneous remission (Carrozzo & Thorpe, 2009). OLP is polymorphous with six main patterns: reticular, erosive (ulcerative), papular, plaque-like, atrophic (erythematous), and bullous. Multiple forms may be present simultaneously and may change over time within the same patient, a finding that can aid in distinguishing OLP from pemphigus vulgaris and mucous membrane pemphigoid since mixed lesions are usually exclusive to OLP (Schlosser, 2010). The reticular and erosive forms of OLP are the most common (Axéll & Rundquist, 1987; Eisen, 2002; Schlosser, 2010). The reticular type is usually asymptomatic and is characterized by numerous white anastomosing lace-like lesions, known as Wickham's striae. In contrast, the erosive form tends to be painful and is usually comprised of both ulcerated and reticular areas.

OLP lesions may be present on any intraoral surface; however, they are most commonly found bilaterally on the buccal mucosa followed by the gingiva, dorsal tongue, lateral tongue, labial mucosa, and floor of mouth (Fig. 4.8A-B) (Eisen, 2002). Depending on the population studied, OLP has a prevalence of 0.11% to 1.9% and affects middle aged women more often than men in an approximately 2:1 to 3:1 ratio (Axéll & Rundquist, 1987; Bouquot & Gorlin, 1986; Eisen, 1999; 2002). The histology of

OLP is similar to cutaneous forms with a band-like infiltrate of lymphocytes at the junction of the epithelium and connective tissue, hyperparakeratosis, basal keratinocyte vacuolar changes, and apoptotic cells (Civatte bodies). Unlike cutaneous forms of lichen planus, OLP lesions show deposition of fibrinogen along the basement membrane, which can be detected using direct immunofluorescence and is often helpful in establishing the diagnosis (Fig. 4.8C-D). The microscopic findings should always be correlated with the patient's clinical presentation, as the histologic features of OLP are not always pathognomonic and may mimic other conditions such as hypersensitivity reaction.

Prior to treatment, presumptive OLP lesions should be biopsied to confirm the diagnosis. In contrast to cutaneous lichen planus, the generally accepted practice is to biopsy oral lesions with emphasis on atypical or unusual appearing forms. Biopsy also permits microscopic examination to rule out dysplasia and OSCC, both of which can arise in the setting of OLP and can clinically mimic atypical forms of OLP. Oral lesions may precede cutaneous or genital involvement and patients should be assessed for this possibility (Eisen, 1999). OLP is often initially treated with systemic and topical corticosteroids, although the use of other immune modulating drugs, such as cyclosporine and tacrolimus, have been reported (Carrozzo & Thorpe, 2009; Schlosser, 2010). For maintenance therapy, topical corticosteroids such as fluocinonide (0.05%) and clobetasol propionate (0.05%), applied to affected areas one to five times per day, depending on disease severity, are effective. Several delivery methods are available and include ointments and mouth rinses, but clinicians should be aware that a significant challenge is the short contact time between steroid and lesion for many oral

preparations. Corticosteroids in ointment form may be applied topically via a vehicle (modified dental trays or gauze) in order to improve contact time with tissues (Aleinikov, Jordan, & Main, 1996). Additionally, corticosteroids can be compounded with orabase-b, a sticky dental paste containing benzocaine, in a 1:1 ratio that can be very helpful in achieving adequate contact time with oral mucous membranes. If corticosteroids in liquid form are used, such as dexamethasone elixir (0.1mg/ml), rinsing for one minute one to two times daily and abstaining from eating or drinking for 60 minutes afterwards can also be helpful in treating widespread OLP lesions.

The risk of OLP transforming into oral cancer is controversial and not fully understood (Bombeccari et al., 2011; Eisen, 2002; Rödström, Jontell, Mattsson, & Holmberg, 2004; van der Meij et al., 1999). Current studies estimate the incidence of oral squamous cell carcinoma (OSCC) in OLP patients to be between 0.36% and 1% over five years (Carrozzo & Thorpe, 2009; van der Meij et al., 1999). Since patients with OLP may have a slightly increased risk of developing OSCC, they should be routinely clinically screened, often every six months to once a year, to ensure that their OLP is well controlled and to monitor for the development of dysplasia and OSCC (Mignogna, Fedele, & Russo, 2006). Routine biopsies of OLP lesions are usually not indicated unless clinically observable changes have occurred, such as changes in color, texture, pain, etc. or the presence of non-healing, treatment refractory ulcers. Biopsies in these instances are warranted in order to ensure that any such changes are not pre-neoplastic or malignant.

**Figure 4.8**

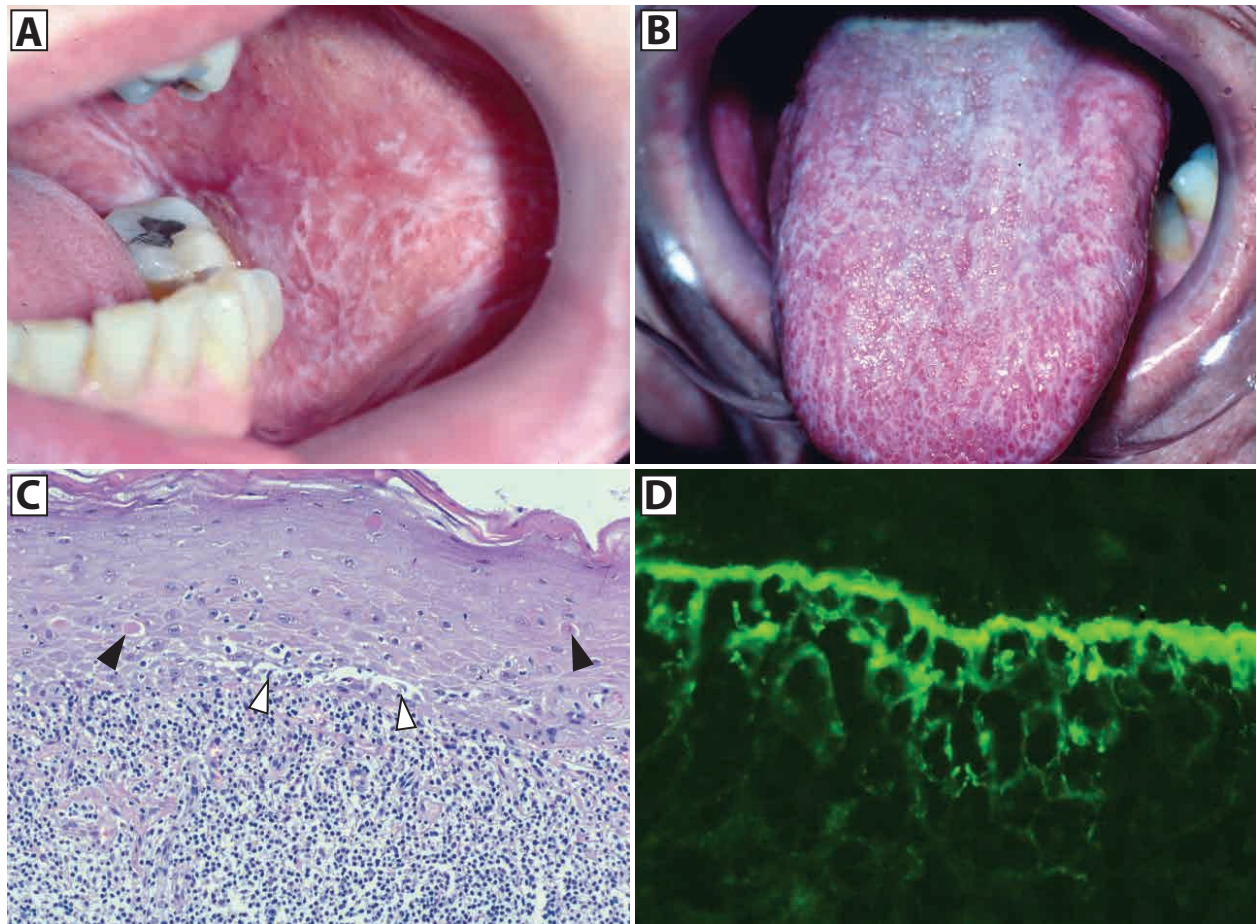


**Figure 4.8 Oral lichen planus.** (A) Reticular form of OLP on the left buccal mucosa. (B) Reticular form of OLP on the dorsal tongue. (C) Lesional biopsy showing a band-like infiltrate of lymphocytes at the epithelial-connective tissue junction, hyperkeratosis, and basal layer keratinocyte destruction in the form of vacuolar degeneration (white arrowheads) and dying keratinocytes (black arrowheads). (D) Direct immunofluorescence showing deposits of fibrinogen at the basement membrane. *OLP*, oral lichen planus

#### 4.5.2 Oral Lichenoid Reactions

Oral lichenoid reactions (OLR) are nearly identical clinically and histologically to OLP (Fig. 4.9). OLR occur less frequently intraorally than they do in the skin and tend to present unilaterally, occasionally with ulcerations (McCartan & McCreary, 1997). Although the pathogenesis of these reactions is not well understood, various medications have been implicated and the list of possible offenders is legion. The most commonly reported drugs associated with OLR are non-steroidal anti-inflammatory medications, antihypertensives, and HIV antiretrovirals (Schlosser, 2010). Treatment of these lesions involves removal of the offending drug, if possible, or management with topical corticosteroids. Other lichenoid reactions can be caused by dental restorative materials and certain food flavorings. Amalgam fillings containing mercury are one of the most common causes of OLR, although similar reactions to many other dental restorative materials such as nickel and composite resins have been documented (Issa, Duxbury, Macfarlane, & Brunton, 2005; Schlosser, 2010). Flavoring agents like cinnamaldehyde and peppermint oil used in chewing gum or dental hygiene products are also known to cause OLR (Morton, Garioch, Todd, & Lamey, 1995; Tremblay & Avon, 2008). OLR lesions are normally in close proximity to the source of irritation and often present with reticular or erosive lesions nearly identical to those seen in OLP. Treating lesions can be challenging, as it is sometimes difficult to identify the source of irritation. Once the irritant is removed, oral lesions normally completely resolve. Lichenoid lesions that do not resolve should be biopsied to rule out dysplasia and OSCC. If the irritant cannot be identified, treatment with topical corticosteroids should be initiated.



Distinguishing OLP from OLR is nearly impossible by microscopy alone. Four features that have been suggested to differentiate OLR from OLP are: 1) an inflammatory infiltrate located deep to the superficial infiltrate in some or all areas, 2) a focal perivascular infiltrate, 3) plasma cells in the connective tissue, and 4) neutrophils in the connective tissue. Clinically, OLRs tend to present unilaterally whereas OLP has a symmetric distribution. Ultimately, a final diagnosis is made based on a synthesis of both clinical and pathological information (Thornhill et al., 2006).

**Figure 4.9**

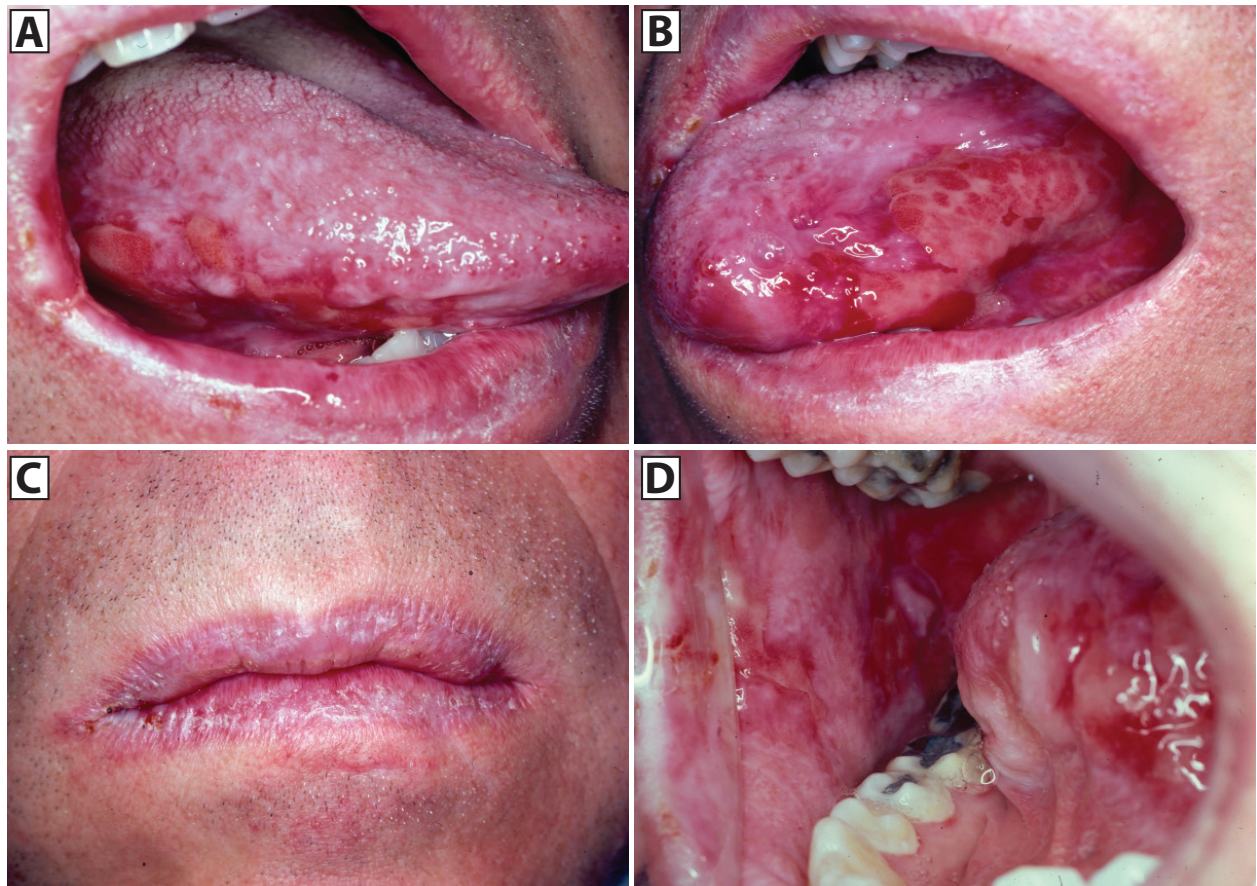


**Figure 4.9 Oral lichenoid reaction.** Drug induced OLR on the **(A)** right lateral tongue; **(B)** left lateral tongue; **(C)** lips; **(D)** right buccal mucosa from the same patient. The reticular and erosive patterns seen here are clinically similar to changes seen in OLP. *OLR*, oral lichenoid reaction; *OLP*, oral lichen planus

## **4.6 PRE-NEOPLASTIC/NEOPLASTIC**

### **4.6.1 Oral Leukoplakia**

The usage and application of the term 'oral leukoplakia' (OL) has generated confusion and controversy. In its simplest form, OL simply means a white patch found within the oral cavity. This broad definition encompasses all pathologic processes of the oral mucosa that culminate in the formation of an intraoral white patch. Since some benign intraoral white lesions can be diagnosed clinically, several groups have advocated a narrower definition of OL. Although the exact terminology continues to evolve, OL in this context is generally defined as an idiopathic white lesion that cannot be wiped off, cannot be characterized as any other definable lesion, and has malignant potential (Warnakulasuriya, Johnson, & van der Waal, 2007). This definition implies that a biopsy has yet to be performed, making the preliminary clinical diagnosis of OL a placeholder until a histologic diagnosis can be made. When biopsied, OL lesions often show hyperkeratosis or grades of epithelial dysplasia microscopically; once a microscopic diagnosis has been rendered, this diagnosis then becomes the correct clinical diagnostic term (Fig. 4.10).

Four clinical patterns of OL have been described: homogeneous, nodular, speckled (i.e. contains red and white changes), and proliferative verrucous leukoplakia (Warnakulasuriya, 2001). These lesions occur within a wide age range, although the majority develop during the 5<sup>th</sup> and 6<sup>th</sup> decades of life (Chi et al., 2007; Natarajan & Woo, 2008; Silverman, Gorsky, & Lozada, 1984). The male-to-female ratio varies depending on geographic location, although in two retrospective studies conducted

within the United States, the ratios were 1.3:1 and 3.7:1 (Chi et al., 2007; Natarajan & Woo, 2008; van der Waal, 2014). Several risk factors associated with developing OL have been identified. These include certain genetic disorders such as dyskeratosis congenita and fanconi anemia, the use of tobacco or areca/betel nut, and alcohol consumption (Grein Cavalcanti et al., 2015; Napier & Speight, 2008; Shiu, Chen, Chang, & Hahn, 2000; Treister, Lehmann, Cherrick, Guinan, & Woo, 2004). In one retrospective review of 1,676 clinically diagnosed OLs, most lesions originated from the tongue (28%) followed by the buccal mucosa (19%), mandibular sulcus (15%), palate (13%), maxillary sulcus (11%), floor of mouth (11%), and labial mucosa (2%). The vast majority of these lesions were diagnosed as idiopathic hyperkeratosis without dysplasia (75%), mild to moderate dysplasia (19%), severe dysplasia to carcinoma in-situ (5%), and OSCC (1%) (Chi et al., 2007). In general, any intraoral white lesion fitting the clinical criteria of OL should be biopsied, especially if it has any associated red changes, as these mixed red and white lesions (known as erythroleukoplakias) have a significantly higher risk of presenting with, or progressing to, OSCC (Napier & Speight, 2008; Silverman et al., 1984).

Any OL, as defined in this review, has pre-malignant potential, but those that contain epithelial dysplasia microscopically have a higher risk of transforming into OSCC than those without dysplasia (Lumerman, Freedman, & Kerpel, 1995; Mehanna, Rattay, Smith, & McConkey, 2009; Silverman, Gorsky, & Kaugars, 1996). A recent meta-analysis analyzing the overall malignant transformation rate of OLs reported ranges of 0.0% to 36.4%, with an overall pooled average of 12.3%. When accounting for the histologic grade of dysplasia present (mild to moderate vs. severe to carcinoma

in-situ), the rates were 10.3% and 24.1%, respectively (Mehanna et al., 2009). In another study, the pooled malignant transformation rate of OLs with severe dysplasia or carcinoma in-situ was 15.6% (Bouquot, Speight, & Farthing, 2006). In contrast, some studies report that for the individual patient the grade of dysplasia does not predict the risk of transformation to OSCC (Arduino et al., 2009). Several risk factors for malignant transformation of OL have been assessed and include a history of never smoking (presumably due to underlying genetic aberrations), a history of heavy smoking, female gender, intraoral site where the lesion is located (e.g. the floor of mouth and lateral borders of the tongue are at higher risk of malignant transformation than other intraoral sites such as the buccal mucosa and gingiva), size of the lesion, homogeneity vs. heterogeneity of the lesion, presence of dysplasia, and altered p53, p16INK4a, and Ki-67 expression patterns; none, however, are reliably predictive (Ho et al., 2012; Holmstrup, Vedtofte, Reibel, & Stoltze, 2006; Nasser, Flechtenmacher, Holzinger, Hofele, & Bosch, 2011; Silverman et al., 1996).

Clinical management of OL lesions has proven difficult. Various treatment options such as surgical excision, laser ablation, photodynamic therapy, cryotherapy, and topical/systemic therapies have been used; however, strong evidence in the form of randomized, controlled trials evaluating their effectiveness in preventing recurrence and/or transformation to OSCC is lacking (Lodi & Porter, 2008; M Clin Dent et al., 2014). Currently, idiopathic hyperkeratotic and mildly dysplastic lesions are usually carefully monitored, whereas lesions with moderate to severe dysplasia or carcinoma in-situ are removed along with normal marginal tissue. Surgical excision is preferred because unlike laser ablation that destroys lesional tissue, surgical excision allows for

histologic study of the specimen in order to assess for variations in the grade of dysplasia and the presence of OSCC. Although some smaller studies do not show a decrease in OSCC transformation rates for patients who have had their dysplastic lesions removed surgically, a meta-analysis of 14 studies comprising over 900 patients showed that these rates actually do decrease by more than half from 14.6% to 5.4% after surgical excision (Lodi & Porter, 2008; Mehanna et al., 2009).

Recurrence is a common problem following excision of any OL. One retrospective study of 52 patients that underwent surgical excision of OL lesions reported a recurrence rate of around 15%, although recurrence rates ranging from 5% to 39.5% have also been reported (Brouns et al., 2013; Kuribayashi, Tsushima, Sato, Morita, & Omura, 2012). Interestingly, the grade of dysplasia in these studies did not predict the risk of recurrence (Brouns et al., 2013; Kuribayashi et al., 2012). Significant risks for recurrence included age over 59 years, lesions on the gingiva, positive surgical margins, and surgical margins less than 3mm. The median time between surgery and recurrence was 17 months (range 2 to 40 months) (Kuribayashi et al., 2012). Smoking cessation has been shown to reduce the rate of recurrence as well as lower the risk of transformation into OSCCs (Silverman et al., 1984; Vladimirov & Schiødt, 2009). Some studies have even shown that smoking cessation may cause a reduction or complete regression of OL lesions over time (Napier & Speight, 2008; Silverman et al., 1984).

Clinicians should be particularly cautious of OLs on the floor of mouth, gingiva, and lateral/ventral tongue since conversion rates to OSCC are higher at these sites. Some groups report that the majority of OLs that will transform into OSCCs do so during the first two to five years of follow-up after biopsy, with lower transformation rates in

subsequent years (Arduino et al., 2009; Napier & Speight, 2008; Silverman et al., 1984). For this reason, we believe it is critical to closely monitor patients every three to four months following a diagnosis of idiopathic hyperkeratosis/dysplasia, even though some question whether this practice actually improves survival rates of patients that eventually convert to OSCC (van der Waal, 2014). Any change in the color and texture of OL or the development of discomfort/pain in the vicinity of these lesions warrants a new biopsy. More research is needed to identify and validate molecular markers that can predict which OL lesions will progress to OSCC as well as which treatment modalities offer patients the best long-term outcomes.

#### **4.6.2 Squamous Cell Carcinoma**

Squamous cell carcinoma (SCC) of the head and neck, which includes various anatomic sites such as the nasal/paranasal sinuses, oral cavity, oropharynx, hypopharynx, and larynx, is the sixth most common cancer worldwide and affects between 35,000 and 45,000 people annually within the United States (Chung et al., 2014; Warnakulasuriya, 2009; Yan, Wistuba, Emmert-Buck, & Erickson, 2011). The overall 5-year survival rate is approximately 57%, however, those diagnosed at earlier stages may have improved 5-year survival rates of up to 75% to 90% (Bagan, Sarrion, & Jimenez, 2010; Feller & Lemmer, 2012; Yan et al., 2011). Indeed, the stage of the disease at the time of diagnosis, which takes into account tumor size, involvement of regional lymph nodes, and distant metastases, is one of the strongest prognostic factors for patient survival (Feller & Lemmer, 2012). Unfortunately, about two-thirds of patients will present with advanced disease upon initial diagnosis (Feller & Lemmer, 2012).

Although SCC diagnosed in the mouth and throat are often collectively known simply as 'oral cancer', the oral cavity and oropharynx have distinct anatomic boundaries as well as risk factors associated with SCC development and overall prognosis. By convention, the oral cavity includes the anterior two thirds of the tongue and all intraoral soft tissues anterior to the first tonsillar pillar (the palatoglossal arch). In turn, the oropharynx comprises the posterior third of the tongue (base of tongue) and is bordered superiorly by the soft palate, laterally by the tonsillar pillars and palatine tonsils, and inferiorly by the epiglottis. Known risk factors associated with both oral and oropharyngeal SCC include the use of cigarettes, alcohol, and betel quid/paan (Feller & Lemmer, 2012; Warnakulasuriya, 2009). Conversely, high risk human papilloma virus subtypes (usually HPV 16) are a significant risk factor for developing oropharyngeal SCCs, but not oral SCCs, since the virus is found in up to 72% of these cancers compared to only 7% of oral SCCs (Chung et al., 2014).

Oral SCC can present clinically in a number of ways. The classical presentation is that of a non-healing ulcer with indurated borders. However, it can also commonly appear as a white and/or red patch or as an exophytic/verrucous mass (Fig. 4.10) (Feller & Lemmer, 2012; Massano, Regateiro, Januário, & Ferreira, 2006). Although SCC can occur anywhere in the oral cavity, favored high risk sites include the lateral/ventral tongue and floor of mouth (Bagan et al., 2010; Feller & Lemmer, 2012). Because of its ability to clinically mimic other benign and pre-neoplastic intraoral white lesions, a biopsy and microscopic examination are crucial in determining the correct diagnosis. Once diagnosed, patients are typically treated surgically along with radiotherapy and/or chemotherapy, all of which have significant side effects.



Figure 4.10

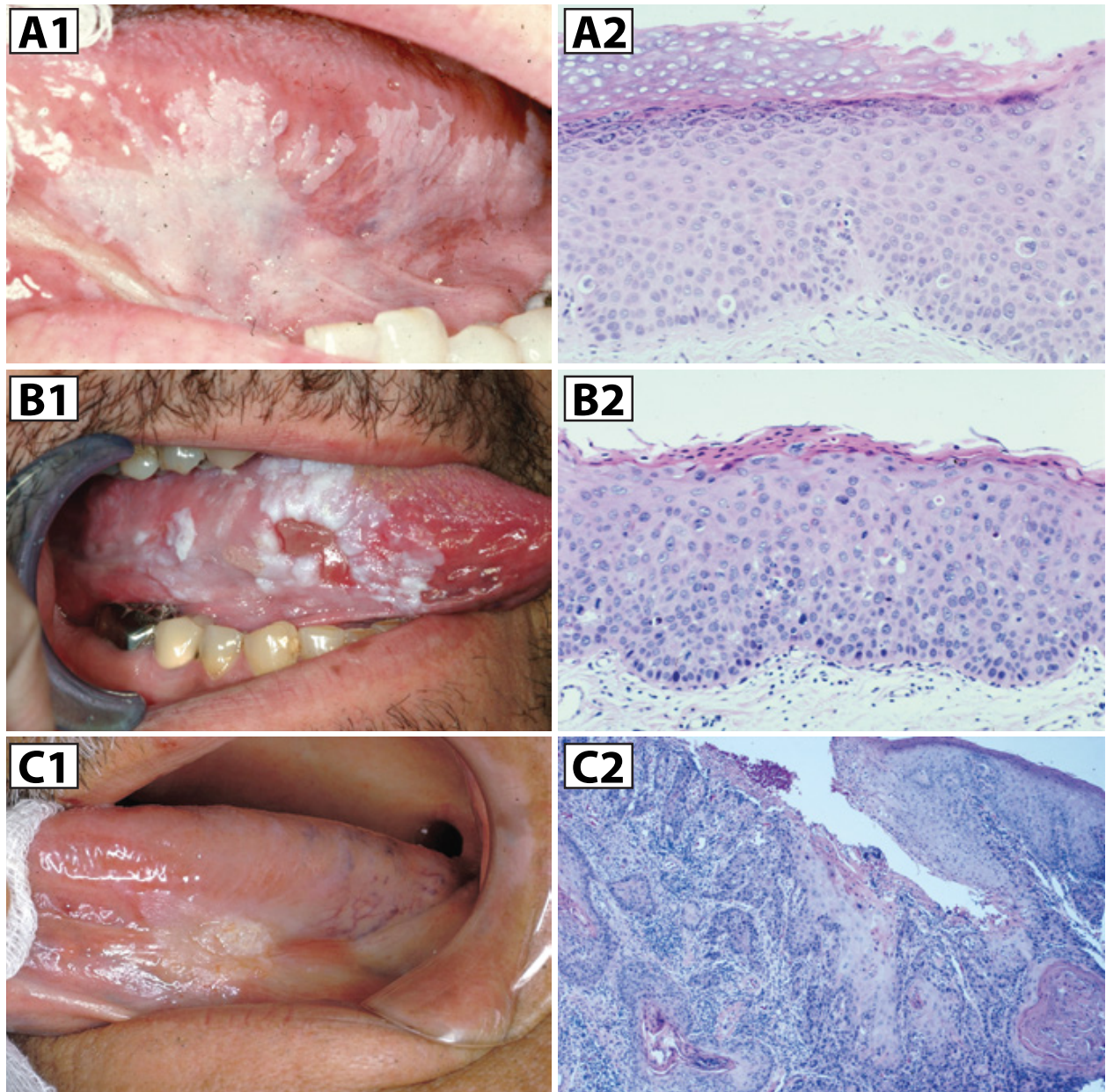


**Figure 4.10 Oral leukoplakia.** (A1, B1, C1) Intraoral white lesions preliminarily described clinically as oral leukoplakia prior to biopsy. The corresponding microscopic diagnosis of each lesion was (A2) moderate dysplasia; (B2), severe dysplasia; (C2), squamous cell carcinoma. Prior to biopsy, oral leukoplakias can look similar clinically, underscoring the need for biopsy in order to properly diagnose and treat these lesions.

## **4.7 OTHER**

### **4.7.1 Geographic Tongue (Benign Migratory Glossitis)**

Geographic tongue, also known as benign migratory glossitis (BMG), is a benign condition of the tongue whose etiology is currently unknown and that affects approximately 2% of the United States population (Regezi et al., 2012). Single or multiple well-defined circinate areas of erythema due to depapillation (loss of filiform papillae) can be seen on the dorsal tongue surrounded by white borders (Fig. 4.11). These lesions may resemble a topographical map (hence the name geographic tongue) and often change shape and location within hours to days (Menni, Boccardi, & Crosti, 2004). Although predominantly located on the dorsal tongue, BMG lesions may also rarely occur on other intraoral surfaces, such as the buccal mucosa and gingiva, and in this context is known as erythema migrans (O'Keefe, Braverman, & Cohen, 1973). Lesions often wax and wane over time and are normally asymptomatic; however, occasionally patients with BMG lesions will complain of burning, dysgeusia (altered taste sensation), or discomfort in response to acidic and/or spicy foods.

Histologically, BMG resembles psoriasis, especially pustular psoriasis (O'Keefe et al., 1973). Sterile spongiotic pustules and subcorneal pustules composed of neutrophils can be identified in areas of depapillation on the tongue along with psoriasiform hyperplasia of the epithelium. These pustular areas are bordered microscopically by hyperkeratotic epithelium that corresponds clinically with the white borders of BMG lesions. Despite the microscopic similarities shared with psoriasis, there is no convincing evidence of a relationship between the two diseases (Darwazeh,

Al-Aboosi, & Bedair, 2012; Miložlu, Göregen, Akgül, & Acemoğlu, 2009; Shulman & Carpenter, 2006).

Patients with symptomatic BMG can be managed in a number of ways. First, it is often helpful to rule out any fungal infection, as this can mimic or exacerbate BMG related signs and symptoms. The avoidance of acidic and/or spicy foods may also prove helpful in relieving symptoms. Pharmacologic treatments include the use of systemic and/or topical corticosteroids (Menni et al., 2004). In cases refractory to corticosteroids, some groups have reported success using systemic cyclosporine and topical tacrolimus (Abe et al., 2007; Ishibashi et al., 2010). BMG lesions do not need to be biopsied since they are usually straightforward to identify clinically and are completely benign.

**Figure 4.11**

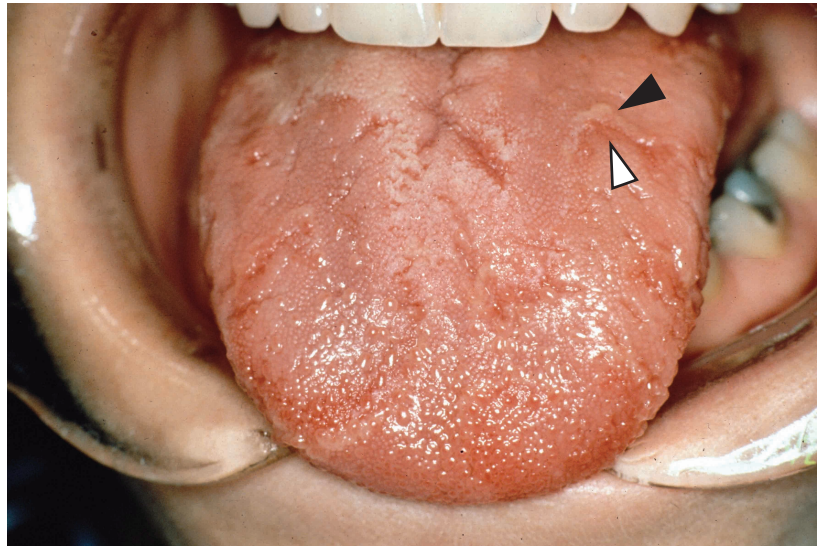


**Figure 4.11 Geographic tongue.** Multiple circinate areas of erythema due to depapillation (i.e. loss of filiform papillae, white arrowhead) surrounded by white borders (black arrowhead) can be seen. These lesions are usually asymptomatic.

## **4.8 CONCLUSION**

Intraoral white lesions have numerous etiologies and include a range of benign and malignant disorders. Most cases require biopsy to establish the diagnosis and to select/initiate the appropriate therapy. Further research into the potential roles that oral epithelial progenitor cells play in the pathogenesis of these lesions could enable the discovery of novel therapeutics and treatment strategies for these diseases.

## CHAPTER 5

### Summary and Future Perspectives

Epithelial progenitor cells in both the epidermis and the oral mucosa are integral to the proper formation of numerous structures within the craniofacial complex during embryonic development, such as teeth, hair follicles, and sweat glands. When problems arise during development that impair the formation of these structures, such as in patients with X-linked hypohidrotic ectodermal dysplasia (XL-HED), the downstream sequelae can be significant. Through the use of several qualitative and quantitative techniques in Chapter 2, I identified the location and organization of oral epithelial progenitor cells, studied their division kinetics and behavior, and showed that they are able to alter their daughter cell fates in response to chemotherapy-induced damage in order to maintain integrity of the mucosa. In Chapter 3, I used novel techniques such as phototrichogram analysis and in-vivo confocal imaging to characterize some of these sequelae, specifically by measuring the hair and sweat gland phenotypes in patients with XL-HED. In addition to their role in development, epithelial progenitor cells also maintain homeostasis in the adult epidermis and oral mucosa. Finally, in Chapter 4, I described numerous pathologies of the oral mucosa that are likely associated with oral epithelial progenitor cell dysfunction. Taken together, these findings underscore the importance that epithelial progenitor cells have in both the development and maintenance of numerous structures and tissues within the craniofacial complex.

Further research into the biology of embryonic and adult epithelial progenitor cells will be vital to understanding their function in normal tissue homeostasis and disease. This will enable the development of novel therapies that precisely target the causes of oral and epidermal epithelial diseases as opposed to merely treating symptoms. For example, the elucidation of the molecular underpinnings in early progenitor epithelial cells that cause XL-HED (i.e. disruption of the ectodysplasin signaling pathway) has led to the creation of novel therapies that, when given at the proper time during development, can significantly abrogate sequelae seen in XL-HED patients. Another example is the possible role that oral epithelial progenitor cells play in the initiation and maintenance of malignant tumors within the oral cavity, such as squamous cell carcinoma. As I indicated in Chapters 1 and 2, the concept of cancer stem cells has gained significant traction over the last several years as a potential explanation for the long-term maintenance of tumors as well as their resistance to anti-tumor therapies. By learning more about the basic biology of oral epithelial progenitor cells, it may be possible to apply this knowledge to tumor biology, which could lead to the development of novel therapies that specifically target the cells giving rise to a tumor as opposed to other tumor cells that may have limited growth potential. The same is true for other pathologies associated with the oral epithelium and mucosa, such as oral epithelial dysplasias. Indeed, understanding the relationship between epithelial progenitor cells and specific disease states within the oral mucosa and craniofacial complex will provide new avenues for potentially groundbreaking research that could significantly affect patients' lives.

There is still significant work that needs to be done in this field and multiple key questions still remain: What are the exact molecular signals that determine daughter cell fate following epithelial progenitor cell division? Is it possible to manipulate these signals for therapeutic outcomes, e.g. improved healing in patients? How are epithelial progenitor cells related to cancer stem cells? What about in other congenital and acquired epithelial diseases? As new technologies and experimental methods are developed, it will be exciting to tackle these questions, along with many others related to craniofacial epithelial progenitor cell biology, with the ultimate goal of improving patients' lives.



**SUPPLEMENTAL MATERIAL**

**Supplemental Table 1 Hair Characteristics of Control and XL-HED Subjects**

|   | Control (N=12) <sup>1</sup> |               | XL-HED (N=11) <sup>1</sup> |            | p-value <sup>3</sup> |
|---|-----------------------------|---------------|----------------------------|------------|----------------------|
|   | Median                      | IQR           | Median                     | IQR        |                      |
| <b>Hair Count Characteristic<sup>2</sup></b>                        |                             |               |                            |            |                      |
| Total hair count  | 212                         | 195.5 – 296.5 | 93                         | 80 – 134   | 0.0001               |
| Total terminal hair count   | 197.5                       | 176.5 – 268   | 84                         | 64 – 97    | <0.0001              |
| Total vellus hair count   | 21                          | 18 – 38       | 26                         | 6 – 40     | 0.56                 |
| Ratio of terminal to vellus hairs                                   | 8.7                         | 6.4 – 11.1    | 3.2                        | 2.4 – 14.5 | 0.30                 |
| Number of subjects with a terminal to vellus hair ratio <4:1, n (%) | 0 (0%)                      |               | 6 (54.5%)                  |            | 0.0046*              |
| <b>Follicular Unit Characteristic<sup>3</sup></b>                   |                             |               |                            |            |                      |
| Total follicular units  | 135.5                       | 121 – 180.5   | 88                         | 78 – 118   | 0.0021               |
| Hairs per follicular unit   | 1.6                         | 1.4 – 1.8     | 1                          | 1 – 1.1    | 0.0003               |
| % of follicular units with 1 hair                                   | 50.5                        | 44.5 – 59.5   | 97.2                       | 90.6 – 100 | 0.0004               |
| % of follicular units with 2 hairs                                  | 36                          | 32.6 – 40.9   | 2.8                        | 0 – 9.4    | 0.0004               |

| <b>Follicular Unit</b>                        |      |             |      |             |         |
|---|------|-------------|------|-------------|---------|
| <b>Characteristic<sup>3</sup></b>             |      |             |      |             |         |
| % of follicular units with 3 hairs            | 10.6 | 4.2 – 16.6  | 0    | 0 – 0       | 0.0001  |
| % of follicular units with 4+ hairs           | 0.7  | 0 – 3.2     | 0    | 0 – 0       | 0.0064  |
| Mean width per terminal hair (mm)             | 71   | 59 – 76.3   | 50.5 | 44.5 – 56.2 | 0.0007  |
| Mean width per vellus hair (mm)               | 20.1 | 18.7 – 22.1 | 21.3 | 20 – 24.1   | 0.36    |
| <b>Hair Growth Characteristic<sup>2</sup></b> |      |             |      |             |         |
| Number of terminal hairs in anagen growth     | 180  | 161 – 232.5 | 70   | 52 – 97     | <0.0001 |
| Number of vellus hairs in anagen growth       | 5    | 4 – 9.5     | 5    | 1 – 16      | 0.88    |
| % Terminal hairs in anagen growth             | 89.5 | 85.9 – 92.5 | 86.3 | 80.5 – 97.9 | 0.81    |
| % Vellus hairs in anagen growth               | 21.1 | 17.3 – 34.7 | 33.3 | 17.2 – 45.5 | 0.31    |
| Terminal hair growth rate (mm/hour)           | 16.2 | 14.6 – 18   | 10.1 | 9.6 – 12    | 0.0001  |

<sup>1</sup>Alignment of phototrichogram images for full analysis was not possible for control subject #11 and XL-HED subject #4 due to their light hair color. These subjects were thus not included in the hair analyses, decreasing the sample size in each group by one.

<sup>2</sup>All hair analyses are based on a surface area of 1 cm<sup>2</sup>.

<sup>3</sup>p-values marked with \* were calculated using a two-sided Fisher's exact test; otherwise, p-values were calculated using the Wilcoxon rank-sum test.

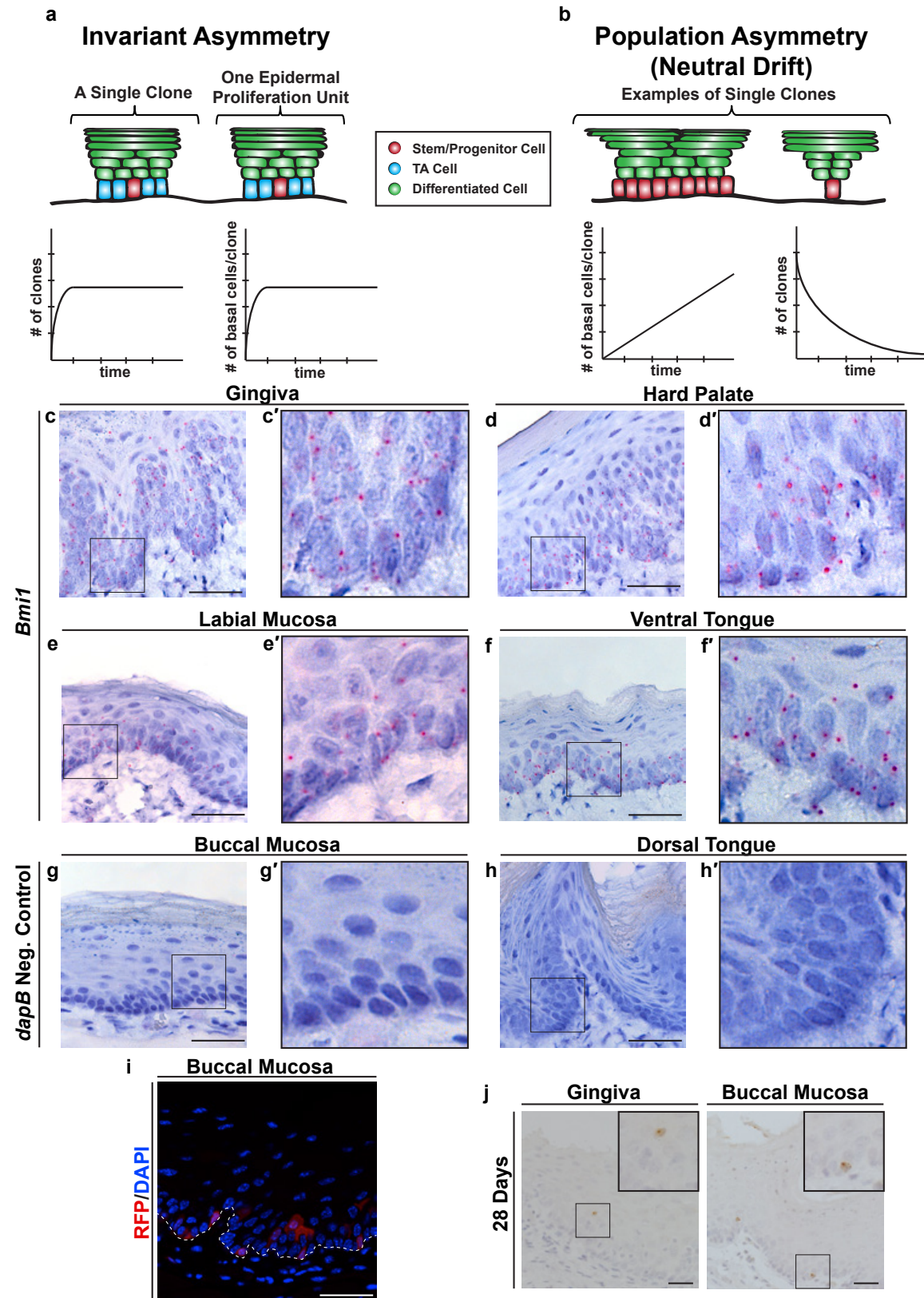
**Supplemental Table 2 *EDA-A1* Genotyping Results for XL-HED Subjects**

| <b><i>EDA-A1</i><br/>Gene<br/>Mutation<sup>1</sup></b> | <b>Exon</b> | <b>Mutation Type</b> | <b>Domain Affected</b> | <b>Previously Reported</b> |
|--|-------------|----------------------|------------------------|----------------------------|
| 895G>A<br>(Gly299Ser)                                  | 7           | Missense             | TNF                    | Reported                   |
| 1070G>C<br>(Arg357Pro)                                 | 8           | Missense             | TNF                    | Reported                   |
| 164T>A<br>(Leu55Gln)                                   | 1           | Missense             | Transmembrane          | Leu55Arg Reported          |
| 164T>A<br>(Leu55Gln)                                   | 1           | Missense             | Transmembrane          | Leu55Arg Reported          |
| 463C>T<br>(Arg155Cys)                                  | 2           | Missense             | Furin                  | Reported                   |
| 463C>T<br>(Arg155Cys)                                  | 2           | Missense             | Furin                  | Reported                   |
| 553_588del   | 4           | Deletion             | Collagen               | Reported                   |
| 467G>A<br>(Arg156 His)                                 | 2           | Missense             | Furin                  | Reported                   |

| <b><i>EDA-A1</i></b><br><b>Gene</b><br><b>Mutation<sup>1</sup></b> | <b>Exon</b> | <b>Mutation Type</b>     | <b>Domain Affected</b> | <b>Previously Reported</b>    |
|--|-------------|--------------------------|------------------------|-------------------------------|
| 822delG  | 7           | Deletion<br>(Truncating) | TNF                    | Novel                         |
| 1087A>G<br>(Lys363Glu)   | 8           | Missense                 | TNF                    | Novel                         |
| 822G>T<br>(Trp274Cys)  | 7           | Missense                 | TNF                    | Trp274Arg and Gly<br>Reported |
| E67X   | 1           | Nonsense                 | Extracellular          | Novel                         |

<sup>1</sup>All mutations are hemizygous and located on the X-chromosome in the *EDA-A1* gene locus

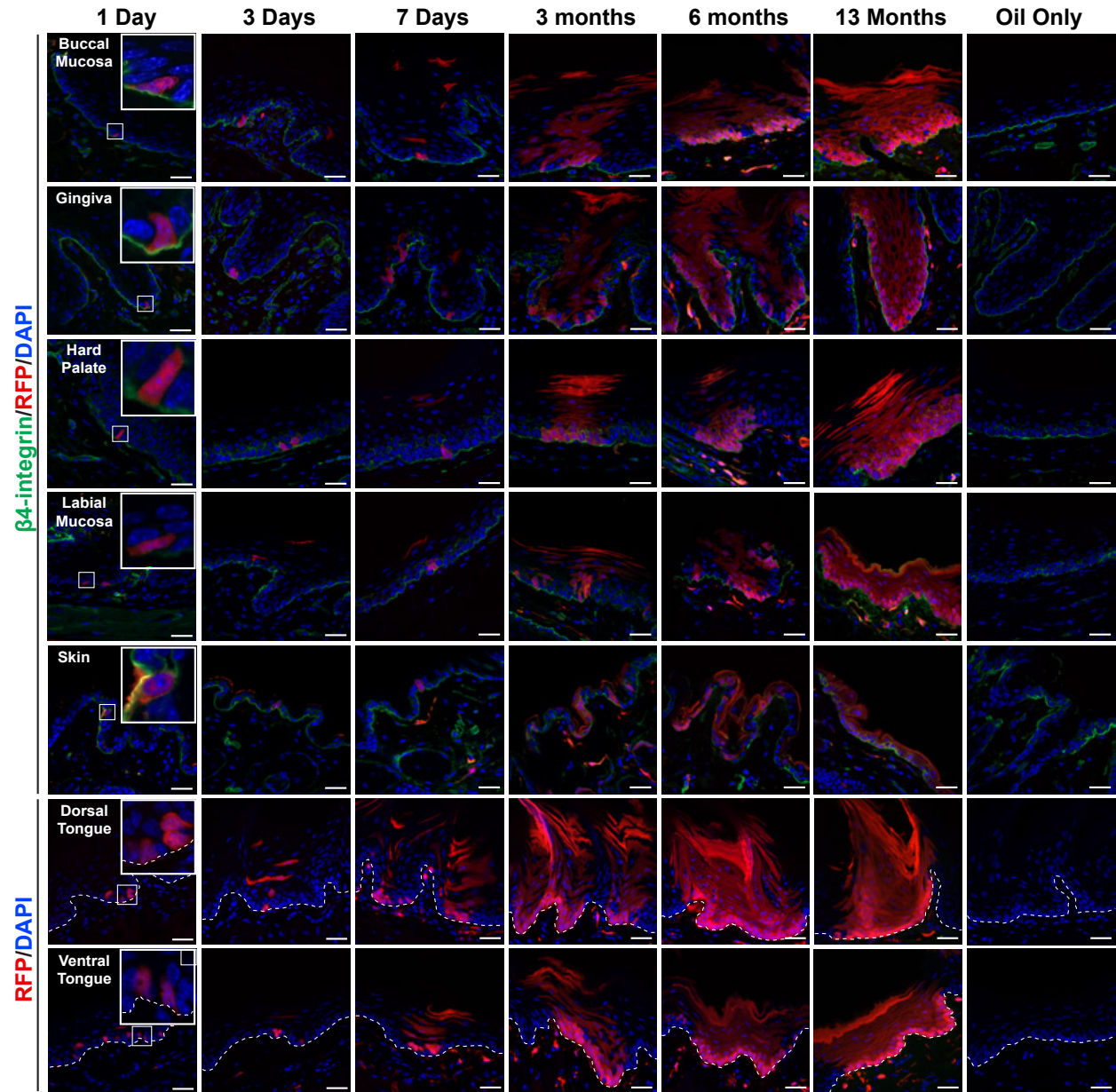
Supplemental Figure S1



**Supplemental Figure S1 *Bmi1* is expressed predominantly in basal layer keratinocytes throughout the oral mucosa.** (a,b) Predicted behavior of clones originating from a single, labeled OEPC following invariant asymmetric divisions in the setting of the epidermal proliferation unit model (a) or population asymmetric divisions with neutral competition between clones (b). (c-h) Similar to the buccal mucosa and dorsal tongue epithelia, *Bmi1* is also expressed predominantly within the basal layer keratinocytes at other oral mucosal sites (individual *Bmi1* transcripts are represented by red dots). The bacterial gene *dapB* was used as a negative control to assess for background staining and routinely showed no signal (g,h). Scale bars, 30µm. (i) With escalating doses of tamoxifen administered to *Bmi1<sup>CreER</sup>;R26<sup>tdTomato</sup>* mice, increased numbers of *Bmi1*-labeled cells can be seen in the basal and suprabasal layers of the buccal mucosa along with other oral mucosal sites. Dashed white line represents epithelial/connective tissue interface. Scale bars, 30µm. (j) Extremely rare BrdU-labeled cells were observed in a seemingly random distribution within the basal and suprabasal layers of the oral mucosa. The intensity of the BrdU staining was typically very weak in these cells, indicating that they had undergone mitosis during the 28 day chase and were not completely quiescent. Scale bars, 30µm. BrdU, 5-bromo-2'-deoxyuridine.

## Supplemental Figure S2

### *Bmi1* Lineage Tracing



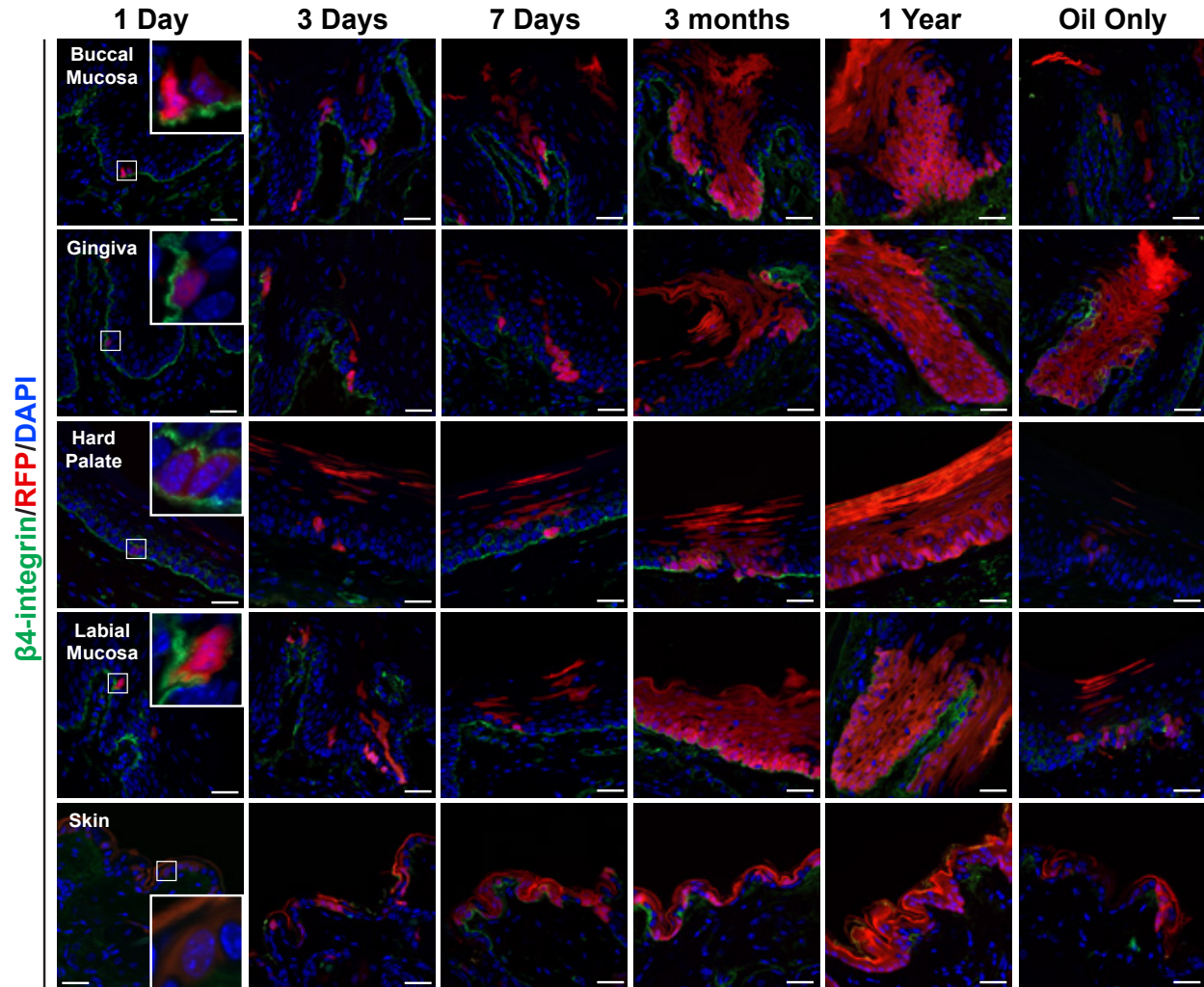
**Supplemental Figure S2** *Bmi1* labels long-lived OEPCs in the oral mucosal epithelium. After a single injection with tamoxifen in *Bmi1*<sup>CreER</sup>;*R26*<sup>tdTomato</sup> mice, at the 1 day chase most labeled cells are found in the basal layer. RFP expression is sustained in basal and suprabasal layer keratinocytes for as long as 13 months post-treatment. RFP expression was almost completely absent in *Bmi1*<sup>CreER</sup>;*R26*<sup>tdTomato</sup>



mice that did not receive tamoxifen. Scale bars, 30 $\mu$ m; OEPC, oral epithelial progenitor cell; dashed line represents epithelial/connective tissue interface. DAPI, 4,6-diamidino-2-phenylindole; RFP, red fluorescent protein.

Supplemental Figure S3

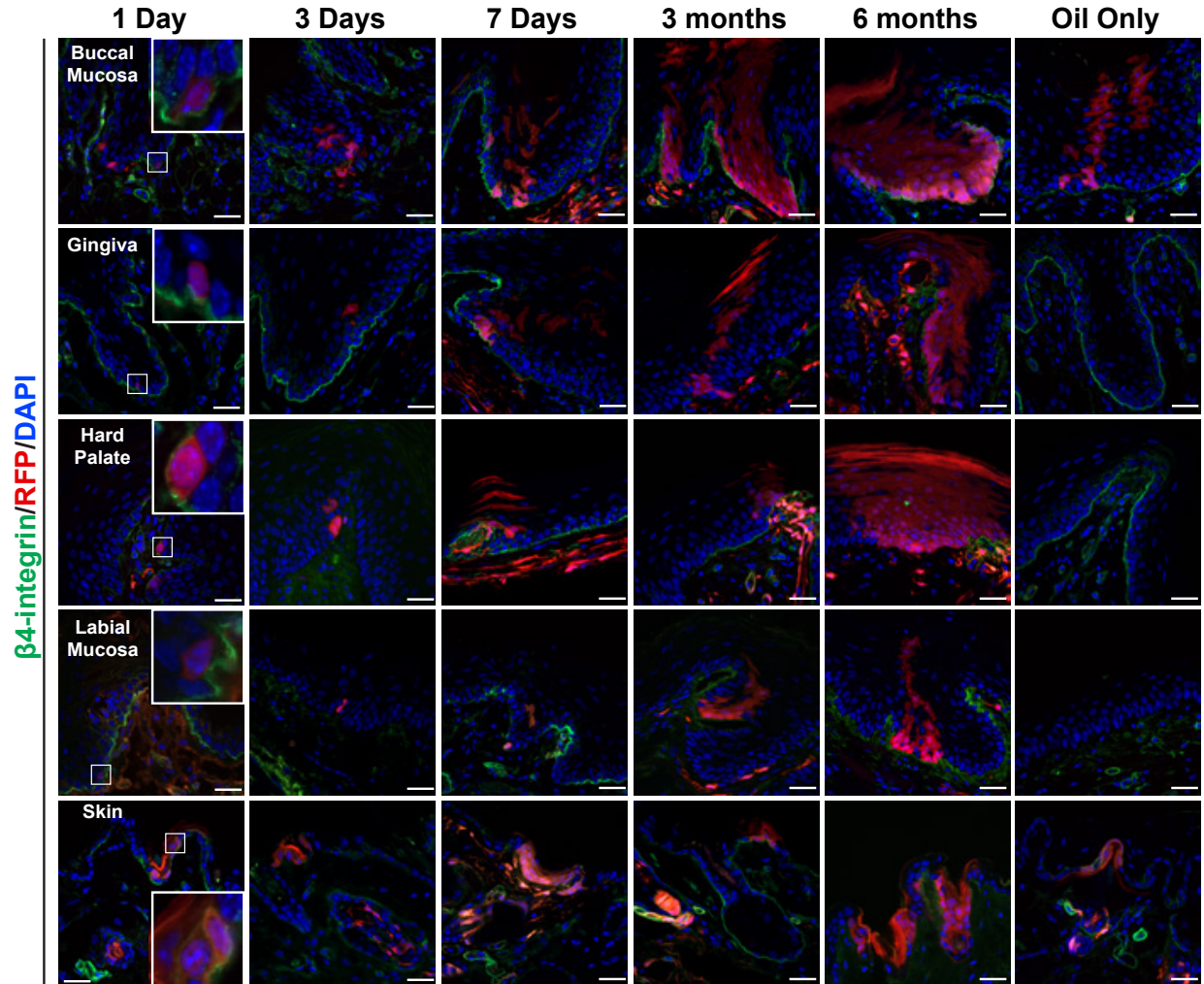
## K14 Lineage Tracing



**Supplemental Figure S3** *Krt14* labels long-lived OEPCs in the oral mucosal epithelium. *Krt14*, a type I keratin intermediate filament, is expressed mainly by basal layer cells in stratified epithelia. After a single low-dose injection with tamoxifen in *K14<sup>CreER</sup>;R26<sup>tdTomato</sup>* mice, at the 1 day chase most labeled cells are found in the basal layer. RFP expression is sustained in basal and suprabasal layer keratinocytes for as long as 1 year post-treatment. The *K14<sup>CreER</sup>* construct did exhibit some leakiness since areas of RFP expression were observed in mice that did not receive tamoxifen. Scale bars, 30 $\mu$ m. OEPC, oral epithelial progenitor cell; DAPI, 4,6-diamidino-2-phenylindole; RFP, red fluorescent protein.

## Supplemental Figure S4

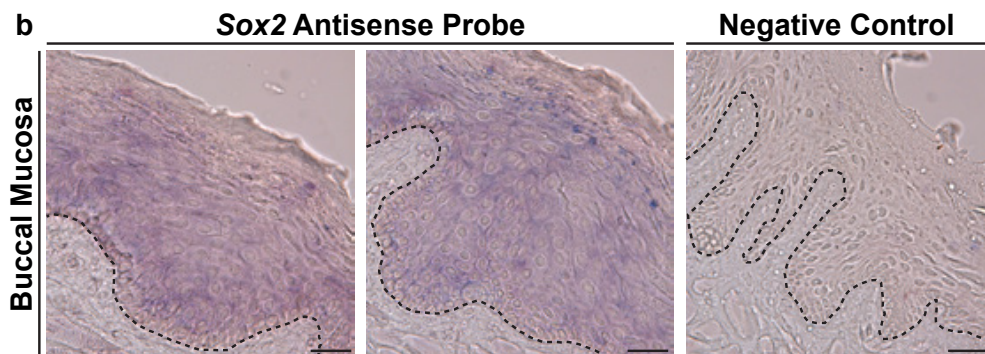
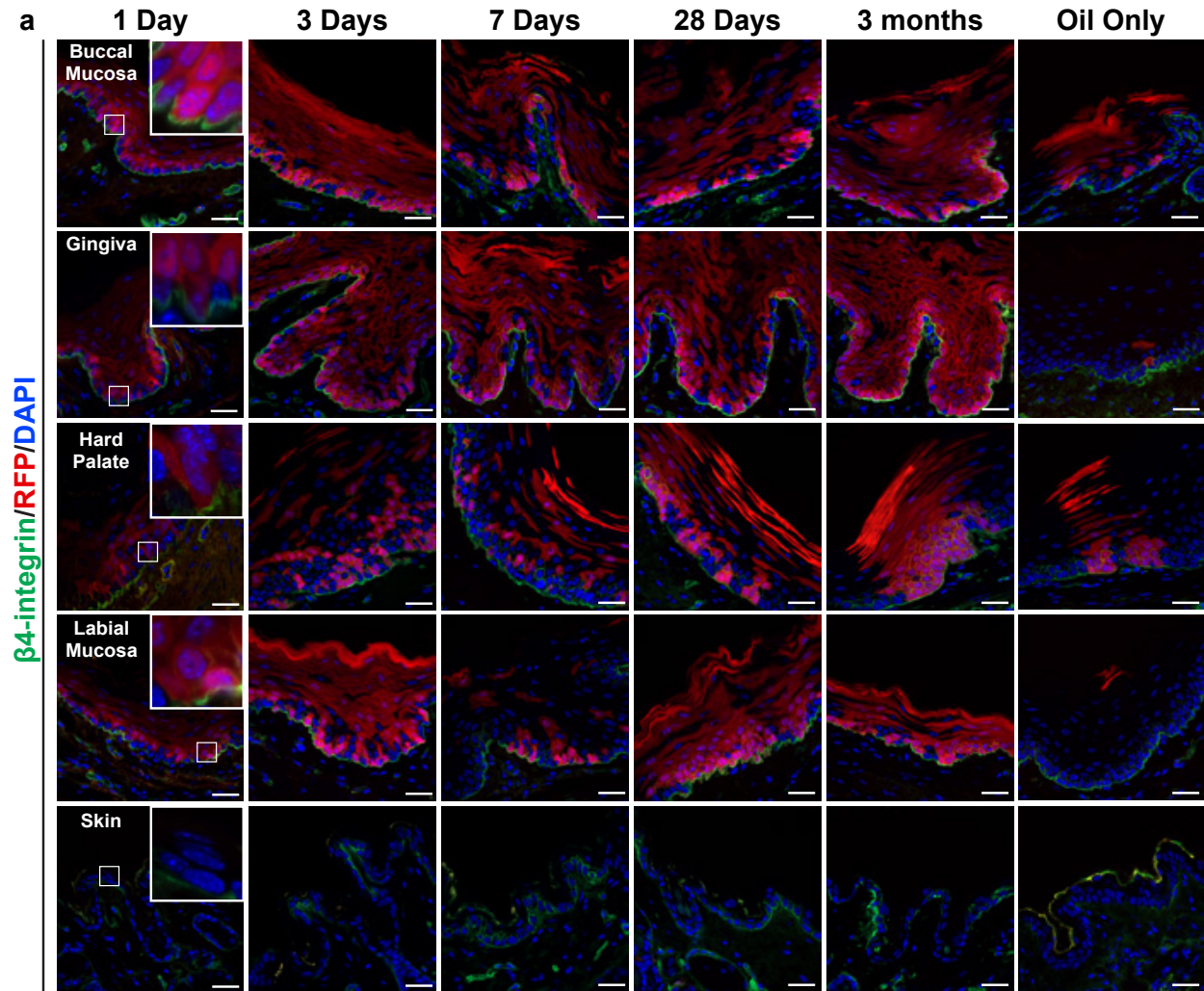
### *Gli1* Lineage Tracing



**Supplemental Figure S4** *Gli1* labels long-lived OEPCs in the oral mucosal epithelium. Following activation of the sonic hedgehog (SHH) signaling pathway, *Gli1* translocates to the nucleus and, among other functions, leads to increased transcription of additional *Gli1* mRNA. By using the *Gli1*<sup>CreER</sup>;R26<sup>tdTomato</sup> mouse, RFP positivity at early time points post-tamoxifen treatment indicates that the SHH pathway has been activated in these cells. The SHH pathway plays an integral role during embryonic development as well as in the maintenance of some adult stem/progenitor cell populations under normal homeostatic and repair conditions. After a single injection with tamoxifen in

*Gli1*<sup>CreER</sup>;R26<sup>tdTomato</sup> mice, at the 1 day chase most labeled cells are found in the basal layer. RFP expression is sustained in basal and suprabasal layer keratinocytes for as long as 6 months post-treatment. The *Gli1*<sup>CreER</sup> construct did exhibit some leakiness since rare RFP expression was observed in a few mice that did not receive tamoxifen. Scale bars, 30µm. OEPC, oral epithelial progenitor cell; DAPI, 4,6-diamidino-2-phenylindole; RFP, red fluorescent protein.

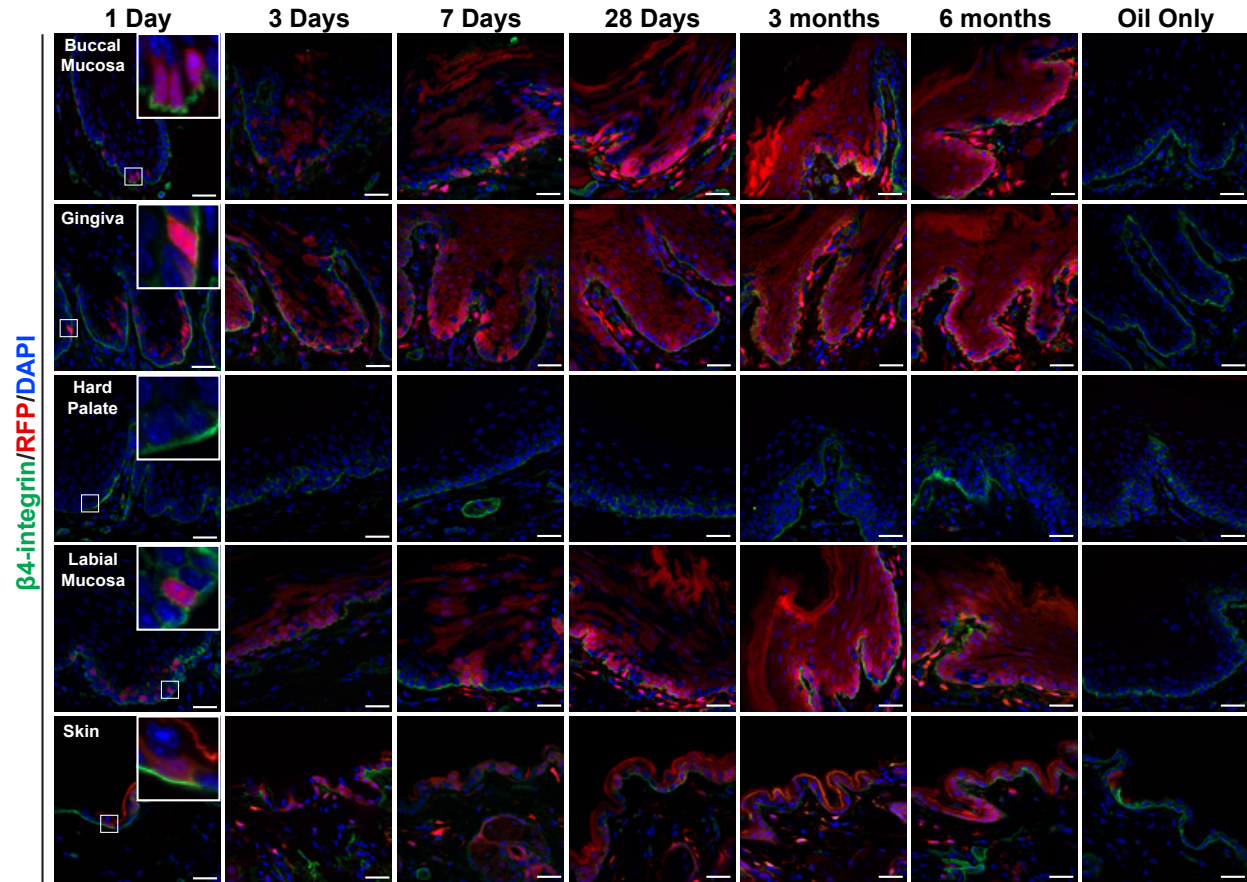
## Sox2 Lineage Tracing



**Supplemental Figure S5 Sox2 labels long-lived OEPCs in the oral mucosal epithelium, but not in lower lip skin.** (a) *Sox2* plays an integral role in the maintenance of embryonic stem cells in an undifferentiated state and is also expressed within several adult stem cell populations. Following treatment with a single dose of tamoxifen in *Sox2<sup>CreER</sup>;R26<sup>tdTomato</sup>* mice, both basal and suprabasal layer keratinocytes are labeled following a 1 day chase. RFP expression is sustained in basal and suprabasal layer keratinocytes for as long as 3 months post-treatment. The *Sox2<sup>CreER</sup>* construct did exhibit some leakiness since RFP expression was observed in mice that did not receive tamoxifen. (b) To confirm the expression pattern of *Sox2* observed in the 1 day chase from (a), in-situ hybridization using a *Sox2* antisense probe was performed in the buccal mucosa, which also showed generalized *Sox2* mRNA expression in both basal and suprabasal layer keratinocytes. Black dashed lines represent the interface between the connective tissue and epithelium. Scale bars, 30µm. OEPC, oral epithelial progenitor cell; DAPI, 4,6-diamidino-2-phenylindole; RFP, red fluorescent protein.

## Supplemental Figure S6

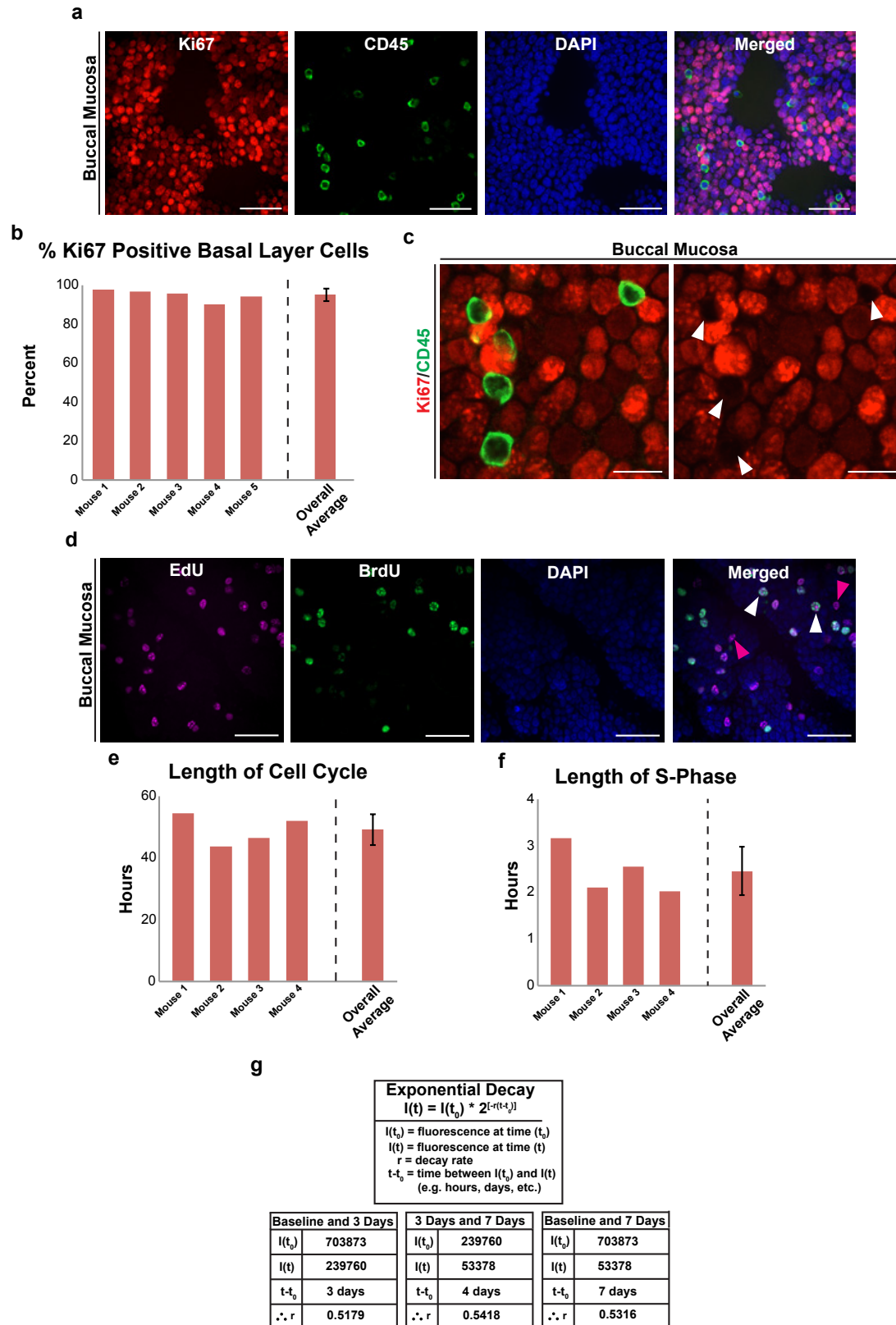
### *Lrig1* Lineage Tracing



#### Supplemental Figure S6 *Lrig1* labels long-lived OEPCs in most, but not all, oral mucosal sites.

*Lrig1* is an endogenous late-stage negative regulator of receptor tyrosine kinase signaling. It is also a marker and regulator of various stem/progenitor cell populations in the skin and intestine. After a single injection with tamoxifen in *Sox2<sup>CreER</sup>;R26<sup>tdTomato</sup>* mice, at the 1 day chase most labeled cells are found in the basal layer. RFP expression is sustained in basal and suprabasal layer keratinocytes for as long as 6 months post-treatment. Interestingly, RFP-labeled cells were never detected in the hard palate epithelium. Therefore, *Lrig1* does not appear to label OEPCs at this intraoral site. Except for extremely rare instances in the lower lip skin, almost no RFP expression was observed in *Lrig1CreER;RFP* mice that did not receive tamoxifen. Scale bars, 30 $\mu$ m. OEPC, oral epithelial progenitor cell; DAPI, 4,6-diamidino-2-phenylindole; RFP, red fluorescent protein.

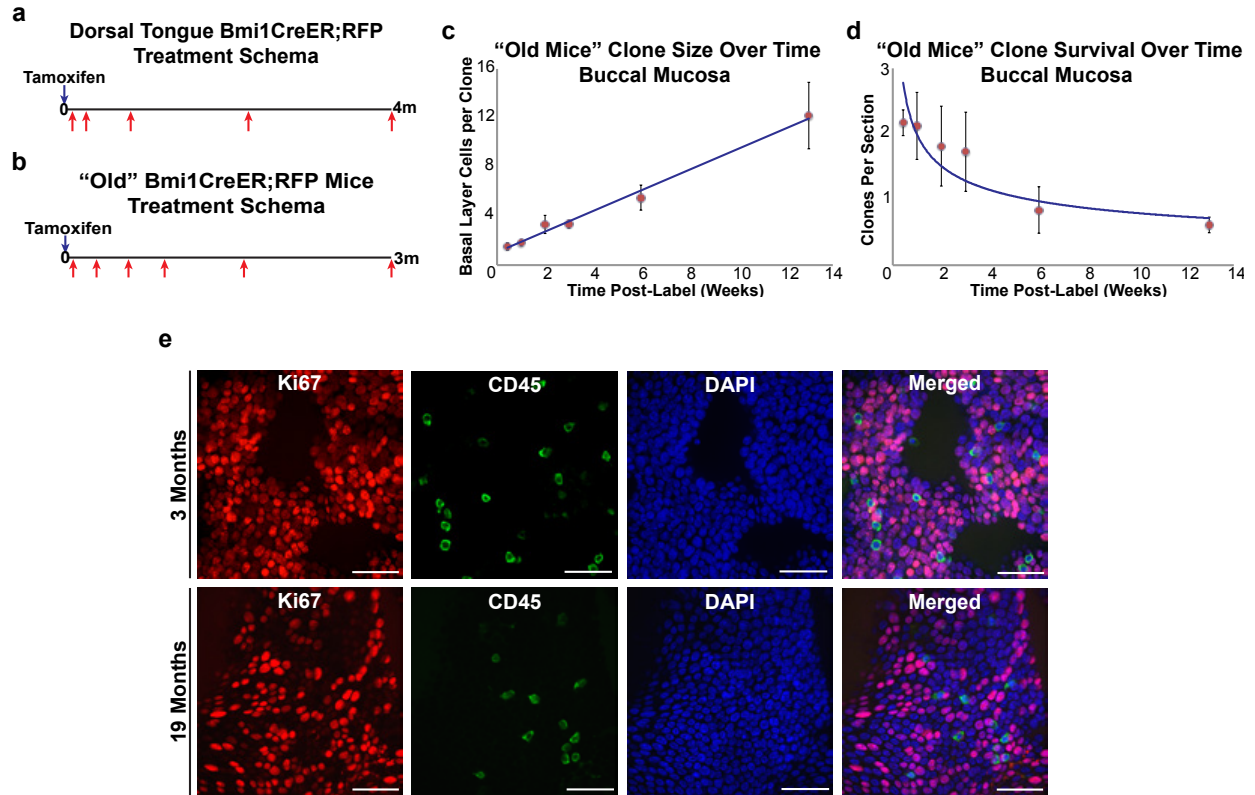
# Supplemental Figure S7





**Supplemental Figure S7 Buccal mucosal basal layer keratinocytes are highly proliferative and exhibit rapid cell turnover.** (a) Whole-mount imaging shows that the majority of buccal mucosal basal layer keratinocytes in 10 week old C57BL/6 mice express Ki-67. Scale bars, 30 $\mu$ m. (b) Bar graphs represent the percentage of basal layer keratinocytes positive for Ki-67 staining along with the overall average  $\pm$  SD. (c) Although there is a range of Ki-67 staining intensity within basal layer keratinocytes, there is nearly no background staining present as evidenced by the lack of RFP signal in the nuclei of several CD45 positive cells (white arrowheads). This supports the conclusion that the observed Ki-67 staining is sensitive and specific, albeit faint in some cells. Scale bars, 10 $\mu$ m. (d) Following temporally spaced injections of EdU and BrdU, cells that exit the S-phase prior to euthanasia only label with EdU (pink arrow heads), whereas cells still within the S-phase label with both EdU and BrdU (white arrow heads); see text for further details. Scale bars, 30 $\mu$ m. (e,f) Bar graphs represent the individual S-phase and total cell cycle times calculated for each of the 8 week old C57BL/6 mice analyzed, along with the overall average  $\pm$  SD. (g) The exponential decay equation and the decay rate constants calculated from comparisons of different time points in doxycycline treated *K5tTa; tetO-H2B-EGFP* mice. SD, standard deviation; BrdU, 5-bromo-2'-deoxyuridine; EdU, 5-ethynyl-2'-deoxyuridine; DAPI, 4,6-diamidino-2-phenylindole.

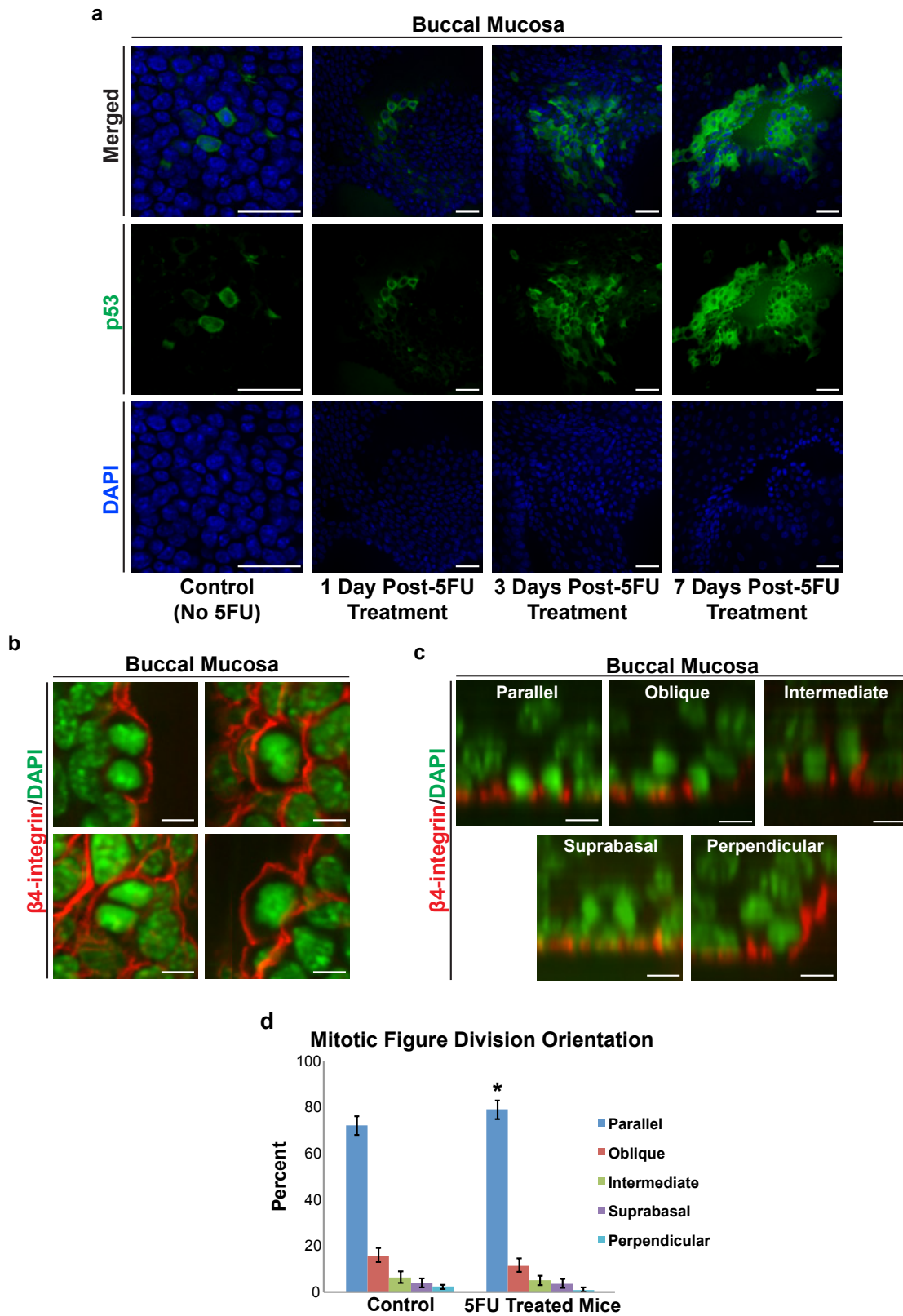
## Supplemental Figure S8



**Supplemental Figure S8** *Bmi1*-labeled basal layer progenitor cells in the buccal mucosa and dorsal tongue divide via population asymmetry—not invariant asymmetry—and follow neutral drift dynamics. **(a)** 2-3 month old *Bmi1*<sup>CreER</sup>;R26<sup>tdTomato</sup> mice were treated with a single dose of tamoxifen, chased at the designated time points, and RFP-labeled clones analyzed in the dorsal tongue epithelium. **(b)** 15 month old *Bmi1*<sup>CreER</sup>;R26<sup>tdTomato</sup> mice were treated with a single dose of tamoxifen, chased at the designated time points, and RFP-labeled clones analyzed. **(c,d)** Similar to clones analyzed in the younger 2-3 month old *Bmi1*<sup>CreER</sup>;R26<sup>tdTomato</sup> mice, in older mice the number of basal layer keratinocytes per clone increased over time (0.85 cells/week ± 0.12 SE) while the overall total number of clones decreased (0.10 clones/tile/week ± 0.02 SE), supporting the population asymmetry model. Solid curves represent predicted neutral drift values. **(e)** Whole-mount imaging of buccal epithelium revealed that on average, older adult mice (19 months old) had fewer basal layer keratinocytes expressing Ki-67 compared with

younger mice (3 months old). Scale bars, 30 $\mu$ m. SE, standard error; DAPI, 4,6-diamidino-2-phenylindole; RFP, red fluorescent protein.

Supplemental Figure S9



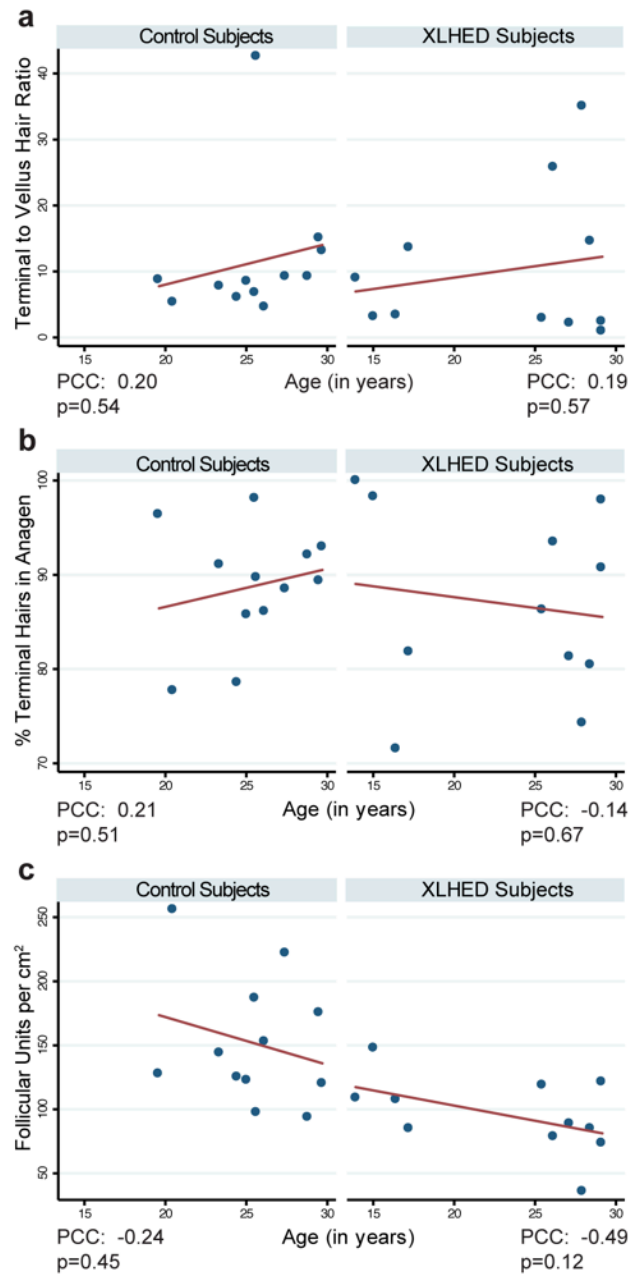
**Supplemental Figure S9 Buccal epithelial basal layer keratinocytes increase both p53 expression and the number of parallel oriented mitoses in response to 5FU-induced damage.** (a) Whole-mount imaging of buccal epithelium from 5FU treated mice reveals progressively increasing levels of cytoplasmic and nuclear p53 protein expression in basal and suprabasal layer keratinocytes. Scale bars, 20 $\mu$ m. (b) Examples of mitotic figures encountered within the buccal mucosa during analysis. The mitotic figures in the left panels would be suitable for mitotic figure orientation analysis due to clear separation of the sister chromatids, whereas the mitotic figures in the right panels would not be. Scale bars, 5 $\mu$ m. (c) Reconstructed confocal microscope cross-sections of whole-mount imaged mitotic figures within the buccal epithelium used for mitotic figure orientation analysis. Mitotic figures were grouped into one of 5 categories based on the relationship of the dividing cells to the underlying BM, represented by  $\beta$ 4-integrin, as well as to one another: parallel (both mitotic figures touch the BM), oblique (one mitotic figure touches the BM while the other has lifted off at an approximately 45° angle to the remaining mitotic figure), perpendicular (one mitotic figure touches the BM while the other is directly above the underlying mitotic figure), intermediate (one mitotic figure touches the BM while the second is barely touching the BM and appears to be in the process of lifting off), and suprabasal (both mitotic figures have simultaneously lifted off the BM and are no longer touching it). Scale bars, 5 $\mu$ m. (d) The vast majority of mitotic figures divide in a parallel orientation with respect to the basement membrane (represented here by  $\beta$ 4-integrin). Following 5FU treatment, there is a small but statistically significant increase in the percentage of parallel oriented mitotic figures (7.1% increase, Fisher's exact test, p=0.01). The bar graphs represent the pooled percentage of mitotic figures in each orientation within control and 5FU treated mice. Error bars represent the 95% confidence interval. 5FU, 5-fluorouracil; BM, basement membrane; DAPI, 4,6-diamidino-2-phenylindole.

# Supplemental Figure S10



**Supplemental Figure S10 Gene ontology terms associated with the upregulated differentially expressed genes for clusters 0-5.** Each horizontal bar represents an enrichment group comprised of related sets of enriched annotation terms identified via DAVID analysis. The enrichment score is the log-transformed geometric mean of p-values calculated from the enriched annotation terms within each enrichment group. The number within each bar represents the total number of genes present in each enrichment group.

## Supplemental Figure S11



**Supplemental Figure S11 Age correlation analysis.** Pearson correlation coefficient (PCC) values were calculated comparing age and (a) the ratio of terminal hairs to vellus hairs, (b) the % of terminal hairs in anagen, and (c) the number of follicular units per square centimeter of surface area for the XL-HED and control subjects. No significant correlation between age and hair properties was determined for either group.



## LITERATURE CITED

- Abe, M., Sogabe, Y., Syuto, T., Ishibuchi, H., Yokoyama, Y., & Ishikawa, O. (2007). Successful treatment with cyclosporin administration for persistent benign migratory glossitis. *The Journal of Dermatology*, 34(5), 340–343. <http://doi.org/10.1111/j.1346-8138.2007.00284.x>
- Aleinikov, A., Jordan, R. C., & Main, J. H. (1996). Topical steroid therapy in oral lichen planus: review of a novel delivery method in 24 patients. *J Can Dent Assoc*, 62(4), 324–327.
- Allen, C. M., Vigneswaran, N., Tilashalski, K., Rodu, B., & Cole, P. (1995). Tobacco use and cancer. *Oral Surgery, Oral Medicine, Oral Pathology, Oral Radiology, and Endodontology*, 80(2), 178–182. [http://doi.org/10.1016/S1079-2104\(05\)80199-4](http://doi.org/10.1016/S1079-2104(05)80199-4)
- Arai, Y., Pulvers, J. N., Haffner, C., Schilling, B., Nüsslein, I., Calegari, F., & Huttner, W. B. (2011). Neural stem and progenitor cells shorten S-phase on commitment to neuron production. *Nature Communications*, 2, 154. <http://doi.org/10.1038/ncomms1155>
- Arduino, P. G., Surace, A., Carbone, M., Elia, A., Massolini, G., Gandolfo, S., & Broccoletti, R. (2009). Outcome of oral dysplasia: a retrospective hospital-based study of 207 patients with a long follow-up. *Journal of Oral Pathology & Medicine : Official Publication of the International Association of Oral Pathologists and the American Academy of Oral Pathology*, 38(6), 540–544. <http://doi.org/10.1111/j.1600-0714.2009.00782.x>

- Arnold, K., Sarkar, A., Yram, M. A., Polo, J. M., Bronson, R., Sengupta, S., et al. (2011). Sox2(+) adult stem and progenitor cells are important for tissue regeneration and survival of mice. *Cell Stem Cell*, 9(4), 317–329. <http://doi.org/10.1016/j.stem.2011.09.001>
- Asaka, T., Akiyama, M., Kitagawa, Y., & Shimizu, H. (2009). Higher density of label-retaining cells in gingival epithelium. *Journal of Dermatological Science*, 55(2), 132–134. <http://doi.org/10.1016/j.jdermsci.2009.03.006>
- Axéll, T., & Rundquist, L. (1987). Oral lichen planus--a demographic study. *Community Dentistry and Oral Epidemiology*, 15(1), 52–56.
- Bagan, J., Sarrion, G., & Jimenez, Y. (2010). Oral cancer: Clinical features. *Oral Oncology*, 46(6), 414–417. <http://doi.org/10.1016/j.oraloncology.2010.03.009>
- Barrandon, Y., & Green, H. (1985). Cell size as a determinant of the clone-forming ability of human keratinocytes. *Proceedings of the National Academy of Sciences of the United States of America*, 82(16), 5390–5394.
- Barrandon, Y., & Green, H. (1987). Three clonal types of keratinocyte with different capacities for multiplication. *Proceedings of the National Academy of Sciences of the United States of America*, 84(8), 2302–2306.
- Barrett, A. W., Selvarajah, S., Franey, S., Wills, K. A., & Berkovitz, B. K. (1998). Interspecies variations in oral epithelial cytokeratin expression. *Journal of Anatomy*, 193 ( Pt 2), 185–193.
- Bhajee, F., Pepper, D. J., Pitman, K. T., & Bell, D. (2012). Cancer stem cells in head

and neck squamous cell carcinoma: a review of current knowledge and future applications. *Head & Neck*, 34(6), 894–899. <http://doi.org/10.1002/hed.21801>

Bhattacharyya, N. (2012). Trends in the use of smokeless tobacco in United States, 2000-2010. *The Laryngoscope*, 122(10), 2175–2178. <http://doi.org/10.1002/lary.23448>

Bickenbach, J. R. (1981). Identification and behavior of label-retaining cells in oral mucosa and skin. *Journal of Dental Research*, 60 Spec No C, 1611–1620.

Bickenbach, J. R., & Mackenzie, I. C. (1984). Identification and localization of label-retaining cells in hamster epithelia. *The Journal of Investigative Dermatology*, 82(6), 618–622.

Blüschke, G., Nüsken, K.-D., & Schneider, H. (2010). Prevalence and prevention of severe complications of hypohidrotic ectodermal dysplasia in infancy. *Early Human Development*, 86(7), 397–399. <http://doi.org/10.1016/j.earlhumdev.2010.04.008>

Bombeccari, G. P., Guzzi, G., Tettamanti, M., Gianni, A. B., Baj, A., Pallotti, F., & Spadari, F. (2011). Oral lichen planus and malignant transformation: a longitudinal cohort study. *Oral Surgery, Oral Medicine, Oral Pathology, Oral Radiology, and Endodontics*, 112(3), 328–334. <http://doi.org/10.1016/j.tripleo.2011.04.009>

Bouquot, J. E., & Gorlin, R. J. (1986). Leukoplakia, lichen planus, and other oral keratoses in 23,616 white Americans over the age of 35 years. *Oral Surgery, Oral Medicine, Oral Pathology*, 61(4), 373–381. [http://doi.org/10.1016/0030-4220\(86\)90422-6](http://doi.org/10.1016/0030-4220(86)90422-6)

- Bouquot, J. E., Speight, P. M., & Farthing, P. M. (2006, February 1). Epithelial dysplasia of the oral mucosa—Diagnostic problems and prognostic features. Retrieved November 11, 2014, from <http://www.sciencedirect.com/science/article/pii/S0968605305001067>
- Boyapati, A., & Sinclair, R. (2013). Combination therapy with finasteride and low-dose dutasteride in the treatment of androgenetic alopecia. *The Australasian Journal of Dermatology*, *54*(1), 49–51. <http://doi.org/10.1111/j.1440-0960.2012.00909.x>
- Brasileiro, C. B., Abreu, M. H. N., & Mesquita, R. A. (2014). Critical review of topical management of oral hairy leukoplakia. *World Journal of Clinical Cases*, *2*(7), 253–256. <http://doi.org/10.12998/wjcc.v2.i7.253>
- Brouns, E. R. E. A., Baart, J. A., Karagozoglu, K. H., Aartman, I. H. A., Bloemena, E., & van der Waal, I. (2013). Treatment results of CO2 laser vaporisation in a cohort of 35 patients with oral leukoplakia. *Oral Diseases*, *19*(2), 212–216. <http://doi.org/10.1111/odi.12007>
- Bryder, D., Rossi, D. J., & Weissman, I. L. (2006). Hematopoietic stem cells: the paradigmatic tissue-specific stem cell. *The American Journal of Pathology*, *169*(2), 338–346. <http://doi.org/10.2353/ajpath.2006.060312>
- Calenic, B., Ishkitiev, N., Yaegaki, K., Imai, T., Costache, M., Tovar, M., et al. (2010a). Characterization of oral keratinocyte stem cells and prospects of its differentiation to oral epithelial equivalents. *Romanian Journal of Morphology and Embryology = Revue Roumaine De Morphologie Et Embryologie*, *51*(4), 641–645.

- Calenic, B., Ishkitiev, N., Yaegaki, K., Imai, T., Kumazawa, Y., Nasu, M., & Hirata, T. (2010b). Magnetic separation and characterization of keratinocyte stem cells from human gingiva. *Journal of Periodontal Research*, 45(6), 703–708. <http://doi.org/10.1111/j.1600-0765.2010.01284.x>
- Canfield, D. (1996). Photographic documentation of hair growth in androgenetic alopecia. *Dermatologic Clinics*, 14(4), 713–721.
- Carrozzo, M., & Thorpe, R. (2009). Oral lichen planus: a review. *Minerva Stomatologica*, 58(10), 519–537.
- Casal, M. L., Lewis, J. R., Mauldin, E. A., Tardivel, A., Ingold, K., Favre, M., et al. (2007). Significant correction of disease after postnatal administration of recombinant ectodysplasin A in canine X-linked ectodermal dysplasia. *American Journal of Human Genetics*, 81(5), 1050–1056. <http://doi.org/10.1086/521988>
- Casal, M. L., Scheidt, J. L., Rhodes, J. L., Henthorn, P. S., & Werner, P. (2005). Mutation identification in a canine model of X-linked ectodermal dysplasia. *Mammalian Genome : Official Journal of the International Mammalian Genome Society*, 16(7), 524–531. <http://doi.org/10.1007/s00335-004-2463-4>
- Castellanos, J. L., & Díaz-Guzmán, L. (2008). Lesions of the oral mucosa: an epidemiological study of 23785 Mexican patients. *Oral Surgery, Oral Medicine, Oral Pathology, Oral Radiology, and Endodontology*, 105(1), 79–85. <http://doi.org/10.1016/j.tripleo.2007.01.037>
- Chambers, A. E., Conn, B., Pemberton, M., Robinson, M., Banks, R., & Sloan, P.

- (2015). Twenty-first-century oral hairy leukoplakia-a non-HIV-associated entity. *Oral Surgery, Oral Medicine, Oral Pathology and Oral Radiology*, 119(3), 326–332. <http://doi.org/10.1016/j.oooo.2014.11.012>
- Chambers, I., Colby, D., Robertson, M., Nichols, J., Lee, S., Tweedie, S., & Smith, A. (2003). Functional expression cloning of Nanog, a pluripotency sustaining factor in embryonic stem cells. *Cell*, 113(5), 643–655.
- Chen, D., Wu, M., Li, Y., Chang, I., Yuan, Q., Ekimyan-Salvo, M., et al. (2017). Targeting BMI1(+) Cancer Stem Cells Overcomes Chemoresistance and Inhibits Metastases in Squamous Cell Carcinoma. *Cell Stem Cell*, 20(5), 621–634.e6. <http://doi.org/10.1016/j.stem.2017.02.003>
- Chi, A. C., Lambert, P. R., Pan, Y., Li, R., Vo, D.-T., Edwards, E., et al. (2007). Is alveolar ridge keratosis a true leukoplakia?: A clinicopathologic comparison of 2,153 lesions. *Journal of the American Dental Association (1939)*, 138(5), 641–651.
- Chiou, S. H., Yu, C. C., Huang, C. Y., Lin, S. C., Liu, C. J., Tsai, T. H., et al. (2008). Positive Correlations of Oct-4 and Nanog in Oral Cancer Stem-Like Cells and High-Grade Oral Squamous Cell Carcinoma. *Clinical Cancer Research*, 14(13), 4085–4095. <http://doi.org/10.1158/1078-0432.CCR-07-4404>
- Chu, Y. H., Tatakis, D. N., & Wee, A. G. (2010). Smokeless tobacco use and periodontal health in a rural male population. *Journal of Periodontology*, 81(6), 848–854. <http://doi.org/10.1902/jop.2010.090310>
- Chung, C. H., Zhang, Q., Kong, C. S., Harris, J., Fertig, E. J., Harari, P. M., et al.

- (2014). p16 protein expression and human papillomavirus status as prognostic biomarkers of nonoropharyngeal head and neck squamous cell carcinoma. *Journal of Clinical Oncology : Official Journal of the American Society of Clinical Oncology*, 32(35), 3930–3938. <http://doi.org/10.1200/JCO.2013.54.5228>
- Cinausero, M., Aprile, G., Ermacora, P., Basile, D., Vitale, M. G., Fanotto, V., et al. (2017). New Frontiers in the Pathobiology and Treatment of Cancer Regimen-Related Mucosal Injury. *Frontiers in Pharmacology*, 8, 354. <http://doi.org/10.3389/fphar.2017.00354>
- Clarke, A., Phillips, D. I., Brown, R., & Harper, P. S. (1987). Clinical aspects of X-linked hypohidrotic ectodermal dysplasia. *Archives of Disease in Childhood*, 62(10), 989–996.
- Clauss, F., Manière, M.-C., Obry, F., Waltmann, E., Hadj-Rabia, S., Bodemer, C., et al. (2008). Dento-craniofacial phenotypes and underlying molecular mechanisms in hypohidrotic ectodermal dysplasia (HED): a review. *Journal of Dental Research*, 87(12), 1089–1099. <http://doi.org/10.1177/154405910808701205>
- Clay, M. R., Tabor, M., Owen, J. H., Carey, T. E., Bradford, C. R., Wolf, G. T., et al. (2010). Single-marker identification of head and neck squamous cell carcinoma cancer stem cells with aldehyde dehydrogenase. *Head & Neck*, 32(9), 1195–1201. <http://doi.org/10.1002/hed.21315>
- Clayton, E., Doupé, D. P., Klein, A. M., Winton, D. J., Simons, B. D., & Jones, P. H. (2007). A single type of progenitor cell maintains normal epidermis. *Nature*, 446(7132), 185–189. <http://doi.org/10.1038/nature05574>

- Cluzeau, C., Hadj-Rabia, S., Bal, E., Clauss, F., Munnich, A., Bodemer, C., et al. (2012). The EDAR370A allele attenuates the severity of hypohidrotic ectodermal dysplasia caused by EDA gene mutation. *The British Journal of Dermatology*, 166(3), 678–681. <http://doi.org/10.1111/j.1365-2133.2011.10620.x>
- Courtney, J.-M., Blackburn, J., & Sharpe, P. T. (2005). The Ectodysplasin and NFkappaB signalling pathways in odontogenesis. *Archives of Oral Biology*, 50(2), 159–163. <http://doi.org/10.1016/j.archoralbio.2004.11.019>
- Cui, C.-Y., & Schlessinger, D. (2006). EDA signaling and skin appendage development. *Cell Cycle (Georgetown, Tex.)*, 5(21), 2477–2483. <http://doi.org/10.4161/cc.5.21.3403>
- Cui, C.-Y., Kunisada, M., Esibizione, D., Douglass, E. G., & Schlessinger, D. (2009). Analysis of the temporal requirement for eda in hair and sweat gland development. *The Journal of Investigative Dermatology*, 129(4), 984–993. <http://doi.org/10.1038/jid.2008.318>
- Cutlan, J. E., Saunders, N., Olsen, S. H., & Fullen, D. R. (2010). White sponge nevus presenting as genital lesions in a 28-year-old female. *Journal of Cutaneous Pathology*, 37(3), 386–389. <http://doi.org/10.1111/j.1600-0560.2009.01294.x>
- Cutright, D. E., & Bauer, H. (1967). Cell renewal in the oral mucosa and skin of the rat. I. Turnover time. *Oral Surgery, Oral Medicine, and Oral Pathology*, 23(2), 249–259.
- Dale, B. A., Salonen, J., & Jones, A. H. (1990). New approaches and concepts in the study of differentiation of oral epithelia. *Critical Reviews in Oral Biology and*



*Medicine : an Official Publication of the American Association of Oral Biologists*, 1(3), 167–190.

Dang, D., & Ramos, D. M. (2009). Identification of  $\alpha\gamma\beta$ 6-positive stem cells in oral squamous cell carcinoma. *Anticancer Research*, 29(6), 2043–2049.

Daniels, T. E. (1984). Human mucosal Langerhans cells: postmortem identification of regional variations in oral mucosa. *Journal of Investigative Dermatology*, 82(1), 21–24.

Daniels, T. E., Greenspan, D., Greenspan, J. S., Lennette, E., Schiodt, M., Petersen, V., & de Souza, Y. (1987). Absence of Langerhans Cells in Oral Hairy Leukoplakia, an AIDS-Associated Lesion. *Journal of Investigative Dermatology*, 89(2), 178–182. <http://doi.org/10.1111/1523-1747.ep12470556>

Darwazeh, A. M., Al-Aboosi, M. M., & Bedair, A. A. (2012). Prevalence of oral mucosal lesions in psoriatic patients: A controlled study. *Journal of Clinical and Experimental Dentistry*, 4(5), e286–91. <http://doi.org/10.4317/jced.50905>

DCCPS: Behavioral Research Program: TCRB: Smoking and Tobacco Control Monographs. (1992, September 1). DCCPS: Behavioral Research Program: TCRB: Smoking and Tobacco Control Monographs. Retrieved November 2, 2014, from <http://cancercontrol.cancer.gov/brp/tcrb/monographs/2/index.html>

Ding, X.-W., Wu, J.-H., & Jiang, C.-P. (2010). ABCG2: a potential marker of stem cells and novel target in stem cell and cancer therapy. *Life Sciences*, 86(17-18), 631–637. <http://doi.org/10.1016/j.lfs.2010.02.012>

Doupe, D. P., Alcolea, M. P., Roshan, A., Zhang, G., Klein, A. M., Simons, B. D., & Jones, P. H. (2012). A Single Progenitor Population Switches Behavior to Maintain and Repair Esophageal Epithelium. *Science*, 337(6098), 1091–1093. <http://doi.org/10.1126/science.1218835>

Doupe, D. P., Alcolea, M. P., Roshan, A., Zhang, G., Klein, A. M., Simons, B. D., & Jones, P. H. (2012). A Single Progenitor Population Switches Behavior to Maintain and Repair Esophageal Epithelium. *Science*. <http://doi.org/10.1126/science.1218835>

Doupe, D. P., Klein, A. M., Simons, B. D., & Jones, P. H. (2010). The ordered architecture of murine ear epidermis is maintained by progenitor cells with random fate. *Developmental Cell*, 18(2), 317–323. <http://doi.org/10.1016/j.devcel.2009.12.016>

Du, L., Yang, Y., Xiao, X., Wang, C., Zhang, X., Wang, L., et al. (2011). Sox2 nuclear expression is closely associated with poor prognosis in patients with histologically node-negative oral tongue squamous cell carcinoma. *Oral Oncology*, 47(8), 709–713. <http://doi.org/10.1016/j.oraloncology.2011.05.017>

Eisen, D. (1999). The evaluation of cutaneous, genital, scalp, nail, esophageal, and ocular involvement in patients with oral lichen planus. *Oral Surgery, Oral Medicine, Oral Pathology, Oral Radiology, and Endodontics*, 88(4), 431–436.

Eisen, D. (2002). The clinical features, malignant potential, and systemic associations of oral lichen planus: a study of 723 patients. *Journal of the American Academy of Dermatology*, 46(2), 207–214.

- Engeland, C. G., Bosch, J. A., Cacioppo, J. T., & Marucha, P. T. (2006). Mucosal wound healing: the roles of age and sex. *Archives of Surgery (Chicago, Ill. : 1960)*, 141(12), 1193–7– discussion 1198. <http://doi.org/10.1001/archsurg.141.12.1193>
- Epstein, J. B., Sherlock, C. H., & Greenspan, J. S. (1991). Hairy leukoplakia-like lesions following bone-marrow transplantation. *AIDS (London, England)*, 5(1), 101–102.
- Epstein, J. B., Sherlock, C. H., & Wolber, R. A. (1993). Hairy leukoplakia after bone marrow transplantation. *Oral Surgery, Oral Medicine, and Oral Pathology*, 75(6), 690–695.
- Feller, L., & Lemmer, J. (2012). Oral Squamous Cell Carcinoma: Epidemiology, Clinical Presentation and Treatment. *Journal of Cancer Therapy*, 03(04), 263–268. <http://doi.org/10.4236/jct.2012.34037>
- Fuchs, E. (1995). Keratins and the Skin. *Annual Review of Cell and Developmental Biology*, 11(1), 123–154. <http://doi.org/10.1146/annurev.cb.11.110195.001011>
- Fuchs, E. (2007). Scratching the surface of skin development. *Nature*, 445(7130), 834–842. <http://doi.org/10.1038/nature05659>
- Fujimoto, A., Kimura, R., Ohashi, J., Omi, K., Yuliwulandari, R., Batubara, L., et al. (2008). A scan for genetic determinants of human hair morphology: EDAR is associated with Asian hair thickness. *Human Molecular Genetics*, 17(6), 835–843. <http://doi.org/10.1093/hmg/ddm355>
- Gaide, O., & Schneider, P. (2003). Permanent correction of an inherited ectodermal dysplasia with recombinant EDA. *Nature Medicine*, 9(5), 614–618.

<http://doi.org/10.1038/nm861>

Ghazizadeh, S., & Taichman, L. B. (2001). Multiple classes of stem cells in cutaneous epithelium: a lineage analysis of adult mouse skin. *The EMBO Journal*, *20*(6), 1215–1222. <http://doi.org/10.1093/emboj/20.6.1215>

Giroux, V., Lento, A. A., Islam, M., Pitarresi, J. R., Kharbanda, A., Hamilton, K. E., et al. (2017). Long-lived keratin 15+ esophageal progenitor cells contribute to homeostasis and regeneration. *Journal of Clinical Investigation*, *127*(6), 2378–2391. <http://doi.org/10.1172/JCI88941>

Grady, D., Greene, J., Daniels, T. E., Ernster, V. L., Robertson, P. B., Hauck, W., et al. (1990). Oral mucosal lesions found in smokeless tobacco users. *Journal of the American Dental Association (1939)*, *121*(1), 117–123.

Greenspan, D., Greenspan, J. S., Conant, M., Petersen, V., Silverman, S., & de Souza, Y. (1984). Oral “hairy” leucoplakia in male homosexuals: evidence of association with both papillomavirus and a herpes-group virus. *Lancet*, *2*(8407), 831–834.

Greenspan, J. S., & Greenspan, D. (1989). Oral hairy leukoplakia: diagnosis and management. *Oral Surgery, Oral Medicine, and Oral Pathology*, *67*(4), 396–403.

Greenspan, J. S., Greenspan, D., Lennette, E. T., Abrams, D. I., Conant, M. A., Petersen, V., & Freese, U. K. (1985). Replication of Epstein-Barr virus within the epithelial cells of oral “hairy” leukoplakia, an AIDS-associated lesion. *The New England Journal of Medicine*, *313*(25), 1564–1571. <http://doi.org/10.1056/NEJM198512193132502>

- Grein Cavalcanti, L., Fátima Lyko, K., Lins Fuentes Araújo, R., Miguel Amenábar, J., Bonfim, C., & Carvalho Torres-Pereira, C. (2015). Oral leukoplakia in patients with Fanconi anaemia without hematopoietic stem cell transplantation. *Pediatric Blood & Cancer*, 62(6), 1024–1026. <http://doi.org/10.1002/pbc.25417>
- Hammersen, J. E., Neukam, V., Nüsken, K.-D., & Schneider, H. (2011). Systematic evaluation of exertional hyperthermia in children and adolescents with hypohidrotic ectodermal dysplasia: an observational study. *Pediatric Research*, 70(3), 297–301. <http://doi.org/10.1203/PDR.0b013e318227503b>
- Häyry, V., Mäkinen, L. K., Atula, T., Sariola, H., Mäkitie, A., Leivo, I., et al. (2010). Bmi-1 expression predicts prognosis in squamous cell carcinoma of the tongue. *British Journal of Cancer*, 102(5), 892–897. <http://doi.org/10.1038/sj.bjc.6605544>
- Ho, M. W., Risk, J. M., Woolgar, J. A., Field, E. A., Field, J. K., Steele, J. C., et al. (2012). The clinical determinants of malignant transformation in oral epithelial dysplasia. *Oral Oncology*, 48(10), 969–976. <http://doi.org/10.1016/j.oraloncology.2012.04.002>
- Hoess, R. H., Ziese, M., & Sternberg, N. (1982). P1 site-specific recombination: nucleotide sequence of the recombining sites. *Proceedings of the ...*
- Holmstrup, P., Vedtofte, P., Reibel, J., & Stoltze, K. (2006). Long-term treatment outcome of oral premalignant lesions. *Oral Oncology*, 42(5), 461–474. <http://doi.org/10.1016/j.oraloncology.2005.08.011>
- Horsley, V., O'Carroll, D., Tooze, R., Ohinata, Y., Saitou, M., Obukhanych, T., et al.

- (2006). Blimp1 defines a progenitor population that governs cellular input to the sebaceous gland. *Cell*, 126(3), 597–609. <http://doi.org/10.1016/j.cell.2006.06.048>
- Huang, D. W., Sherman, B. T., & Lempicki, R. A. (2009a). Bioinformatics enrichment tools: paths toward the comprehensive functional analysis of large gene lists. *Nucleic Acids Research*, 37(1), 1–13. <http://doi.org/10.1093/nar/gkn923>
- Huang, D. W., Sherman, B. T., & Lempicki, R. A. (2009b). Systematic and integrative analysis of large gene lists using DAVID bioinformatics resources. *Nature Protocols*, 4(1), 44–57. <http://doi.org/10.1038/nprot.2008.211>
- Huang, Y.-L., Tao, X., Xia, J., Li, C.-Y., & Cheng, B. (2009c). Distribution and quantity of label-retaining cells in rat oral epithelia. *Journal of Oral Pathology and Medicine*, 38(8), 663–667. <http://doi.org/10.1111/j.1600-0714.2009.00798.x>
- Hume, W. J., & Potten, C. S. (1976). The ordered columnar structure of mouse filiform papillae. *Journal of Cell Science*.
- Hume, W. J., & Potten, C. S. (1979). Advances in epithelial kinetics-An oral view. *Journal of Oral Pathology and Medicine*, 8(1), 3–22. <http://doi.org/10.1111/j.1600-0714.1979.tb01618.x>
- Igarashi, T., Shimmura, S., Yoshida, S., Tonogi, M., Shinozaki, N., & Yamane, G.-Y. (2008). Isolation of oral epithelial progenitors using collagen IV. *Oral Diseases*, 14(5), 413–418. <http://doi.org/10.1111/j.1601-0825.2007.01390.x>
- Ishibashi, M., Tojo, G., Watanabe, M., Tamabuchi, T., Masu, T., & Aiba, S. (2010). Geographic tongue treated with topical tacrolimus. *Journal of Dermatological Case*

*Reports*, 4(4), 57–59. <http://doi.org/10.3315/jdcr.2010.1058>

Issa, Y., Duxbury, A. J., Macfarlane, T. V., & Brunton, P. A. (2005). Verifiable CPD Paper: Oral lichenoid lesions related to dental restorative materials : Abstract : British Dental Journal. *British Dental Journal*.

Jaks, V., Barker, N., Kasper, M., van Es, J. H., Snippert, H. J., Clevers, H., & Toftgård, R. (2008). Lgr5 marks cycling, yet long-lived, hair follicle stem cells. *Nature Genetics*, 40(11), 1291–1299. <http://doi.org/10.1038/ng.239>

Jensen, K. B., Collins, C. A., Nascimento, E., Tan, D. W., Frye, M., Itami, S., & Watt, F. M. (2009). Lrig1 expression defines a distinct multipotent stem cell population in mammalian epidermis. *Cell Stem Cell*, 4(5), 427–439. <http://doi.org/10.1016/j.stem.2009.04.014>

Jones, K. B., & Jordan, R. (2015). White lesions in the oral cavity: clinical presentation, diagnosis, and treatment. *Seminars in Cutaneous Medicine and Surgery*, 34(4), 161–170. <http://doi.org/10.12788/j.sder.2015.0180>

Jones, K. B., & Klein, O. D. (2013). Oral epithelial stem cells in tissue maintenance and disease: the first steps in a long journey. *International Journal of Oral Science*. <http://doi.org/10.1038/ijos.2013.46>

Jones, K. B., Goodwin, A. F., Landan, M., Seidel, K., Tran, D.-K., Hogue, J., et al. (2013). Characterization of X-linked Hypohidrotic Ectodermal Dysplasia (XL-HED) Hair and Sweat Gland Phenotypes Using Phototrichogram Analysis and Live Confocal Imaging. *American Journal of Medical Genetics Part A*.

<http://doi.org/10.1002/ajmg.a.35959>

Jones, P. H., & Watt, F. M. (1993). Separation of human epidermal stem cells from transit amplifying cells on the basis of differences in integrin function and expression. *Cell*, 73(4), 713–724. [http://doi.org/10.1016/0092-8674\(93\)90251-K](http://doi.org/10.1016/0092-8674(93)90251-K)

Jorgenson, R. J., & Levin, S. L. (1981, October 30). White Sponge Nevus. Retrieved October 30, 2014, from <http://archderm.jamanetwork.com/article.aspx?articleid=541740>

Joyner, A. L., & Zervas, M. (2006). Genetic inducible fate mapping in mouse: Establishing genetic lineages and defining genetic neuroanatomy in the nervous system. *Developmental Dynamics : an Official Publication of the American Association of Anatomists*, 235(9), 2376–2385. <http://doi.org/10.1002/dvdy.20884>

Kang, H. S., Lee, H. E., Ro, Y. S., & Lee, C. W. (2012). Three cases of 'morsicatio labiorum'. *Annals of Dermatology*, 24(4), 455–458. <http://doi.org/10.5021/ad.2012.24.4.455>

Kanitakis, J. (2002). Anatomy, histology and immunohistochemistry of normal human skin. *European Journal of Dermatology : EJD*, 12(4), 390–9– quiz 400–1.

Kaur, P., & Li, A. (2000). Adhesive properties of human basal epidermal cells: an analysis of keratinocyte stem cells, transit amplifying cells, and postmitotic differentiating cells. *The Journal of Investigative Dermatology*, 114(3), 413–420. <http://doi.org/10.1046/j.1523-1747.2000.00884.x>

Kiyosue, T., Kawano, S., Matsubara, R., Goto, Y., Hirano, M., Jinno, T., et al. (2011).



Immunohistochemical location of the p75 neurotrophin receptor (p75NTR) in oral leukoplakia and oral squamous cell carcinoma. *International Journal of Clinical Oncology / Japan Society of Clinical Oncology*. <http://doi.org/10.1007/s10147-011-0358-4>

Klein, A. M., & Simons, B. D. (2011). Universal patterns of stem cell fate in cycling adult tissues. *Development (Cambridge, England)*, 138(15), 3103–3111. <http://doi.org/10.1242/dev.060103>

Klein, A. M., Doupé, D. P., Jones, P. H., & Simons, B. D. (2007). Kinetics of cell division in epidermal maintenance. *Physical Review. E, Statistical, Nonlinear, and Soft Matter Physics*, 76(2 Pt 1), 021910.

Klein, A. M., Nakagawa, T., Ichikawa, R., Yoshida, S., & Simons, B. D. (2010). Mouse germ line stem cells undergo rapid and stochastic turnover. *Cell Stem Cell*, 7(2), 214–224. <http://doi.org/10.1016/j.stem.2010.05.017>

Kolios, G., & Moodley, Y. (2013). Introduction to stem cells and regenerative medicine. *Respiration; International Review of Thoracic Diseases*, 85(1), 3–10. <http://doi.org/10.1159/000345615>

Korber, A., & Dissemond, J. (2006). Black Hairy Tongue — NEJM. *New England Journal of Medicine*.

Körber, A., & Voshege, N. (2012). Black hairy tongue in an infant. *CMAJ : Canadian Medical Association Journal = Journal De l'Association Médicale Canadienne*, 184(1), 68–68. <http://doi.org/10.1503/cmaj.111013>

- Köse, O., Lalli, A., Kutulola, A. O., Odell, E. W., & Waseem, A. (2007). Changes in the expression of stem cell markers in oral lichen planus and hyperkeratotic lesions. *Journal of Oral Science*, *49*(2), 133–139.
- Kuribayashi, Y., Tsushima, F., Sato, M., Morita, K.-I., & Omura, K. (2012). Recurrence patterns of oral leukoplakia after curative surgical resection: important factors that predict the risk of recurrence and malignancy. *Journal of Oral Pathology & Medicine : Official Publication of the International Association of Oral Pathologists and the American Academy of Oral Pathology*, *41*(9), 682–688. <http://doi.org/10.1111/j.1600-0714.2012.01167.x>
- Lalla, R. V., Sonis, S. T., & Peterson, D. E. (2008). Management of oral mucositis in patients who have cancer. *Dental Clinics of North America*, *52*(1), 61–77– viii. <http://doi.org/10.1016/j.cden.2007.10.002>
- Legg, J., Jensen, U. B., Broad, S., Leigh, I., & Watt, F. M. (2003). Role of melanoma chondroitin sulphate proteoglycan in patterning stem cells in human interfollicular epidermis. *Development (Cambridge, England)*, *130*(24), 6049–6063. <http://doi.org/10.1242/dev.00837>
- Legué, E., & Joyner, A. L. (2010). Genetic fate mapping using site-specific recombinases. *Methods in Enzymology*, *477*, 153–181. [http://doi.org/10.1016/S0076-6879\(10\)77010-5](http://doi.org/10.1016/S0076-6879(10)77010-5)
- Li, L., & Clevers, H. (2010). Coexistence of quiescent and active adult stem cells in mammals. *Science*, *327*(5965), 542–545. <http://doi.org/10.1126/science.1180794>

- Lim, J., & Ng, S. K. (1992). Oral tetracycline rinse improves symptoms of white sponge nevus. *Journal of the American Academy of Dermatology*, 26(6), 1003–1005. [http://doi.org/10.1016/S0190-9622\(08\)80340-4](http://doi.org/10.1016/S0190-9622(08)80340-4)
- Lim, X., Tan, S. H., Koh, W. L. C., Chau, R. M. W., Yan, K. S., Kuo, C. J., et al. (2013). Interfollicular epidermal stem cells self-renew via autocrine Wnt signaling. *Science*, 342(6163), 1226–1230. <http://doi.org/10.1126/science.1239730>
- Liu, Y., Lyle, S., Yang, Z., & Cotsarelis, G. (2003). Keratin 15 promoter targets putative epithelial stem cells in the hair follicle bulge. *The Journal of Investigative Dermatology*, 121(5), 963–968. <http://doi.org/10.1046/j.1523-1747.2003.12600.x>
- Lodi, G., & Porter, S. (2008). Management of potentially malignant disorders: evidence and critique. (Vol. 37, pp. 63–69). Presented at the Journal of oral pathology & medicine : official publication of the International Association of Oral Pathologists and the American Academy of Oral Pathology. <http://doi.org/10.1111/j.1600-0714.2007.00575.x>
- Longley, D. B., Harkin, D. P., & Johnston, P. G. (2003). 5-fluorouracil: mechanisms of action and clinical strategies. *Nature Reviews. Cancer*, 3(5), 330–338. <http://doi.org/10.1038/nrc1074>
- Lumerman, H., Freedman, P., & Kerpel, S. (1995). Oral epithelial dysplasia and the development of invasive squamous cell carcinoma. *Oral Surgery, Oral Medicine, Oral Pathology, Oral Radiology, and Endodontics*, 79(3), 321–329.
- Luo, X., Okubo, T., Randell, S., & Hogan, B. L. M. (2009). Culture of endodermal

stem/progenitor cells of the mouse tongue. *In Vitro Cellular & Developmental Biology. Animal*, 45(1-2), 44–54. <http://doi.org/10.1007/s11626-008-9149-2>

Lyle, S., Christofidou-Solomidou, M., Liu, Y., Elder, D. E., Albelda, S., & Cotsarelis, G. (1998). The C8/144B monoclonal antibody recognizes cytokeratin 15 and defines the location of human hair follicle stem cells. *Journal of Cell Science*, 111 ( Pt 21), 3179–3188.

M Clin Dent, F. V., Al-Kheraif, A. A., Qadri, T., Hassan, M. I. A., Ahmed, A., Warnakulasuriya, S., & Javed, F. (2014). Efficacy of photodynamic therapy in the management of oral premalignant lesions. A systematic review. *Photodiagnosis and Photodynamic Therapy*, 12(1), 150–159. <http://doi.org/10.1016/j.pdpdt.2014.10.001>

Mackenzie, I. (2005). Stem Cells in Oral Mucosal Epithelia, 1–9.

Mackenzie, I. C. (1997). Retroviral Transduction of Murine Epidermal Stem Cells Demonstrates Clonal Units of Epidermal Structure. *The Journal of Investigative Dermatology*, 109(3), 377–383. <http://doi.org/10.1111/1523-1747.ep12336255>

Macosko, E. Z., Basu, A., Satija, R., Nemesh, J., Shekhar, K., Goldman, M., et al. (2015). Highly Parallel Genome-wide Expression Profiling of Individual Cells Using Nanoliter Droplets. *Cell*, 161(5), 1202–1214. <http://doi.org/10.1016/j.cell.2015.05.002>

Mannelli, G., & Gallo, O. (2012). Cancer stem cells hypothesis and stem cells in head and neck cancers. *Cancer Treatment Reviews*, 38(5), 515–539. <http://doi.org/10.1016/j.ctrv.2011.11.007>

- Marrelli, M., Tatullo, M., Dipalma, G., & Inchingolo, F. (2012). Oral infection by *Staphylococcus aureus* in patients affected by White Sponge Nevus: a description of two cases occurred in the same family. *International Journal of Medical Sciences*, 9(1), 47–50.
- Martin, J. L. (1992). Leukoedema: a review of the literature. *Journal of the National Medical Association*, 84(11), 938–940.
- Martynoga, B., Morrison, H., Price, D. J., & Mason, J. O. (2005). Foxg1 is required for specification of ventral telencephalon and region-specific regulation of dorsal telencephalic precursor proliferation and apoptosis. *Developmental Biology*, 283(1), 113–127. <http://doi.org/10.1016/j.ydbio.2005.04.005>
- Mascré, G., Dekoninck, S., Drogat, B., Youssef, K. K., Broheé, S., Sotiropoulou, P. A., et al. (2012). Distinct contribution of stem and progenitor cells to epidermal maintenance. *Nature*, 489(7415), 257–262. <http://doi.org/10.1038/nature11393>
- Massano, J., Regateiro, F. S., Januário, G., & Ferreira, A. (2006). Oral squamous cell carcinoma: review of prognostic and predictive factors. *Oral Surgery, Oral Medicine, Oral Pathology, Oral Radiology, and Endodontics*, 102(1), 67–76. <http://doi.org/10.1016/j.tripleo.2005.07.038>
- Mauldin, E. A., Gaide, O., Schneider, P., & Casal, M. L. (2009). Neonatal treatment with recombinant ectodysplasin prevents respiratory disease in dogs with X-linked ectodermal dysplasia. *American Journal of Medical Genetics Part A*, 149A(9), 2045–2049. <http://doi.org/10.1002/ajmg.a.32916>

- McCartan, B. E., & McCreary, C. E. (1997). Oral lichenoid drug eruptions - McCartan - 2008 - Oral Diseases - Wiley Online Library. *Oral Diseases*.
- MCDONAGH, A. J. G., GAWKRODGER, D. J., & WALKER, A. E. (1990). White sponge naevus successfully treated with topical tetracycline. *Clinical and Experimental Dermatology*, 15(2), 152–153. <http://doi.org/10.1111/j.1365-2230.1990.tb02056.x>
- Mehanna, H. M., Rattay, T., Smith, J., & McConkey, C. C. (2009). Treatment and follow-up of oral dysplasia — A systematic review and meta-analysis - Mehanna - 2009 - Head & Neck - Wiley Online Library. *Head & Neck*.
- Menni, S., Boccardi, D., & Crosti, C. (2004). Painful geographic tongue (benign migratory glossitis) in a child. *Journal of the European Academy of Dermatology and Venereology* : *JEADV*, 18(6), 737–738. <http://doi.org/10.1111/j.1468-3083.2004.01032.x>
- Michel, M., Török, N., Godbout, M. J., Lussier, M., Gaudreau, P., Royal, A., & Germain, L. (1996). Keratin 19 as a biochemical marker of skin stem cells in vivo and in vitro: keratin 19 expressing cells are differentially localized in function of anatomic sites, and their number varies with donor age and culture stage. *Journal of Cell Science*, 109 ( Pt 5), 1017–1028.
- Mignogna, M. D., Fedele, S., & Russo, Lo, L. (2006). Dysplasia/neoplasia surveillance in oral lichen planus patients: a description of clinical criteria adopted at a single centre and their impact on prognosis. *Oral Oncology*, 42(8), 819–824. <http://doi.org/10.1016/j.oraloncology.2005.11.022>

- Mikkola, M. L. (2009). Molecular aspects of hypohidrotic ectodermal dysplasia. *American Journal of Medical Genetics Part A*, 149A(9), 2031–2036. <http://doi.org/10.1002/ajmg.a.32855>
- Mikkola, M. L., & Thesleff, I. (2003). Ectodysplasin signaling in development. *Cytokine & Growth Factor Reviews*, 14(3-4), 211–224.
- Miloğlu, O., Göregen, M., Akgül, H. M., & Acemoğlu, H. (2009). The prevalence and risk factors associated with benign migratory glossitis lesions in 7619 Turkish dental outpatients. *Oral Surgery, Oral Medicine, Oral Pathology, Oral Radiology, and Endodontics*, 107(2), e29–33. <http://doi.org/10.1016/j.tripleo.2008.10.015>
- Moll, R., Divo, M., & Langbein, L. (2008). The human keratins: biology and pathology. *Histochemistry and Cell Biology*, 129(6), 705–733. <http://doi.org/10.1007/s00418-008-0435-6>
- Morton, C. A., Garioch, J., Todd, P., & Lamey, P. J. (1995). Contact sensitivity to menthol and peppermint in patients with intra-oral symptoms - Morton - 2006 - Contact Dermatitis - Wiley Online Library. *Contact* ....
- Mou, C., Thomason, H. A., Willan, P. M., Clowes, C., Harris, W. E., Drew, C. F., et al. (2008). Enhanced ectodysplasin-A receptor (EDAR) signaling alters multiple fiber characteristics to produce the East Asian hair form. *Human Mutation*, 29(12), 1405–1411. <http://doi.org/10.1002/humu.20795>
- Mustafa Baydar, M. D. A. S. I. A. (2005). Prevention of oral mucositis due to 5-fluorouracil treatment with oral cryotherapy. *Journal of the National Medical*

*Association*, 97(8), 1161.

Nakagawa, M., Koyanagi, M., Tanabe, K., Takahashi, K., Ichisaka, T., Aoi, T., et al. (2007). Generation of induced pluripotent stem cells without Myc from mouse and human fibroblasts. *Nature Biotechnology*, 26(1), 101–106. <http://doi.org/10.1038/nbt1374>

Nakamura, T., Endo, K.-I., & Kinoshita, S. (2007). Identification of human oral keratinocyte stem/progenitor cells by neurotrophin receptor p75 and the role of neurotrophin/p75 signaling. *Stem Cells (Dayton, Ohio)*, 25(3), 628–638. <http://doi.org/10.1634/stemcells.2006-0494>

Napier, S. S., & Speight, P. M. (2008). Natural history of potentially malignant oral lesions and conditions: an overview of the literature. *Journal of Oral Pathology & Medicine : Official Publication of the International Association of Oral Pathologists and the American Academy of Oral Pathology*, 37(1), 1–10. <http://doi.org/10.1111/j.1600-0714.2007.00579.x>

Nasser, W., Flechtenmacher, C., Holzinger, D., Hofele, C., & Bosch, F. X. (2011). Aberrant expression of p53, p16INK4a and Ki-67 as basic biomarker for malignant progression of oral leukoplakias. *Journal of Oral Pathology and Medicine*, 40(8), 629–635. <http://doi.org/10.1111/j.1600-0714.2011.01026.x>

Natarajan, E., & Woo, S.-B. (2008). Benign alveolar ridge keratosis (oral lichen simplex chronicus): A distinct clinicopathologic entity. *Journal of the American Academy of Dermatology*, 58(1), 151–157. <http://doi.org/10.1016/j.jaad.2007.07.011>



- Niwa, H., Miyazaki, J., & Smith, A. G. (2000). Quantitative expression of Oct-3/4 defines differentiation, dedifferentiation or self-renewal of ES cells. *Nature Genetics*.
- O'Keefe, E., Braverman, I. M., & Cohen, I. (1973). Annulus migrans. Identical lesions in pustular psoriasis, Reiter's syndrome, and geographic tongue. *Archives of Dermatology*, 107(2), 240–244.
- Okada, S., Nakauchi, H., Nagayoshi, K., Nishikawa, S., Miura, Y., & Suda, T. (1991). Enrichment and characterization of murine hematopoietic stem cells that express c-kit molecule. *Blood*, 78(7), 1706–1712.
- Okubo, T., Clark, C., & Hogan, B. L. M. (2009). Cell lineage mapping of taste bud cells and keratinocytes in the mouse tongue and soft palate. *Stem Cells (Dayton, Ohio)*, 27(2), 442–450. <http://doi.org/10.1634/stemcells.2008-0611>
- Okumura, T., Shimada, Y., Imamura, M., & Yasumoto, S. (2003). Neurotrophin receptor p75(NTR) characterizes human esophageal keratinocyte stem cells in vitro. *Oncogene*, 22(26), 4017–4026. <http://doi.org/10.1038/sj.onc.1206525>
- Otobe, I. F., de Sousa, S. O. M., Matthews, R. W., & Migliari, D. A. (2007). White sponge naevus: improvement with tetracycline mouth rinse: report of four cases. *Clinical and Experimental Dermatology*, 32(6), 749–751. <http://doi.org/10.1111/j.1365-2230.2007.02538.x>
- Pellegrini, G., Dellambra, E., Golisano, O., Martinelli, E., Fantozzi, I., Bondanza, S., et al. (2001). p63 identifies keratinocyte stem cells. *Proceedings of the National Academy of Sciences of the United States of America*, 98(6), 3156–3161.

<http://doi.org/10.1073/pnas.061032098>

Pispa, J., & Thesleff, I. (2003). Mechanisms of ectodermal organogenesis. *Developmental Biology*, 262(2), 195–205.

Pittenger, M. F. (1999). Multilineage Potential of Adult Human Mesenchymal Stem Cells. *Science*, 284(5411), 143–147. <http://doi.org/10.1126/science.284.5411.143>

Potten, C. S. (1974). The Epidermal Proliferative Unit: The Possible Role Of The Central Basal Cell. *Cell Proliferation*, 7(1), 77–88. <http://doi.org/10.1111/j.1365-2184.1974.tb00401.x>

Potten, C. S. (1975). EPIDERMAL CELL PRODUCTION RATES. *The Journal of Investigative Dermatology*, 65(6), 488–500. <http://doi.org/10.1111/1523-1747.ep12610194>

Prince, M. E., Sivanandan, R., Kaczorowski, A., Wolf, G. T., Kaplan, M. J., Dalerba, P., et al. (2007). Identification of a subpopulation of cells with cancer stem cell properties in head and neck squamous cell carcinoma. *Proceedings of the National Academy of Sciences of the United States of America*, 104(3), 973–978. <http://doi.org/10.1073/pnas.0610117104>

Raimondi, A. R., Molinolo, A., & Gutkind, J. S. (2009). Rapamycin Prevents Early Onset of Tumorigenesis in an Oral-Specific K-ras and p53 Two-Hit Carcinogenesis Model. *Cancer Research*, 69(10), 4159–4166. <http://doi.org/10.1158/0008-5472.CAN-08-4645>

Rajadhyaksha, M., González, S., Zavislan, J. M., Anderson, R. R., & Webb, R. H.

- (1999). In vivo confocal scanning laser microscopy of human skin II: advances in instrumentation and comparison with histology. *Journal of Investigative Dermatology*, 113(3), 293–303. <http://doi.org/10.1046/j.1523-1747.1999.00690.x>
- Ramulu, C., Raju, M. V. S., Venkatarathnam, G., & Reddy, C. R. R. M. (n.d.). Nicotine Stomatitis and its Relation to Carcinoma of the Hard Palate in Reverse Smokers of Chuttas. *Jdr.Sagepub.com*.
- Ravindran, G., & Devaraj, H. (2012). Aberrant expression of CD133 and musashi-1 in preneoplastic and neoplastic human oral squamous epithelium and their correlation with clinicopathological factors. *Head & Neck*, 34(8), 1129–1135. <http://doi.org/10.1002/hed.21896>
- Regezi, J. A., Sciubba, J. J., & Jordan, R. (2012). Oral Pathology: Clinical Pathologic Correlations, 85–86– 95.
- Richard, G., De Laurenzi, V., Didona, B., Bale, S. J., & Compton, J. G. (1995). Keratin 13 point mutation underlies the hereditary mucosal epithelial disorder white sponge nevus. *Nature Genetics*, 11(4), 453–455. <http://doi.org/10.1038/ng1295-453>
- Ro, S., & Rannala, B. (2004). A stop-EGFP transgenic mouse to detect clonal cell lineages generated by mutation. *EMBO Reports*, 5(9), 914–920. <http://doi.org/10.1038/sj.embor.7400218>
- Ro, S., & Rannala, B. (2005). Evidence from the stop-EGFP mouse supports a niche-sharing model of epidermal proliferative units. *Experimental Dermatology*, 14(11), 838–843. <http://doi.org/10.1111/j.1600-0625.2005.00366.x>

- Roosaar, A., Johansson, A. L. V., Sandborgh-Englund, G., Nyrén, O., & Axéll, T. (2006). A long-term follow-up study on the natural course of snus-induced lesions among Swedish snus users. *International Journal of Cancer. Journal International Du Cancer*, *119*(2), 392–397. <http://doi.org/10.1002/ijc.21841>
- Rosen, J. M., & Jordan, C. T. (2009). The increasing complexity of the cancer stem cell paradigm. *Science*, *324*(5935), 1670–1673. <http://doi.org/10.1126/science.1171837>
- Rouse, C., Siegfried, E., Breer, W., & Nahass, G. (2004). Hair and sweat glands in families with hypohidrotic ectodermal dysplasia: further characterization. *Archives of Dermatology*, *140*(7), 850–855. <http://doi.org/10.1001/archderm.140.7.850>
- Rödström, P.-O., Jontell, M., Mattsson, U., & Holmberg, E. (2004). Cancer and oral lichen planus in a Swedish population. *Oral Oncology*, *40*(2), 131–138.
- Rugg, E. L., McLean, W. H., Allison, W. E., Lunny, D. P., Macleod, R. I., Felix, D. H., et al. (1995). A mutation in the mucosal keratin K4 is associated with oral white sponge nevus. *Nature Genetics*, *11*(4), 450–452. <http://doi.org/10.1038/ng1295-450>
- Satija, R., Farrell, J. A., Gennert, D., Schier, A. F., & Regev, A. (2015). Spatial reconstruction of single-cell gene expression data. *Nature Biotechnology*, *33*(5), 495–502. <http://doi.org/10.1038/nbt.3192>
- SATRIANO, R. A., ERRICHETTI, E., & BARONI, A. (2012). White sponge nevus treated with chlorhexidine. *The Journal of Dermatology*, *39*(8), 742–743. <http://doi.org/10.1111/j.1346-8138.2012.01508.x>
- Schindelin, J., Arganda-Carreras, I., Frise, E., Kaynig, V., Longair, M., Pietzsch, T., et

- al. (2012). Fiji: an open-source platform for biological-image analysis. *Nature Methods*, 9(7), 676–682. <http://doi.org/10.1038/nmeth.2019>
- Schindelin, J., Rueden, C. T., Hiner, M. C., & Eliceiri, K. W. (2015). The ImageJ ecosystem: An open platform for biomedical image analysis. *Molecular Reproduction and Development*, 82(7-8), 518–529. <http://doi.org/10.1002/mrd.22489>
- Schiødt, M., Greenspan, D., Daniels, T. E., & Greenspan, J. S. (1987). Clinical and histologic spectrum of oral hairy leukoplakia. *Oral Surgery, Oral Medicine, and Oral Pathology*, 64(6), 716–720.
- Schlosser, B. J. (2010). Lichen planus and lichenoid reactions of the oral mucosa - Schlosser - 2010 - Dermatologic Therapy - Wiley Online Library. *Dermatologic Therapy*, 23(3), 251–267. <http://doi.org/10.1111/j.1529-8019.2010.01322.x>
- Schneider, H., Hammersen, J., Preisler-Adams, S., Huttner, K., Rascher, W., & Bohring, A. (2011). Sweating ability and genotype in individuals with X-linked hypohidrotic ectodermal dysplasia. *Journal of Medical Genetics*, 48(6), 426–432. <http://doi.org/10.1136/jmg.2010.084012>
- Seidel, K., Ahn, C. P., Lyons, D., Nee, A., Ting, K., Brownell, I., et al. (2010). Hedgehog signaling regulates the generation of ameloblast progenitors in the continuously growing mouse incisor. *Development (Cambridge, England)*, 137(22), 3753–3761. <http://doi.org/10.1242/dev.056358>
- Sen, S., Sharma, S., Gupta, A., Gupta, N., Singh, H., Roychoudhury, A., et al. (2011).

- Molecular characterization of explant cultured human oral mucosal epithelial cells. *Investigative Ophthalmology & Visual Science*, 52(13), 9548–9554. <http://doi.org/10.1167/iovs.11-7946>
- Severson, H. H., Klein, K., Lichtensein, E., Kaufman, N., & Orleans, C. T. (2005). Smokeless tobacco use among professional baseball players: survey results, 1998 to 2003. *Tobacco Control*, 14(1), 31–36. <http://doi.org/10.1136/tc.2004.007781>
- Shiu, M. N., Chen, T. H., Chang, S. H., & Hahn, L. J. (2000). Risk factors for leukoplakia and malignant transformation to oral carcinoma: a leukoplakia cohort in Taiwan. *British Journal of Cancer*, 82(11), 1871–1874. <http://doi.org/10.1054/bjoc.2000.1208>
- Shulman, J. D., & Carpenter, W. M. (2006). Prevalence and risk factors associated with geographic tongue among US adults. *Oral Diseases*, 12(4), 381–386. <http://doi.org/10.1111/j.1601-0825.2005.01208.x>
- Siddique, H. R., & Saleem, M. (2012). Role of BMI1, a stem cell factor, in cancer recurrence and chemoresistance: preclinical and clinical evidences. *Stem Cells (Dayton, Ohio)*, 30(3), 372–378. <http://doi.org/10.1002/stem.1035>
- Silverman, S., Gorsky, M., & Kaugars, G. E. (1996). Leukoplakia, dysplasia, and malignant transformation. *Oral Surgery, Oral Medicine, Oral Pathology, Oral Radiology, and Endodontics*, 82(2), 117.
- Silverman, S., Gorsky, M., & Lozada, F. (1984). Oral leukoplakia and malignant transformation. A follow-up study of 257 patients. *Cancer*, 53(3), 563–568.
- Sinclair, R. D., & Dawber, R. P. (2001). Androgenetic alopecia in men and women.

*Clinics in Dermatology*, 19(2), 167–178.

Smith, J. F. (1975). Snuff-dippers lesion. A ten-year follow-up. *Archives of Otolaryngology (Chicago, Ill. : 1960)*, 101(5), 276–277.

Smith, J. F., Mincer, H. A., Hopkins, K. P., & Bell, J. (1970). Snuff-dipper's lesion. A cytological and pathological study in a large population. *Archives of Otolaryngology (Chicago, Ill. : 1960)*, 92(5), 450–456.

Snippert, H. J., Haegebarth, A., Kasper, M., Jaks, V., van Es, J. H., Barker, N., et al. (2010a). Lgr6 marks stem cells in the hair follicle that generate all cell lineages of the skin. *Science*, 327(5971), 1385–1389. <http://doi.org/10.1126/science.1184733>

Snippert, H. J., van der Flier, L. G., Sato, T., van Es, J. H., van den Born, M., Kroon-Veenboer, C., et al. (2010b). Intestinal crypt homeostasis results from neutral competition between symmetrically dividing Lgr5 stem cells. *Cell*, 143(1), 134–144. <http://doi.org/10.1016/j.cell.2010.09.016>

Squier, C. A., & Kremer, M. J. (2001). Biology of oral mucosa and esophagus. *Journal of the National Cancer Institute. Monographs*, (29), 7–15.

Sternberg, N., & Hamilton, D. (1981). Bacteriophage P1 site-specific recombination. *Journal of Molecular Biology*, 150(4), 467–486. [http://doi.org/10.1016/0022-2836\(81\)90375-2](http://doi.org/10.1016/0022-2836(81)90375-2)

Supek, F., Bošnjak, M., Škunca, N., & Šmuc, T. (2011). REVIGO summarizes and visualizes long lists of gene ontology terms. *PLoS ONE*, 6(7), e21800. <http://doi.org/10.1371/journal.pone.0021800>

- Takeda, T., Sugihara, K., Hirayama, Y., Hirano, M., Tanuma, J.-I., & Semba, I. (2006). Immunohistological evaluation of Ki-67, p63, CK19 and p53 expression in oral epithelial dysplasias. *Journal of Oral Pathology and Medicine*, 35(6), 369–375. <http://doi.org/10.1111/j.1600-0714.2006.00444.x>
- Tamura, T., Kuwahara, A., Kadoyama, K., Yamamori, M., Nishiguchi, K., Inokuma, T., et al. (2011). Effects of bolus injection of 5-fluorouracil on steady-state plasma concentrations of 5-fluorouracil in Japanese patients with advanced colorectal cancer. *International Journal of Medical Sciences*, 8(5), 406–412.
- Tanaka, T., Komai, Y., Tokuyama, Y., Yanai, H., Ohe, S., Okazaki, K., & Ueno, H. (2013). Identification of stem cells that maintain and regenerate lingual keratinized epithelial cells. *Nature Cell Biology*, 15(5), 511–518. <http://doi.org/10.1038/ncb2719>
- Tani, H., Morris, R. J., & Kaur, P. (2000). Enrichment for murine keratinocyte stem cells based on cell surface phenotype. *Proceedings of the National Academy of Sciences of the United States of America*, 97(20), 10960–10965.
- Tao, Q., Qiao, B., Lv, B., Zheng, C., Chen, Z., & Huang, H. (2009). p63 and its isoforms as markers of rat oral mucosa epidermal stem cells in vitro. *Cell Biochemistry and Function*, 27(8), 535–541. <http://doi.org/10.1002/cbf.1612>
- Taybos, G. (2003). Oral changes associated with tobacco use. *The American Journal of the Medical Sciences*, 326(4), 179–182.
- Thompson, D. F., & Kessler, T. L. (2010). Drug-induced black hairy tongue. *Pharmacotherapy*, 30(6), 585–593. <http://doi.org/10.1592/phco.30.6.585>



- Thornhill, M. H., Sankar, V., Xu, X.-J., Barrett, A. W., High, A. S., Odell, E. W., et al. (2006). The role of histopathological characteristics in distinguishing amalgam-associated oral lichenoid reactions and oral lichen planus. *Journal of Oral Pathology & Medicine : Official Publication of the International Association of Oral Pathologists and the American Academy of Oral Pathology*, 35(4), 233–240. <http://doi.org/10.1111/j.1600-0714.2006.00406.x>
- Tian, H., Biehs, B., Warming, S., Leong, K. G., Rangell, L., Klein, O. D., & de Sauvage, F. J. (2011). A reserve stem cell population in small intestine renders Lgr5-positive cells dispensable. *Nature*, 478(7368), 255–259. <http://doi.org/10.1038/nature10408>
- Timmer, R., Seldenrijk, C. A., Gorp, von, L. H., Dingemans, K. P., Bartelsman, J. F., & Smout, A. J. (1997). Esophageal white sponge nevus associated with severe dysphagia and odynophagia. *Digestive Diseases and Sciences*, 42(9), 1914–1918.
- Tomar, S. L. (2003). Trends and patterns of tobacco use in the United States. *The American Journal of the Medical Sciences*, 326(4), 248–254.
- Treister, N., Lehmann, L. E., Cherrick, I., Guinan, E. C., & Woo, S.-B. (2004). Dyskeratosis congenita vs. chronic graft versus host disease: report of a case and a review of the literature. *Oral Surgery, Oral Medicine, Oral Pathology, Oral Radiology, and Endodontics*, 98(5), 566–571. <http://doi.org/10.1016/S1079210404000678>
- Tremblay, S., & Avon, S. L. (2008). Contact allergy to cinnamon: case report. *J Can Dent Assoc*.

- Trzeciak, W. H., & Koczorowski, R. (2016). Molecular basis of hypohidrotic ectodermal dysplasia: an update. *Journal of Applied Genetics*, *57*(1), 51–61. <http://doi.org/10.1007/s13353-015-0307-4>
- Tsai, L.-L., Yu, C.-C., Chang, Y.-C., Yu, C.-H., & Chou, M.-Y. (2011). Markedly increased Oct4 and Nanog expression correlates with cisplatin resistance in oral squamous cell carcinoma. *Journal of Oral Pathology and Medicine*, *40*(8), 621–628. <http://doi.org/10.1111/j.1600-0714.2011.01015.x>
- Tumbar, T., Guasch, G., Greco, V., Blanpain, C., Lowry, W. E., Rendl, M., & Fuchs, E. (2004). Defining the epithelial stem cell niche in skin. *Science*, *303*(5656), 359–363. <http://doi.org/10.1126/science.1092436>
- van der Meij, E. H., Schepman, K. P., Smeele, L. E., van der Wal, J. E., Bezemer, P. D., & van der Waal, I. (1999). A review of the recent literature regarding malignant transformation of oral lichen planus. *Oral Surgery, Oral Medicine, Oral Pathology, Oral Radiology, and Endodontics*, *88*(3), 307–310.
- van der Waal, I. (2014). Oral potentially malignant disorders: is malignant transformation predictable and preventable? *Medicina Oral, Patología Oral Y Cirugía Bucal*, *19*(4), e386–90.
- Van Keymeulen, A., & Blanpain, C. (2012). Tracing epithelial stem cells during development, homeostasis, and repair. *The Journal of Cell Biology*, *197*(5), 575–584. <http://doi.org/10.1083/jcb.201201041>
- Van Neste, D., & Fuh, V. (2001). Finasteride increases anagen hair in men with

androgenetic alopecia. *British Journal of ...* Retrieved from <http://onlinelibrary.wiley.com/doi/10.1046/j.1365-2133.2000.03780.x/full>

Vasioukhin, V., Degenstein, L., Wise, B., & Fuchs, E. (1999). The magical touch: genome targeting in epidermal stem cells induced by tamoxifen application to mouse skin. *Proceedings of the National Academy of Sciences of the United States of America*, 96(15), 8551–8556.

Visvader, J. E., & Lindeman, G. J. (2008). Cancer stem cells in solid tumours: accumulating evidence and unresolved questions. *Nature Reviews. Cancer*, 8(10), 755–768. <http://doi.org/10.1038/nrc2499>

Vladimirov, B. S., & Schiødt, M. (2009). The effect of quitting smoking on the risk of unfavorable events after surgical treatment of oral potentially malignant lesions. *International Journal of Oral and Maxillofacial Surgery*, 38(11), 1188–1193. <http://doi.org/10.1016/j.ijom.2009.06.026>

Waitzer, S. (1984). Oral Leukoedema. *Archives of Dermatology*, 120(2), 264. <http://doi.org/10.1001/archderm.1984.01650380124028>

Warnakulasuriya, S. (2001). Histological grading of oral epithelial dysplasia: revisited. *The Journal of Pathology*, 194(3), 294–297. [http://doi.org/10.1002/1096-9896\(200107\)194:3<294::AID-PATH911>3.0.CO;2-Q](http://doi.org/10.1002/1096-9896(200107)194:3<294::AID-PATH911>3.0.CO;2-Q)

Warnakulasuriya, S. (2009). Global epidemiology of oral and oropharyngeal cancer. *Oral Oncology*, 45(4-5), 309–316. <http://doi.org/10.1016/j.oraloncology.2008.06.002>

Warnakulasuriya, S., Johnson, N. W., & van der Waal, I. (2007). Nomenclature and

classification of potentially malignant disorders of the oral mucosa. (Vol. 36, pp. 575–580). Presented at the Journal of oral pathology & medicine : official publication of the International Association of Oral Pathologists and the American Academy of Oral Pathology. <http://doi.org/10.1111/j.1600-0714.2007.00582.x>

Watt, F. M. (2002). NEW EMBO MEMBER'S REVIEW: Role of integrins in regulating epidermal adhesion, growth and differentiation. *The EMBO Journal*, 21(15), 3919–3926. <http://doi.org/10.1093/emboj/cdf399>

WINER, L. H. (1958). Black Hair Tongue. *A.M.a. Archives of Dermatology*, 77(1), 97. <http://doi.org/10.1001/archderm.1958.01560010099013>

Winning, T. A., & Townsend, G. C. (2000). Oral mucosal embryology and histology. *Clinics in Dermatology*, 18(5), 499–511.

Woo, S. B., & Lin, D. (2009). Morsicatio Mucosae Oris—A Chronic Oral Frictional Keratosis, Not a Leukoplakia. *Journal of Oral and Maxillofacial Surgery*.

Wu, T., Xiong, X., Zhang, W., Zou, H., Xie, H., & He, S. (2012). Morphogenesis of Rete Ridges in Human Oral Mucosa: A Pioneering Morphological and Immunohistochemical Study. *Cells, Tissues, Organs*. <http://doi.org/10.1159/000342926>

Yan, W., Wistuba, I. I., Emmert-Buck, M. R., & Erickson, H. S. (2011). Squamous Cell Carcinoma - Similarities and Differences among Anatomical Sites. *American Journal of Cancer Research*, 1(3), 275–300.

Yanamoto, S., Kawasaki, G., Yamada, S.-I., Yoshitomi, I., Kawano, T., Yonezawa, H.,

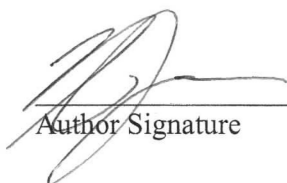
- et al. (2011). Isolation and characterization of cancer stem-like side population cells in human oral cancer cells. *Oral Oncology*, 47(9), 855–860. <http://doi.org/10.1016/j.oraloncology.2011.06.501>
- Zhang, P., Zhang, Y., Mao, L., Zhang, Z., & Chen, W. (2009a). Side population in oral squamous cell carcinoma possesses tumor stem cell phenotypes. *Cancer Letters*, 277(2), 227–234. <http://doi.org/10.1016/j.canlet.2008.12.015>
- Zhang, Q., Shi, S., Yen, Y., Brown, J., Ta, J. Q., & Le, A. D. (2010). A subpopulation of CD133+ cancer stem-like cells characterized in human oral squamous cell carcinoma confer resistance to chemotherapy. *Cancer Letters*, 289(2), 151–160. <http://doi.org/10.1016/j.canlet.2009.08.010>
- Zhang, Y., Tomann, P., Andl, T., Gallant, N. M., Huelsken, J., Jerchow, B., et al. (2009b). Reciprocal requirements for EDA/EDAR/NF-kappaB and Wnt/beta-catenin signaling pathways in hair follicle induction. *Developmental Cell*, 17(1), 49–61. <http://doi.org/10.1016/j.devcel.2009.05.011>
- Zhou, S., Schuetz, J. D., & Bunting, K. D. (2001). The ABC transporter Bcrp1/ABCG2 is expressed in a wide variety of stem cells and is a molecular determinant of the side-population phenotype. *Nature*.
- Zimmerman, L., Lendahl, U., Cunningham, M., McKay, R., Parr, B., Gavin, B., et al. (1994). Independent regulatory elements in the nestin gene direct transgene expression to neural stem cells or muscle precursors. *Neuron*, 12(1), 11–24. [http://doi.org/10.1016/0896-6273\(94\)90148-1](http://doi.org/10.1016/0896-6273(94)90148-1)

**Publishing Agreement**

*It is the policy of the University to encourage the distribution of all theses, dissertations, and manuscripts. Copies of all UCSF theses, dissertations, and manuscripts will be routed to the library via the Graduate Division. The library will make all theses, dissertations, and manuscripts accessible to the public and will preserve these to the best of their abilities, in perpetuity.*

***Please sign the following statement:***

*I hereby grant permission to the Graduate Division of the University of California, San Francisco to release copies of my thesis, dissertation, or manuscript to the Campus Library to provide access and preservation, in whole or in part, in perpetuity.*

  
\_\_\_\_\_  
Author Signature

9/11/2017  
\_\_\_\_\_  
Date